TECTONOSTRATIGRAPHIC STAGES IN THE MESOZOIC OPENING AND SUBSIDENCE OF THE GULF OF MEXICO BASED ON DEEP-PENETRATION SEISMIC REFLECTION DATA IN THE SALT-FREE EASTERN PART OF THE BASIN

A Thesis Presented to

the Faculty of the Department of Earth and Atmospheric Sciences

University of Houston

In Partial Fulfillment

of the Requirements for the Degree

Master of Science

By

Murad Ismael

December 2014

TECTONOSTRATIGRAPHIC STAGES IN THE MESOZOIC OPENING AND SUBSIDENCE OF THE GULF OF MEXICO BASED ON DEEP-PENETRATION SEISMIC REFLECTION DATA IN THE SALT-FREE EASTERN PART OF THE BASIN

____

Murad Ismael

APPROVED:

____

Paul Mann, Supervisor

____

Stuart Hall, Committee member

____

Shuhab Khan, Committee member

____

Peter Bartok, Committee member

____

Dean, College of Natural Sciences and Mathematics

Dedication

To the souls of my fellow Yazidis killed during the ISIS invasion of Sinjar, northwestern Iraq, during the summer and fall of 2014.

Acknowledgements

I would like to thank my master's thesis committee for their support and helpful reviews: Paul Mann (advisor), Stuart Hall (committee member), and Shuhab Khan (committee member). I would also like to thank the 20 sponsoring oil companies of the University of Houston Caribbean Basin, Tectonics and Hydrocarbons project whose financial support has allowed me to be a graduate research assistant for the past two years. I would also like to thank Peter Nuttall and Rob Pascoe of Dynamic Data Services for kindly providing me the seismic reflection data that formed the main observational basis for this thesis and their help in interpreting the data. Finally, I would like to thank my family and friends and co-workers at the CBTH project who have provided support and guidance over the past two years.

November 4, 2014

TECTONOSTRATIGRAPHIC STAGES IN THE MESOZOIC OPENING AND SUBSIDENCE OF THE GULF OF MEXICO BASED ON DEEP-PENETRATION SEISMIC REFLECTION DATA IN THE SALT-FREE EASTERN PART OF THE BASIN

An Abstract of a Thesis

Presented to

the Faculty of the Department of Earth and Atmospheric Sciences

University of Houston

In Partial Fulfillment

of the Requirements for the Degree

Master of Science

By

Murad Ismael

December 2014

ABSTRACT

The eastern and northeastern Gulf of Mexico provide one of the few areas of the Gulf of Mexico continent-ocean boundary that is not obscured by a thick layer of remobilized salt deposits. I used 17,000 km of deep-penetration, long-offset seismic reflection data tied to five oil exploration wells, gravity and magnetic data, and plate reconstructions to propose six major tectonic stages representative for the overall opening of the Gulf of Mexico, including its north-central and southwestern, salt-covered areas: 1) **Triassic stage 1 rifting (230-190 Ma)** occurred in a southeast direction and thinned the 450 km-wide zone of transitional continental crust in the northern Gulf of Mexico; rift basins filled with red beds of the Eagle Mills Formation (Late Triassic to Earliest Jurassic); it is not clear if the Triassic rifting was continuous with later Jurassic rifting or whether there was an intervening period of no rifting; 2) **Late Jurassic stage 2 rifting (174-166 Ma)** occurred during 39 degrees of clockwise rotation of the Yucatan block from its position along the NE GOM and eastern Florida based on the re-alignment of pre-rift, Paleozoic trends seen on regional magnetic maps; rifting in the northeastern GOM is accompanied by subaerial lava flows and interbedded sediments up to 6-8 km thick characteristic of a volcanic passive margin; uplifted rift shoulders led to the formation of a breakup unconformity of latest Jurassic age; 3) **Late Jurassic stage 3 sag basin (166-163 Ma)** occurred immediately before breakup and resulted in more than 4 km of salt deposition that thins in the northeastern GOM to a thickness of 0-0.5 km; salt thickness variations were likely controlled by preexisting rift topography; 4) **Late Jurassic stage 4 separation and formation of 6-8-km-thick oceanic crust**; fracture

zones and arcuate spreading ridges visible on gravity maps of the central GOM constrain a single and stationary pole position for Jurassic opening; seafloor spreading separating salt of the stage 3 sage basin into two salt bodies - one underlying the US Gulf coast, the other underlying the southeastern Mexican margin. Seafloor spreading ended by the earliest Cretaceous (137 Ma); 5) **Cretaceous stage 5 passive margin stage and deposition of overlying stratigraphic sections**: on the east Florida shelf over 5 km of mixed carbonate and clastic rocks accumulated while terrigenous turbidites and shallow marine carbonate rocks were deposited in the deepwater GOM; these deepwater sections overlie stage 2 rifts; 6) **Cenozoic stage 6 sediments influx stage**: on the east Florida shelf thin layer of mainly carbonate accumulated while over 10 km of terrigenous turbidites filled the deepwater GOM; these deepwater sections overlie stage 2 rifts basins and the oceanic crust.

TABLE OF CONTENTS

LIST OF TABLES

LIST OF FIGURES

CHAPTER I

1.1 Introduction to the thesis

The Gulf of Mexico basin (GOM) has been studied by many geoscientists using a variety of geologic and geophysical methods for the last century (Salvador, 1988) (Fig. 1). Despite a century of concentrated research on the geological history of GOM, there remains widespread disagreement on its tectonic origins and main stages of development for the basin (Hudec et al., 2013). The primary reason for the disagreement is the extreme thickness of the sedimentary fill of GOM which - based on its large area (2.5 million km^2) and semi-circular dimensions - has received terrigenous sediment from its northern, western, and southern quadrants since its opening in late Mesozoic times and aggrading carbonate buildups (Galloway, 2008) (Fig 1). Moreover, the fill of the basin contains thick salt deposits up to 8 km thick that act as an acoustic barrier that hampers geophysical imaging of the deeper parts of the basin that record its early opening history (Hudec et al., 2013).

The main areas of controversy involve most of the main aspects of the basin including:

1) **Tectonic setting for the opening of the GOM**. Most workers agree that the same Triassic-Jurassic rift system of the eastern coast of the USA that predated opening of the Central Atlantic also branched to northeast into the North Atlantic and to the southeast into the GOM (Olsen et al., 1997) (Fig. 1). The branch of the rift system in the GOM area was thought to have formed in the Triassic and

rifted either continuously through the late Jurassic (166 Ma) or with a pause of 27 Ma in the middle Jurassic (Hudec et al. (2013). There is disagreement about the Atlantic and GOM rifts were opening about the same poles of rotation (Klitgord, 1984). Pindell and Kennan (2009) pointed out that the GOM may have opened by: 1) a Triassic-early Jurassic period of southeastwardly opening about distant Atlantic poles: and 2) a late Jurassic period of strong rotation of the Yucatan pole about a more proximal pole. In contrast, Stern and Dickinson (2010) proposed that the GOM formed as a back-arc basin whose main influence on its initial rifting was northeast-dipping subduction zones along the Pacific margin of Mexico, rather than its direct linkage to rifts along the eastern coast of North America (Fig. 1).

2) **Volcanic vs. non-volcanic nature of rifting in the GOM.** Rifted margins are generally divided into these two categories based on the presence or absence of massive volcanic flows that accompany the early rift process (Franke, 2013). In the GOM, volcanic margins have been proposed locally for the northeastern (Imbert, 2005) and northwestern GOM (Mickus et al., 2009) but have not been observed in the Cuba area (Escalona and Yang, 2013), eastern Florida (Christeson et al., 2014), or along the Mexican margin (Rodriguez, 2009). The limited availability of refraction data has made an answer to this question especially challenging.

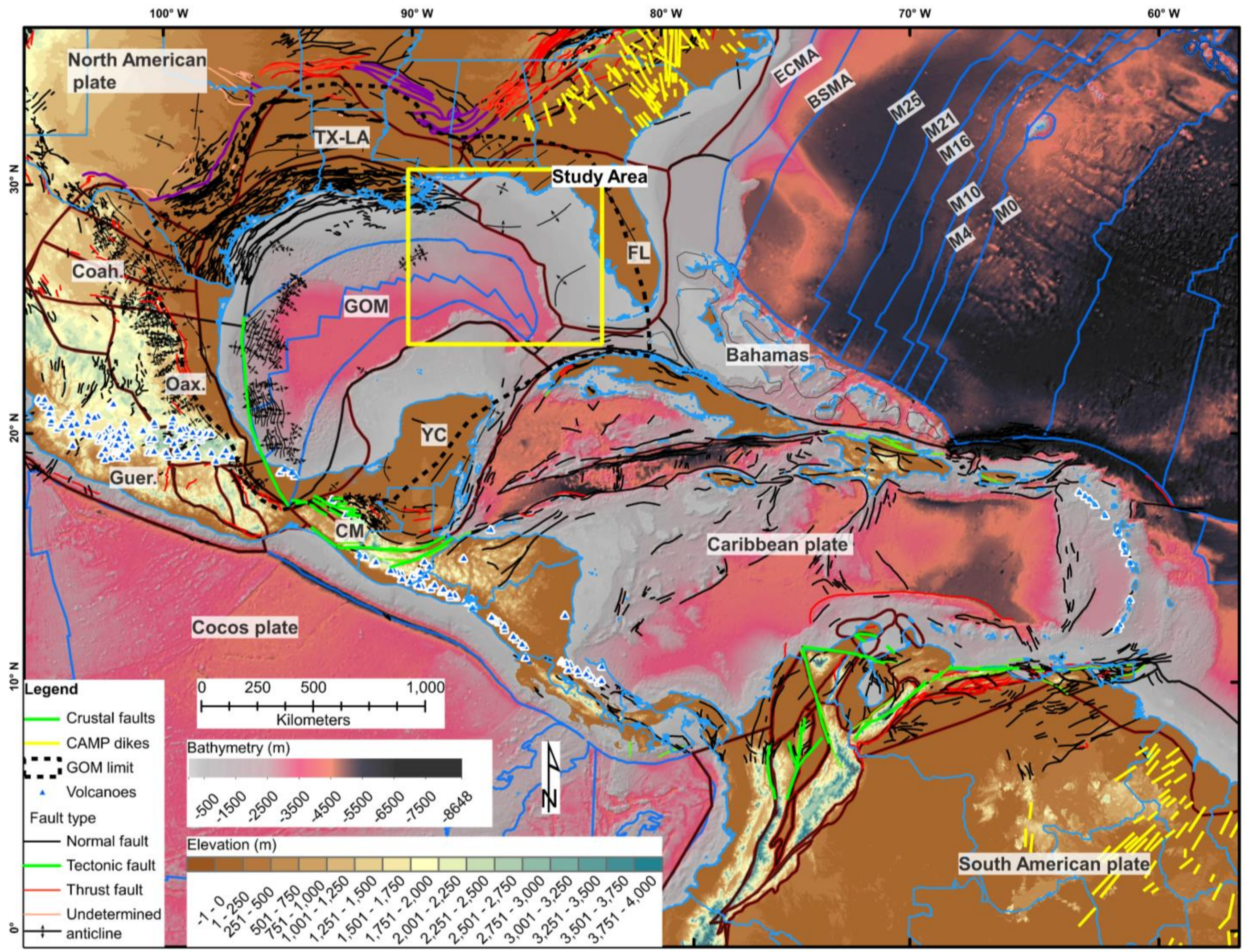

Fig. 1: Geographic setting of Gulf of Mexico and Caribbean region showing location of study area in yellow box.

3) **Tectonostratigraphic stages of GOM opening**. The immense thickness of sediments in the GOM, along with the presence of an obscuring salt layer, have made it difficult to directly relate the older Mesozoic stratigraphic units to the tectonic stages of GOM rifting, breakup, and plate separation (Galloway, 2008). In comparison to better studied rifts, these main rift stages include: 1) rifting of continental crust with the formation of rifts filled by terrigenous rocks; these types of rocks are observed in the subsurface of the northern GOM (Triassic Eagle Mills Formation, Salvador, 1988), in Mexico (Bartok, 1991), but in few other outcrop or subsurface areas around the GOM; 2) non-faulted thermal subsidence of the continental crust to form a sag basin sometimes filled with evaporites; remobilization of evaporites in the GOM from their original, evaporite parent body has made it difficult to understand the original stratigraphic position of the evaporites during their deposition during or following the Mesozoic rifting process; and 3) more regional, non-faulted thermal subsidence led to a thick terrigenous passive margin in the deep-water GOM and either carbonate or mixed carbonate-terrigenous shallow-water deposits (Galloway, 2008).

1.2 Motivation and data used in this thesis

My motivation for revisiting the many, unanswered tectonic and stratigraphic issues related to the origin and development of the GOM came about as a result of my access to state-of-art subsurface seismic data acquired in 2012 and kindly provided by Dynamic Data Services. These data - known as the Supercache dataset - were recorded to a depth of 22 seconds two-way-time - or about 40 km - using a special 2D acquisition configuration, a towed seismic cable 15 km in length, and an exceptionally large air gun source array of 9,100 cubic inches. The energy source and streamer combination provided unprecedented resolution of the deep structure of the GOM including images of the continent-ocean boundary in the northeastern and eastern GOM and the Moho of both the oceanic and thinned continental crust.

The box in Figure 1 shows a box of the area I studied using the Supercache dataset. I used only the data from the salt-free or salt-poor areas of the eastern and northeastern GOM; my area did not include the Supercache data from the thick salt area of the northern GOM (Fig. 1).

In addition to the Supercache data, I used additional datasets from my study area shown in Figure 1 that included: 1) accompanying ship-based gravity and magnetic survey from the Supercache survey along with grids of free air gravity offshore and Bouguer gravity onshore from Decade of North American Geology - or "DNAG" (1997); 2) wells data available from public sources and by purchase from the Bureau of Ocean Energy Management (BOEM); 4) radiometric ages of magmatic rocks in deep wells of Florida (Smith, 1982); and 5) ship-based gravity data acquired simultaneously with the seismic grid by Dynamic Data Services that I used to create a gravity model for the COB in the eastern GOM. For seismic to well ties and for 1-D backstripping analysis, I used publicly available well data (either at no cost or at moderate cost from BOEM) from offshore Florida, Yucatan and the northern GOM region (Fig. 1)

1.3 Personal motivation for this study

I came to begin studying geology in 2011 from a background in civil engineering based on my Bachelor of Science degree in Water Resources Engineering at the University of Dohuk in northern Iraq from 2001 to 2006. Following service as an interpreter with the 101st Airborne Division of the US Army stationed in Kurdistan, northern Iraq, during the second Gulf War in 2004-2009, I emigrated to the US and completed my MS degree in civil engineering at Norwich University in Vermont from 2009 to 2011.

During 2011 to 2012 I worked for Geofields, a midstream oil company in Houston, Texas, where I first applied my GIS and engineering skills to geosciences. After taking several classes in GIS with the University of Houston for a graduate certificate in 2011, I became more interested in geology and tectonics and the application of GIS to regional geology and petroleum exploration. From spring, 2012 to spring, 2013, I worked as a fulltime employee for the CBTH project at the University of Houston as a GIS specialist. With my MS project begun in January of 2013, I was able to enhance my geophysical experience through coursework for my MS degree in geophysics at the University of Houston and to further apply my previous GIS skills. In 2014, I was hired by Shell Oil in Houston as a GIS specialist and will begin my career with them in January, 2015.

CHAPTER II

TECTONOSTRATIGRAPHIC STAGES IN THE MESOZOIC OPENING AND SUBSIDENCE OF THE GULF OF MEXICO BASED ON DEEP-PENETRATION SEISMIC REFLECTION DATA IN THE SALT-FREE EASTERN PART OF THE BASIN

2.1. Introduction

Tectonic history of the GOM. The tectonic history of the GOM and adjacent areas of the circum-Atlantic ocean began with the late Paleozoic formation of the Pangean supercontinent when Gondwana converged on Laurentia, closed the intervening Rheic Ocean, and formed the Appalachian and Ouachita orogenic belts (Sacks and Secor, 1990) (Fig. 1). The Ouachita-Marathon-Sonora suture zone marks the northern extent of GOM basin and separates terranes with Gondwanan and Laurentian affinities (Poole et al., 2005).

Following late Paleozoic collision, the breakup of Pangea began with continuous, Late Triassic to Middle Jurassic rifting along the structural grain of the previous collisional belt in the GOM area and along the eastern coast of the USA and Canada (Hudec et al., 2013; Pindell and Kennan, 2009) (Fig. 2). Other groups including Bartok (1991) and Bird et al. (2005) proposed that this regional rifting event was not continuous but occurred as two distinct rifting episodes: a late Triassic rifting episode that pre-dated the opening of the Central Atlantic and a middle Jurassic rifting episode that predated the opening of the deepwater area of the GOM.

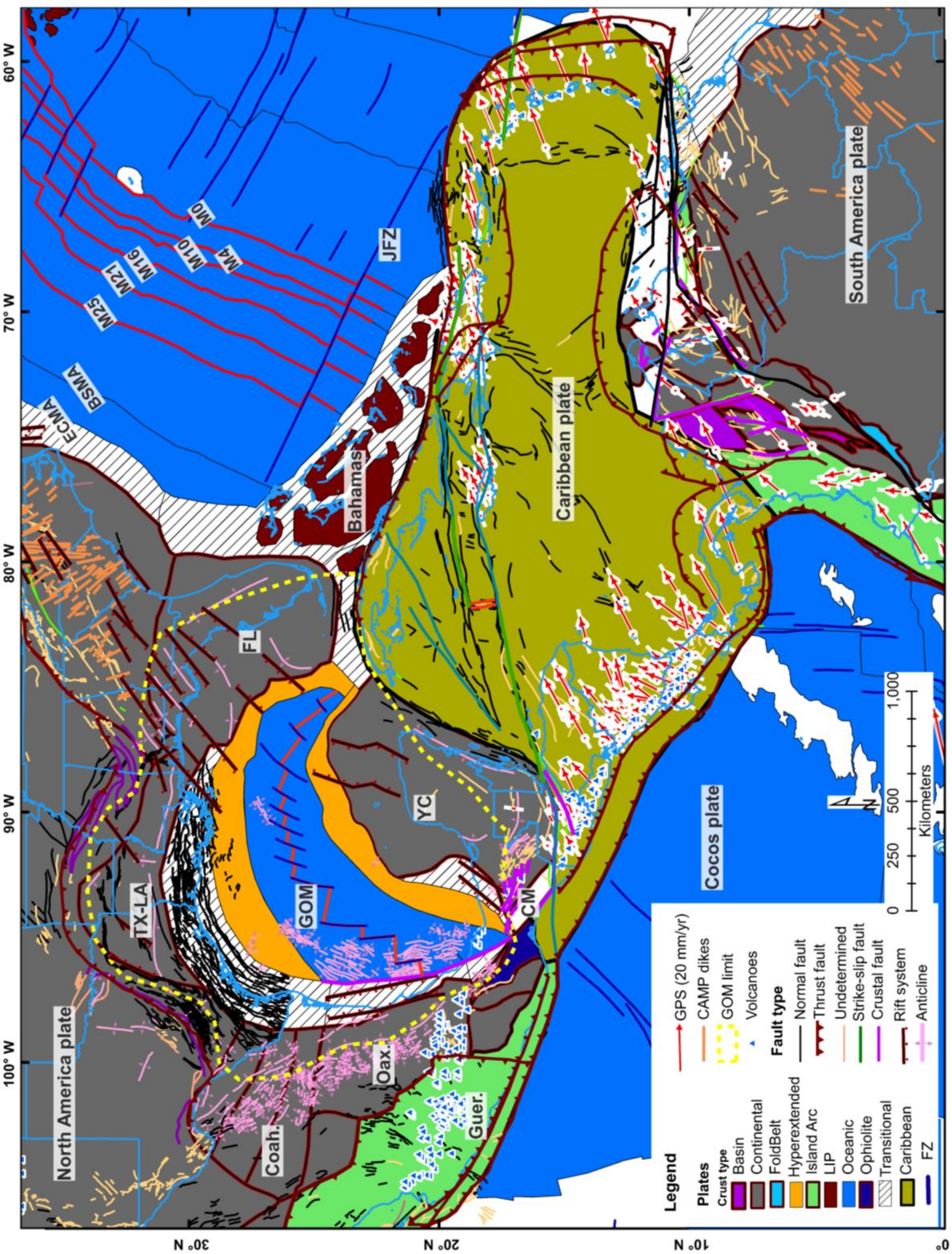
60° W
70° W
80° W
90° W
100° W
30° N
20° N
10° N
0°
North America plate
Caribbean plate
South America plate
Cocos plate
Bahamas
ECMA
BSMA
M25
M21
M16
M10
M4
M0
JFZ
FL
YC
GOM
TX-LA
Coah.
Oax
Guer.
CM
Kilometers
0
250
500
1,000
Legend
Plates
Crust type
Basin
Continental
FoldBelt
Hyperextended
Island Arc
LIP
Oceanic
Ophiolite
Transitional
Caribbean
FZ
GPS (20 mm/yr)
CAMP dikes
GOM limit
Volcanoes
Fault type
Normal fault
Thrust fault
Undetermined
Strike-slip fault
Crustal fault
Rift system
Anticline

The deepwater GOM basin is underlain by a small, oceanic basin formed during the Late Jurassic-Earliest Cretaceous as the Yucatan block rotated in a CCW direction along an arcuate seafloor spreading ridge (Hudec et al, 2013; Escalona and Yang, 2012; Pindell and Kennan, 2009 and 2007; Galloway, 2008; Bird et al, 2005; Mancini and Bucket, 2005; Jacques and Clegg, 2002; Ewing, 2001; Mancini et al, 2001; Marton and Buffler, 1994; Salvador, 1987 and 1991b, Pindell and Dewey, 1982) (Fig. 2). The oceanic crust of the deep GOM is bounded on its northern side by a 500-km-wide zone of transitional continental crust that extends beneath the continental slope and coastal plain of the North America plate of the southeastern USA (Fig. 2).

Figure 2: Tectonic setting of the GOM enclosed by dotted yellow line and Caribbean region in yellow showing crustal types ranging in thickness from normal continental crust (gray) to hyperextended continental crust rimming the GOM with crustal thicknesses as thin as 1 km near the GOM continent-ocean boundary (COB). Stretched continental crust in white extends from the present-day GOM shoreline of Louisiana and Texas for 200 km landward into the southern USA. Accreted terranes in green include the Guerrero island arc terrane of Mexico and accreted Caribbean oceanic plateau terranes in northwestern South America. Central Atlantic Magmatic Province (CAMP) dikes cover larges areas along the east coast of North America and Venezuela and are interbedded with exposed Late Triassic redbeds. Undifferentiated late Triassic to Middle Jurassic rift systems along the east coast of North America and the northern margin of the South American plate are shown with red lines. Red lines show Cretaceous magnetic anomalies in the central Atlantic Ocean. Subduction of Cocos plate beneath Mexico and Central America has created a chain of active arc volcanoes. The Caribbean area is simplified as a single crustal block and is not discussed in this thesis. Eastward motion of the Caribbean plate relative to North America and the GOM is shown by arrows. Abbreviations of blocks include: **Coah** = Coahuila block; **Oax** = Oaxaquia block; **TX-LA** = Texas-Louisiana block; **CM** = Chiapas Massif; and **FL** = Florida block. Other important structural features of the Atlantic crust include: **ECMA** = East Coast Magnetic Anomaly; **BSMA** = Blake Spur Magnetic Anomaly; and **JFZ** = Jacksonville fracture zone. All block names are modified from Bartok et al. (in press).

Marton and Buffler (1994) and Galloway (2008) proposed that Mesozoic thinning of the continental crust beneath the northern GOM occurred as the result of asymmetrical rifting between the rotating Yucatan block and North American plate, which allowed as much as 20 km of evaporites and clastic sedimentary rocks to infill the area of the continental slope and shelf in the US GOM. (Fig. 2). The precise timing of the end of seafloor spreading and the rotation of the Yucatan block in the GOM is uncertain. Galloway (2008) proposed the end of GOM opening by the earliest Cretaceous (~137 Ma), Hudec et al. (2013) proposed seafloor spreading ended between 149-137 Ma, while Pindell and Kennan (2009) proposed an end between158-130 Ma (Table 1).

Following the cessation of rifting and oceanic spreading of the deep GOM by the earliest Cretaceous, the GOM subsided as a passive margin on its eastern, southern, and northern flanks, but remained bounded by an active subduction and collisional margin in Mexico throughout the Cretaceous and Cenozoic (Galloway, 2008). On its eastern edge, the GOM is bounded by Florida block that has been the site of carbonate accumulation since Late Jurassic (Salvador, 1987). Along its Mexican margin the GOM is bounded by pre-Mesozoic continental terranes that include Coahuila, Oaxaquia, and Yucatan (shown in brown on Figure 2) and post-Mesozoic accreted terranes that include the Guerrero terrane (shown in green on Figure 2) (Bartok et al., in press; Centeno-Garcia et al., 2008).

Author	Basin evolution sequence	Magma involvement	Exhumed mantle	Timing of salt deposition	Phase I: Triassic rifting	Phase II: Jurassic rifting	Phase I extension direction	Phase II extension direction	Drifting phase	Pole of Rotation	Seafloor propagation
Christeson et al., 2014	Rifting II> Breakup > Drifting	Increased magmatic input during the rifting process	No	NA	240-210 Ma	NA	NA	NA	(~152–155 Ma) to (~138–142 Ma)	NA	West to east
Eddy et al., 2014	Rifting>breakup>SDRs>Drifting	Magma rich and SDRs	No	NA	230-210 Ma	NA	NA	NA	~158-140 Ma	Na	
Pindell and Horn, 2014	Rifting and stretching > Outer margin collapse and salt deposition > Breakup> Drifting	Magma poor	Yes	Rapid salt deposition (~3Ma)	Undifferentiated rifting phases: Late Triassic to Middle Jurassic		NW-SE in central GOM; NE-SW in eastern GOM		Earliest Cretaceous	Pole migration southward	West to east
Hudec etal, 2013	Rifting > Salt deposition (163 to 161Ma) > Further extension for 12 Ma (161 Ma - 154 Ma)> Breakup (154 Ma) > drifting	NA	No	Callovian (~163 - 161 Ma)	210-163 Ma	210-163 Ma	NE-SE with extension of 200-250 km	NA	154-149 Ma to 137 Ma	NA	East to the west
Johnson and Kneller, 2011	Triassic rifting > Jurassic rifting > Breakup > Drifting	NA	No	NA	240-220	176- 163	NW-SE direction then CCW rotation	Transtensional between Yucatan and Florida	163-154	NA	NA
Pindell and Kennan, 2009	Rifting > Salt deposition > Drifting	NA	NA	NA	Undifferentiated rifting phase:(190 - 158 Ma)		Southeastward direction with probable minor counter-clockwise rotation		154-130	Fixed pole; southeast GOM	NA
Galloway, 2008	Rifting > Salt deposition> Breakup > Drifting	Magma rich and SDRs	NA	168-158 Ma	Undifferentiated rifting phases: Middle to Late Jurassic		NA	NA	158-137	NA	NA

Table 1: Phases and timing of GOM evolution based on a compilation of previous studies.

To the south of the GOM, the Caribbean area has remained tectonically active during the Cretaceous to recent passive margin phase of the GOM. The presence of the Yucatan block acted as a barrier that isolated the GOM from the effects of the Caribbean deformation in all areas except for the southeastern GOM near Cuba (Escalona and Yang, 2013) (Fig 2).

One of the main motivations for studies of the GOM including this thesis is to better understand the relation of hydrocarbons to the rift and passive margin phases of the basin. Most large discoveries have been in the area of the Texas-Louisiana-Alabama coastlines and not along the Florida margin (Fig. 3). This pattern of hydrocarbons reflects the long-term governmental moratorium on offshore drilling in the Florida area for environmental reasons, but also reflects major differences in the basin geology including the lesser amounts of in situ and remobilized Jurassic age salt, an important hydrocarbon seal in the Florida area.

Objectives of this chapter. Objectives include: 1) use the grid of deep-penetration 2D seismic and gravity data to map the COB in the eastern and northeastern GOM; 2) use this newly mapped COB of the GOM for an improved tectonic closure of the entire basin along with an improve understanding in the rifting, breakup and separation process, how these events affected the basin stratigraphy, and whether these processes were accompanied by abundant volcanism or not; and 3) compare my observations on the COB and spreading ridge locations using seismic and gravity data with satellite gravity observations from Sandwell et al. (2014).

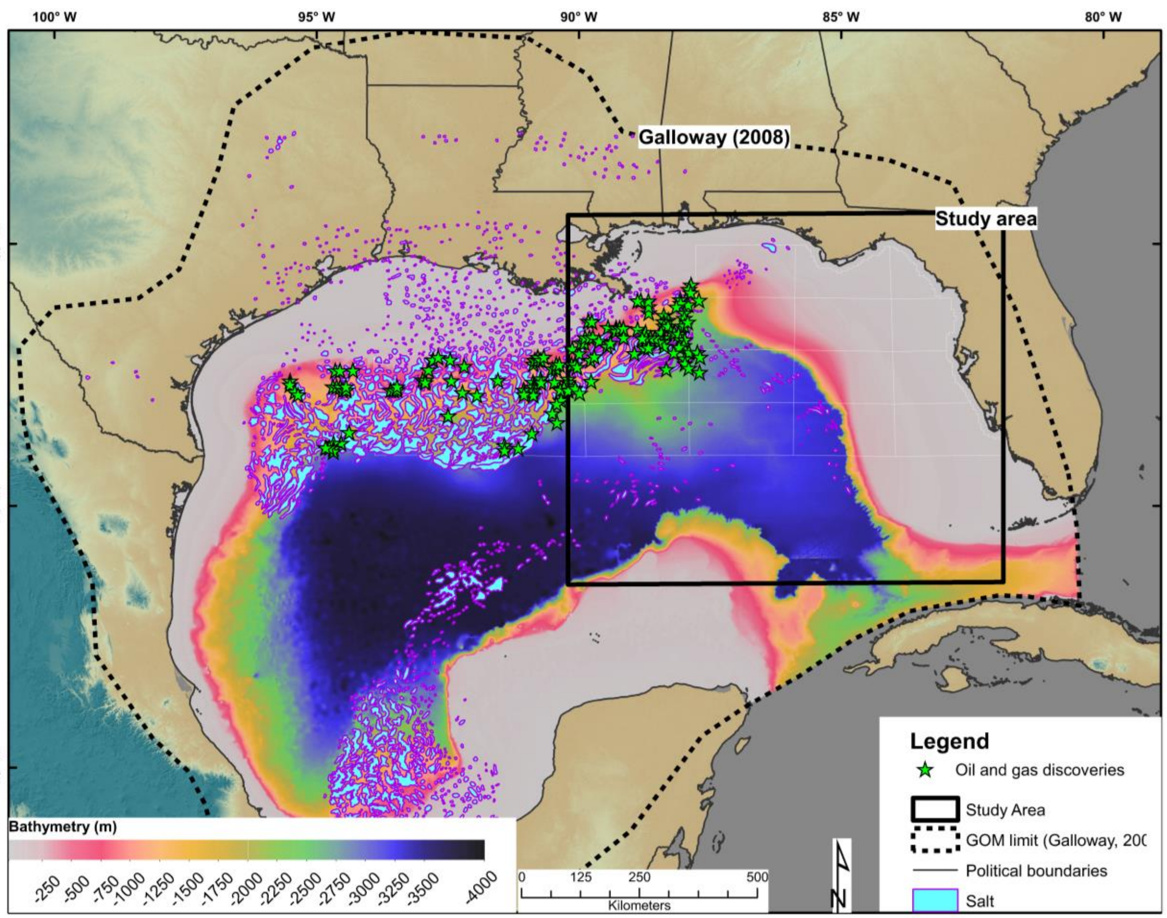

Figure 3: Map of GOM region showing location of study area in black box, salt distribution in cyan polygons, and giant oil and gas discoveries (green stars) from Bureau of Ocean Energy Management (BOEM). The eastern and northeastern GOM were selected for this thesis study because these margins of the GOM have minimal amounts of salt that allows for improved subsurface imaging of the early GOM rift history. Jurassic hydrocarbon plays in NE GOM are prolific and provide an additional incentive for understanding this early GOM rift history.

2.2. Previous models for the opening of the Gulf of Mexico

2.2.1. Summary of previously proposed timing of opening stages

Key stages in previous models are summarized in Table 1, including models by: Christeson et al. (2014), Pindell and Horn (2014), Hudec et al. (2013), Johnson and Kneller (2011), Pindell and Keenan (2009) and Galloway (2008). Each of these models makes different predictions about ages and sequence of major stages. Some propose that the rifting occurred in two phases: an earlier Triassic phase and a younger Jurassic one (Christeson et al., 2014; Johnson and Kneller, 2011; Bartok, 1991), or occurred as a continuous rifting episode from Late Triassic to Middle Jurassic. (Pindell and Horn, 2014; Hudec et al, 2013; Pindell and Kennan, 2009). Whether the two rifting phases were discrete or continuous is unclear given the data presently available on the deeper stratigraphy of the GOM.

Most previous workers agree that oceanic crust formation began soon after the continental breakup between Yucatan and North America with opening initiated by Middle Jurassic (166 Ma to 152 Ma) and completed during the earliest Cretaceous (142 – 130 Ma). Christeson et al. (2014) and Pindell and Horn (2014) proposed a west-to-east propagation of the spreading ridge to explain the shape of the basin (Table 1).

In this thesis, I followed the two-state GOM opening model because the cessation of rifting is different: Late Triassic rifting ended with the opening of central Atlantic at ~190 Ma (Withjack, et al, 2012), while Middle Jurassic rifting ended with opening of

GOM basin at ~163 Ma. There is no concrete evidence showing the rifting continued for the 30 million year period that separated the two rifting events.

2.2.2. Timing and role of salt in the opening of the GOM basin

Thick salt was deposited prior to continental breakup in the accommodation space formed by previous rifting episodes and subsequent rapid subsidence. The thickest salt (3-5 km) was deposited rapidly during relatively short time (~1 to 3 Ma) in the center of the basin (Fig. 3) (Hudec et al., 2013; Pindell and Kennan, 2009; Salvador, 1987) forming the central salt provinces of Luann in the North and Campeche in the south. A thin layer of salt was also deposited in basement lows in the Rio Grande embayment, Houston embayment salt basin, south Louisiana salt basin, and Desoto Canyon salt basin. (Fig. 3).

2.2.3. Timing and role of volcanism in the opening of the GOM basin

Igneous activity is deeply buried and poorly imaged, so its age and presence remains controversial. Refraction studies by Eddy et al. (2014), Christeson et al. (2014); Mickus et al. (2009), and Imbert (2005) suggests that the northeastern GOM was a volcanic margin characterized by extensive syn-rift magmatism in the form of seaward dipping reflectors (SDRs) and continental basalt flows.

The eastern and northern GOM has also been interpreted as a magma-poor or non-volcanic margin where mantle was exhumed during the opening. (Pindell and Horn, 2014) The timing of magmatism relative to the stages of rifting, breakup, and separation is not clear, largely due to imaging problems.

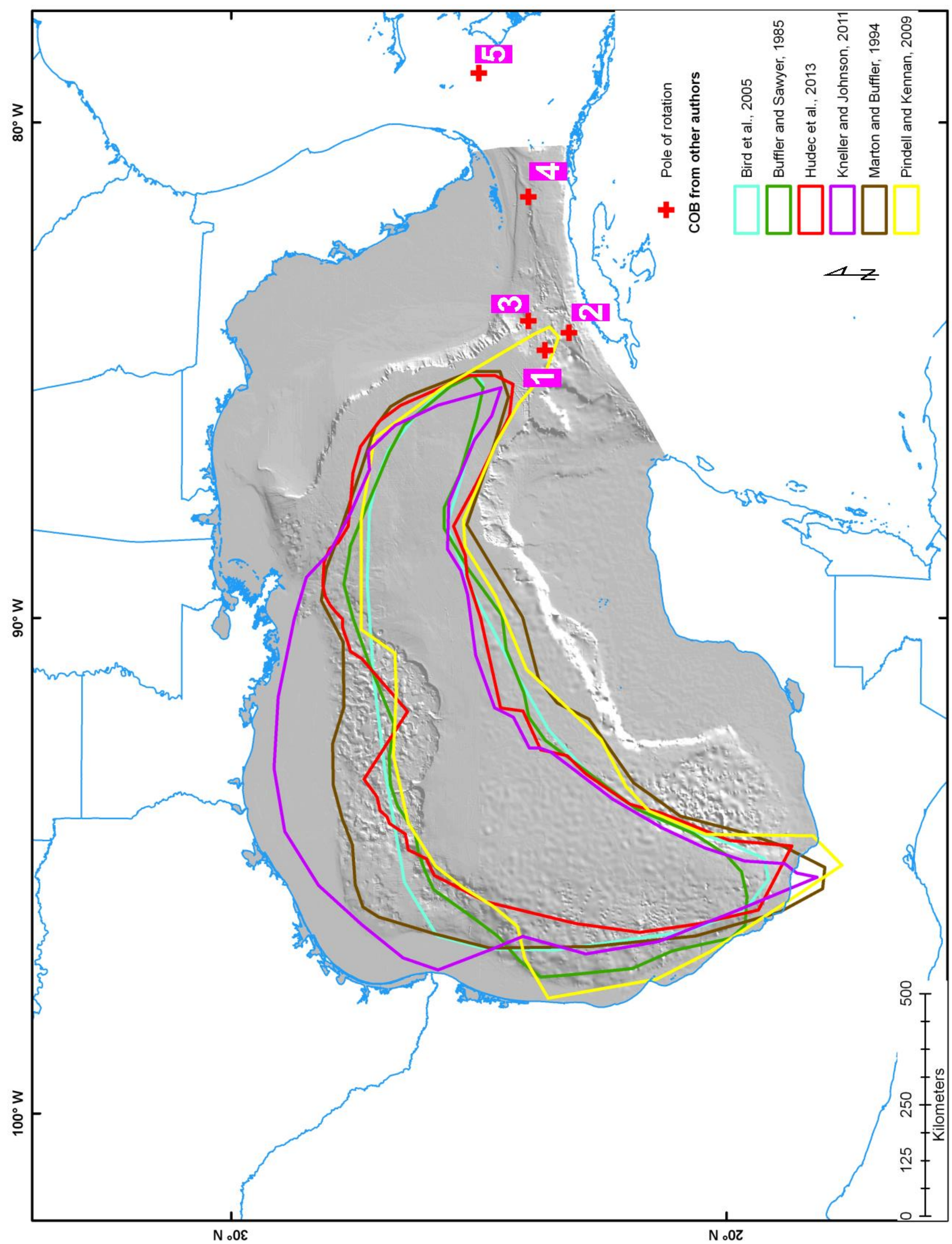
80° W
90° W
100° W
30° N
20° N
Pole of rotation
COB from other authors
Bird et al., 2005
Buffler and Sawyer, 1985
Hudec et al., 2013
Kneller and Johnson, 2011
Marton and Buffler, 1994
Pindell and Kennan, 2009
1
2
3
4
5
N
0
125
250
500
Kilometers

2.2.4. Shape of oceanic crust in the GOM and its constraints on basin opening

The tectonic controls of the rotational history of the Yucatan block on the shape of the oceanic crust in the deep GOM has been described by many previous workers and is summarized on Figure 4 and Table 1. Most workers are in broad agreement on the extent of the oceanic crust except for Johnson and Kneller (2011) and Marton and Baffler (1994) who both propose a much larger oceanic basin that extents to near the southern shoreline of the USA.

Figure 4: Regional map of GOM showing proposed locations of the continent-ocean boundary (COB) separating oceanic crust of the central GOM from thinned crust around the basin margins. Most models use refraction or gravity model and all models converge on the same general shape of the GOM oceanic crust area. The most diverging model is that of Kneller and Johnson (2011) who infer oceanic crust underlying most of the northern GOM. Multiple poles of rotation have been proposed for the opening of the oceanic crust in the center of the GOM: Pindell and Kennan (2009) = 1; Shepherd (1983) = 2; and Marton and Buffler (1994) = 3. These first three poles are located in the deep water Straits of Florida, whereas poles of Hall and Najmuddin (1994) = 4 and Dunbar and Sawyer (1987) = 5 are located in the area northeast of Cuba.

Early attempts to map the COB were largely based on potential field data (Bird et al, 2005; Hall and Najmuddin, 1994) with the extent of the oceanic crust in the GOM following roughly the central free-air gravity high. Deep-penetration seismic reflection data (Pindell and Horn, 2014; Hudec et al, 2013) and tomographic studies using passive seismic data (Eddy et al. 2014) have been also used to propose refinements in the location of the COB in the GOM.

Proposed locations for pole of rotation for the Yucatan block can be grouped to two groups: 1) a stationary pole of rotation located in the deepwater area of the southeastern GOM in the Straits of Florida (Pindell and Kennan, 2009; Marton and Buffler, 1994; Hall and Najmuddin, 1994), or 2) a migrating pole of rotation during basin opening (Pindell, 2014).

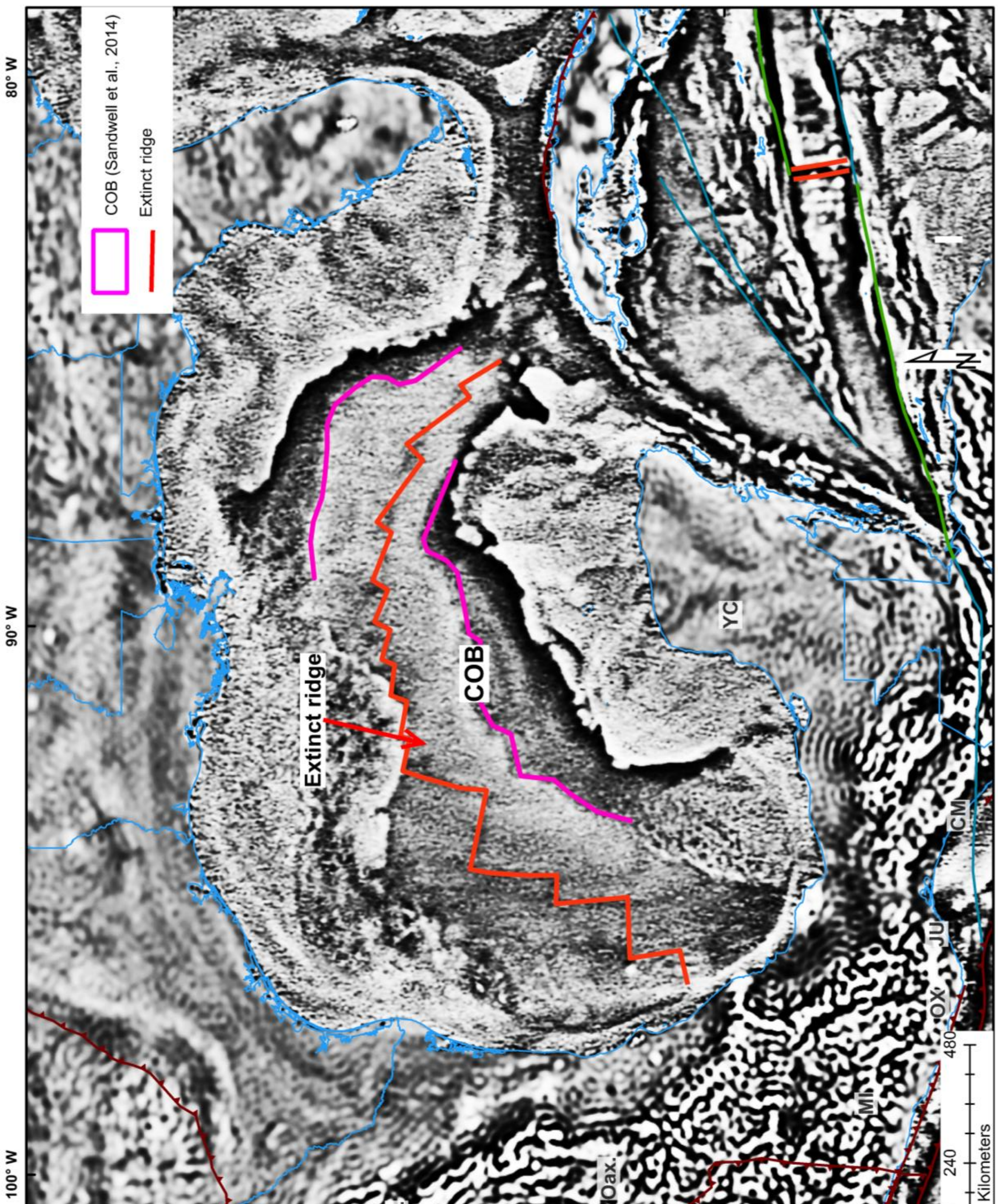
COB (Sandwell et al., 2014)
Extinct ridge
80° W
90° W
100° W
30° N
20° N
Extinct ridge
COB
YC
CM
JU
OX
MI
Oax.
Coah.
Guer.
0
120
240
480
Kilometers
N

2.2.5. High-resolution gravity image of GOM by Sandwell et al. (2014)

Sandwell et al. (2014) proposed a modified locations of the COB and spreading ridge in GOM based on a new vertical gradient of gravity (VGG) grid with spatial resolution twice that of previous, publicly available gravity datasets from the late 1990’s (Fig. 5). The new radar altimeter measurements merged gravity data from CryoSat-2 and Jason-1 the satellites with existing ship-based data. The COB of the GOM is marked by high amplitude of VGG across the eastern and southern margin. The northern margin of the GOM is obscured by salt and the salt-flow front of the Sigsbee escarpment.

The Sandwell et al. (2014) VGG map provides a useful regional framework for seeing the COBs and central spreading ridge on a regional scale and confirms previous rotational models for Yucatan summarized on Figure 4 by the circular shape of the fractures zone and the arcuate shape of the extinct spreading center (Fig. 5). I make frequent use of the Sandwell et al. (2014) map in this thesis to place the reflection and gravity profiles from the Dynamic data set into a regional framework.

Figure 5: Vertical gradient of gravity map by Sandwell et al. (2014) showing their inferred positions of the COB and extinct, Mesozoic spreading center of the GOM. The vertical gravity gradient (VGG) image precisely outlines the arcuate shape of the extinct, Jurassic spreading ridges and circular shape of the fracture zones that have long been speculated on by previous authors. According to Sandwell et al. (2014), the COB is marked by the high-amplitude gravity anomaly along the eastern and southern GOM margin. The COB of the northern GOM is obscured by remobilized salt that forms a southward-protruding salient along the Sigsbee escarpment.

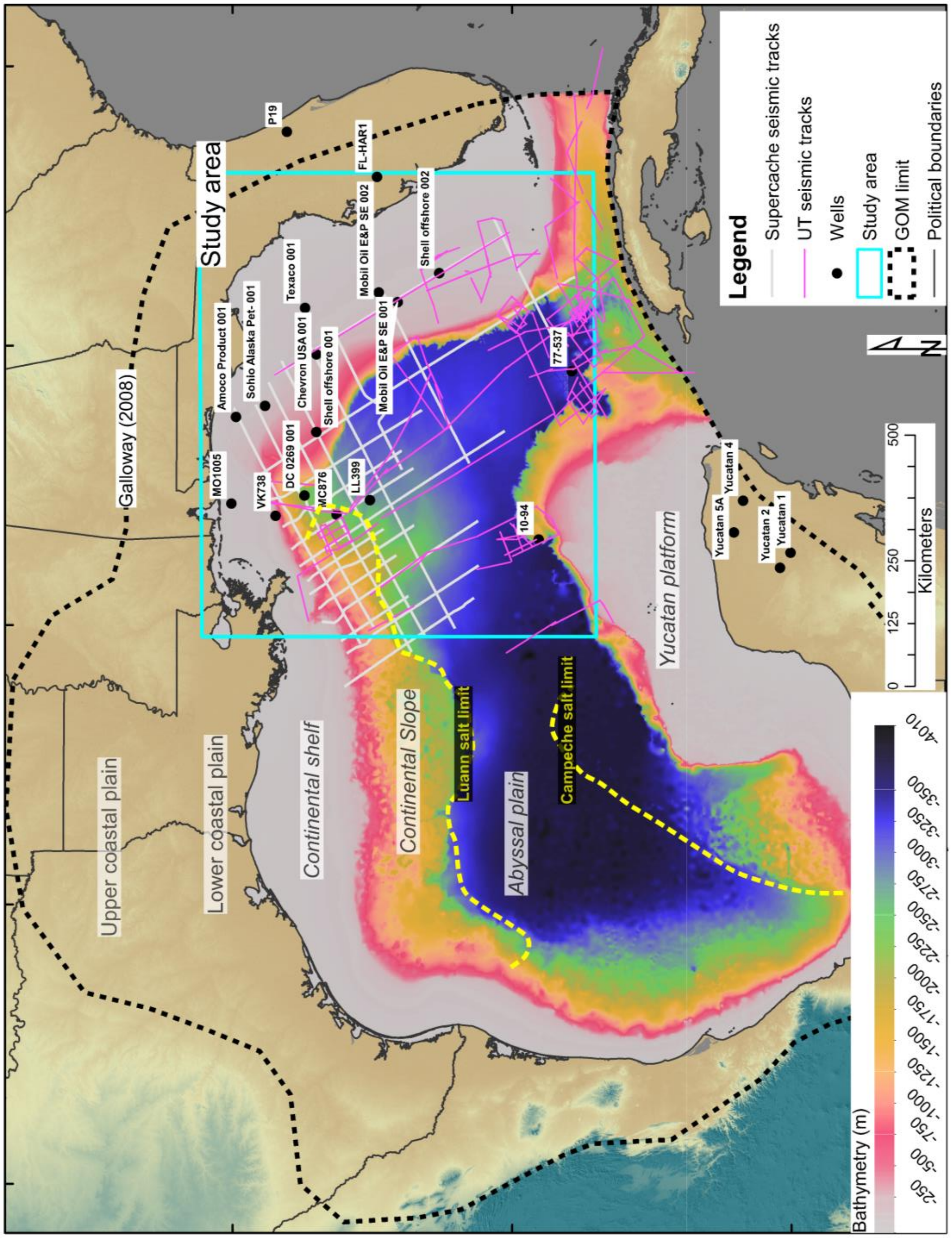
Legend
Supercache seismic tracks
UT seismic tracks
Wells
Study area
GOM limit
Political boundaries
Study area
Galloway (2008)
Upper coastal plain
Lower coastal plain
Continental shelf
Continental Slope
Abyssal plain
Yucatan platform
Luann salt limit
Campeche salt limit
Bathymetry (m)
Kilometers
0
125
250
500
80° W
85° W
90° W
95° W
100° W
30° N
25° N
20° N
P19
FL-HAR1
Shell offshore 002
Mobil Oil E&P SE 002
Mobil Oil E&P SE 001
Texaco 001
Amoco Product 001
Sohio Alaska Pet- 001
Chevron USA 001
Shell offshore 001
MO1005
VK738
DC 0269 001
MC876
LL399
77-537
10-94
Yucatan 5A
Yucatan 4
Yucatan 2
Yucatan 1
-250
-500
-750
-1000
-1250
-1500
-1750
-2000
-2250
-2500
-2750
-3000
-3250
-3500
-4010

2.3. Dataset used and methodology

In this thesis, I integrated the grid of Supercache data with academic seismic lines from the University of Texas at Austin and 20 deep exploration wells on Florida platform, Yucatan platform and deepwater GOM. (Fig. 6). For plate reconstructions, I used the Decade of North America magnetic grid (DNAG) (1989).

For gravity modeling, I used ship-based gravity data acquired simultaneously with the seismic grid by Dynamic. For seismic to well ties and for 1-D backstripping analysis, I used publicly available well data from the US Bureau of Ocean and Energy Management (BOEM) from offshore Florida, Yucatan and the northern GOM region (Fig. 2).

Figure 6: Regional topography and bathymetry map of the GOM showing 17,000 km of 2D, deep-penetration seismic reflection data from Dynamic Data Services that I used in the boxed area of the eastern and northeastern GOM that is known commercially as “Supercache” (gray lines). Other data included the ship-borne gravity and magnetic surveys collected during the Supercache survey, 1970’s vintage seismic lines from UTIG (purple lines), and a suite of exploration wells compiled for this study (black dots).

I followed a standard workflow for interpretation that includes: 1) digitizing well logs obtained from the BOEM and performed seismic well tie for two exploration wells (Shell 001 and Chevron 001); 2) interpreting seismic lines and mapping of the major horizons: top of basement (breakup unconformity) and base of crust (Moho) reflector; Valanginian unconformity; Earliest Cretaceous (Albian); and KT boundary; 3) mapping of basement step-up marking the COB based on subsurface observations on the seismic lines and forward gravity modeling; 4) performing well correlation for two wells sections; an east-west section and a north-south section; 5) performing 1-D backstripping analysis to unravel burial history at three distinct tectonic settings in the study area for three deep exploration wells (LL 399, Shell 001, and Chevron 001); 6) using the mapped COB boundary for plate reconstructions at the following time steps: 200, 174, 163, 154, 147 and 137 Ma; and 7) integrating all of these data to divide GOM basin evolution into six major phases: Late Triassic rifting (not visible on data from my study area), Middle Jurassic rifting, Callovian salt deposition, seafloor spreading, passive margin phase 1, and passive margin phase 2.

2.4. Gravity modeling of the COB in the less salt area of the EGOM

Ship-borne, free-air gravity data acquired during the Supercache seismic survey was used for simple 2D forward gravity modeling for an east-west-striking, 800-km-long transect across the Florida platform, the rifted margin along the eastern GOM, and the deep abyssal plain of the GOM (Fig. 7). The objective of this model was to map crustal boundaries and types including the exact location of the COB.

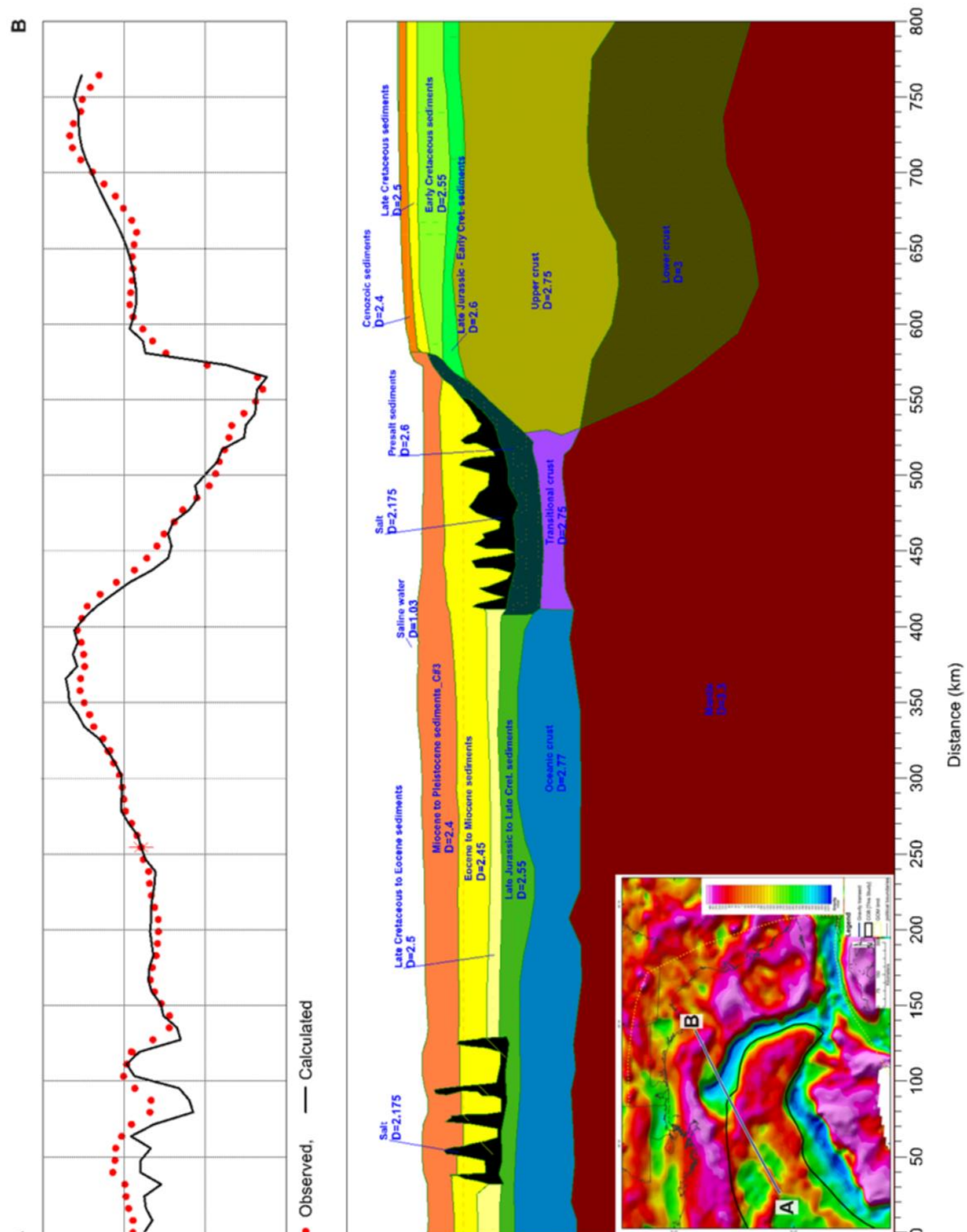

A.
B.
A
B
Gravity (mGal)
50
0
-50
-100
Observed,
Calculated
Depth (km)
0
10
20
30
40
50
Distance (km)
0
50
100
150
200
250
300
350
400
450
500
550
600
650
700
750
800
Salt
D=2.175
Late Cretaceous to Eocene sediments
D=2.5
Miocene to Pleistocene sediments_C#3
D=2.4
Eocene to Miocene sediments
D=2.45
Late Jurassic to Late Cret. sediments
D=2.55
Oceanic crust
D=2.77
Saline water
D=1.03
Salt
D=2.175
Presalt sediments
D=2.6
Transitional crust
D=2.75
Cenozoic sediments
D=2.4
Late Cretaceous sediments
D=2.5
Early Cretaceous sediments
D=2.55
Late Jurassic - Early Cret. sediments
D=2.6
Upper crust
D=2.75
Lower crust
D=3

Observations from a Supercache seismic line converted to depth along the modeled transect were used to control the geometry of the different stratigraphic and crustal units. These horizons taken from the seismic lines included the oceanic Moho, the top of basement, the tops of Early Cretaceous (Albian) and Late Cretaceous (Maestrichtian), the top of Eocene, the top of Miocene and the seafloor top. For the crust beneath the Florida platform, no confirmed picks of the Moho were possible. Standard density values for different crustal units used are based on Bird et al. (2005) and are indicated on the profile in Figure 7.

The gravity model in Figure 7 suggests a normal, 6-8-km-thick, oceanic crust inboard (east) of the edge of central gravity high in the GOM and a ~120-km-wide, rifted margin with a crustal thickness of ~5-km. The crust beneath Florida predicted in this model for this area is of normal continental thickness with only a possibility of minor stretching during the Middle Jurassic phase II rift phase as proposed by previous workers and in this thesis (Table 1).

Figure 7: **A.** Observed and calculated gravity transect along line A-B in the eastern GOM. Inset shows location of the gravity line. **B.** Interpreted gravity transect showing west-to-east transition from 6-8-km-thick oceanic crust of the central GOM that is shown in blue, across a Jurassic rift structure with a crustal thickness of about 5 km, to normal oceanic crust underlying the Florida platform with a crustal thickness of 30-35 km. The gravity peak east and north of the linear gravity anomaly reflects the presence of the basement step-up that most workers agree corresponds to the COB (Bird et al., 2005; Hudec et al., 2013). The rapid increase in gravity amplitude east of the linear gravity anomaly is an edge affect related to the thick, Florida carbonate shelf (Bird et al., 2005).

2.5. Interpretation of two long seismic transects in lesser-salt areas of the eastern GOM

2.5.1 Line 8 seismic interpretation

Line 8 is 160 km-long and crosses the less-salt window from oceanic crust of the deep, central GOM to the shoreline of western Florida (Fig. 9). Line 9 is a strike line, 375 km long, and extending from the southernmost edge of Mississippi fan to the Florida platform ~100 km seaward of the Florida shelf edge (Fig. 10). This line crosses Jurassic oceanic crust of the central GOM to the continental block of Florida. Because of the lack of the salt layer, this line shows well the transition from the GOM oceanic crust to thinned continental crust along western Florida.

2.5.1.1 Line 8 age picks

The top basement pick on this line and the other Supercache seismic reflection lines corresponds to the top of oceanic crust and to the correlative breakup unconformity on continental crust. On oceanic crust, the age of top basement is inferred to be the same age as initial seafloor spreading ranging from 163 Ma near the COB to 137 Ma near the extinct spreading center in the deep GOM basin. The top of oceanic basement is nearly flat at a depth of 9 to 10 km with smaller-scale basement highs and lows likely produced as spreading fabric at the slowly spreading ridge during late Jurassic opening (R. Pascoe, personal communication, 2014). Alternatively, Pindell and Horn (2014) attributed this undulating surface of the top oceanic basement to a scarce supply of magma during generation of the oceanic crust produced in the setting of a non-volcanic margin.

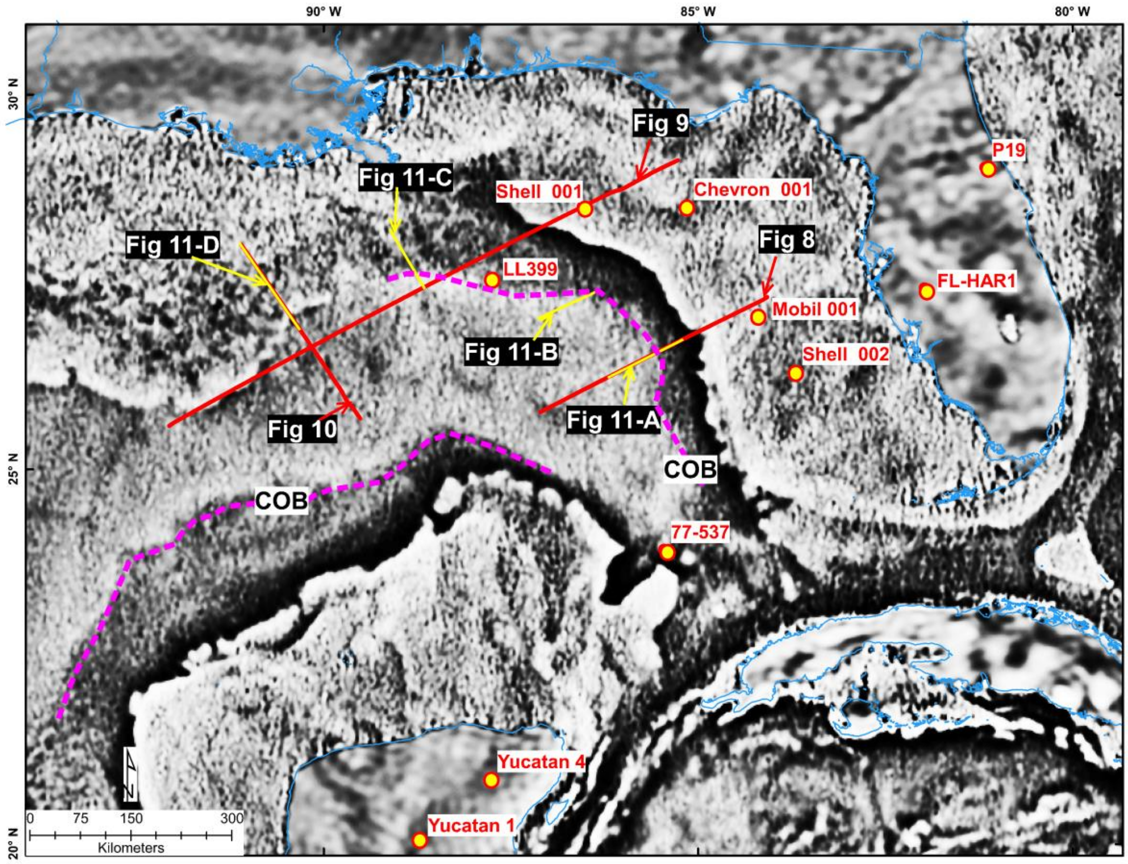

Figure 8: Location map for seismic and well data used in this thesis using the Sandwell et al. (2014) VGG image of the GOM. See text for discussion.

The top of basement and Moho in the area of the rifted continental crust is less continuous and less evident on Line 8 (Fig. 9). The character of the seismic reflectors change at depth of ~ 10 km along the 80-km width of the rifted margin with “chaotic” reflectivity within the syn-rift section overlying the top basement reflector and a more homogenous and layered signature within the basement itself (Fig. 9). The top reflector of continental basement (also termed the breakup unconformity) is also nearly flat on the shelf at a depth of 5.5 km. t0 6) km. The age of breakup unconformity is inferred to be late Jurassic: 170 to 163 Ma (Table 1).

The top of the synrift phase can be mapped along the 80-km wide rifted margin of western Florida. This pick divides the overlying flat-lying strata of the post-rift phase from the underlying synrift strata that are chaotic and lack stratification (Fig. 9).

The top Albian pick (~100 Ma) is assumed in this thesis to be equivalent to the Mid-Cenomanian unconformity that has been described by previous authors in the northeast GOM (Buffler et al. 1980; Wu et al. 1990) (Fig. 9). The updated age for this unconformity is based on micropaleontological work contained in BOEM well reports (Fig. 8).

Figure 9. (next page) A. Uninterpreted regional Dynamic Data Services seismic reflection line 8 showing tectonic transition from oceanic crust of the central GOM to continental crust underlying the Florida platform 160 km to the east. **B.** Interpreted line 8 showing: 1) nearly flat top of GOM oceanic basement at a depth of 8.5 to 9.5 seconds TWT (9.0 to 10.0 km); 2) hummocky topography of top of oceanic crust surface likely reflects high-relief of oceanic crust produced at slow spreading rates at the Mesozoic ridge; 3) top of continental basement beneath the shelf is smoother at a depth of 3.75 to 4.0 seconds TWT (5.5 to 6 km); 4) syn-rift pick divides the overlaying flat strata of post-rift phase from the underlying syn-rift strata that are chaotic and lack stratification; 4) Cretaceous-Tertiary (KT) boundary is continuous throughout GOM deep basin and northeast shelf with a strong reflection contrast especially in deepwater GOM; 5) Cretaceous passive margin strata predating the KT boundary are relatively flat and depositional in nature that thickens from less than 0.5 km1 second two way time near the extinct spreading center to ~1.5 second two way time 2.5 km near COB; 6) Cenozoic terrigenous packages of the Mississippi fan thicken toward the central GOM; 7) the Moho pick for the base of the GOM oceanic crust is semi-continuous and flat at a depth of ~9 seconds TWT(~16 km); and 8) the basement step-up at a depth of ~1 (1.5 km) marks the limit of the oceanic crust.

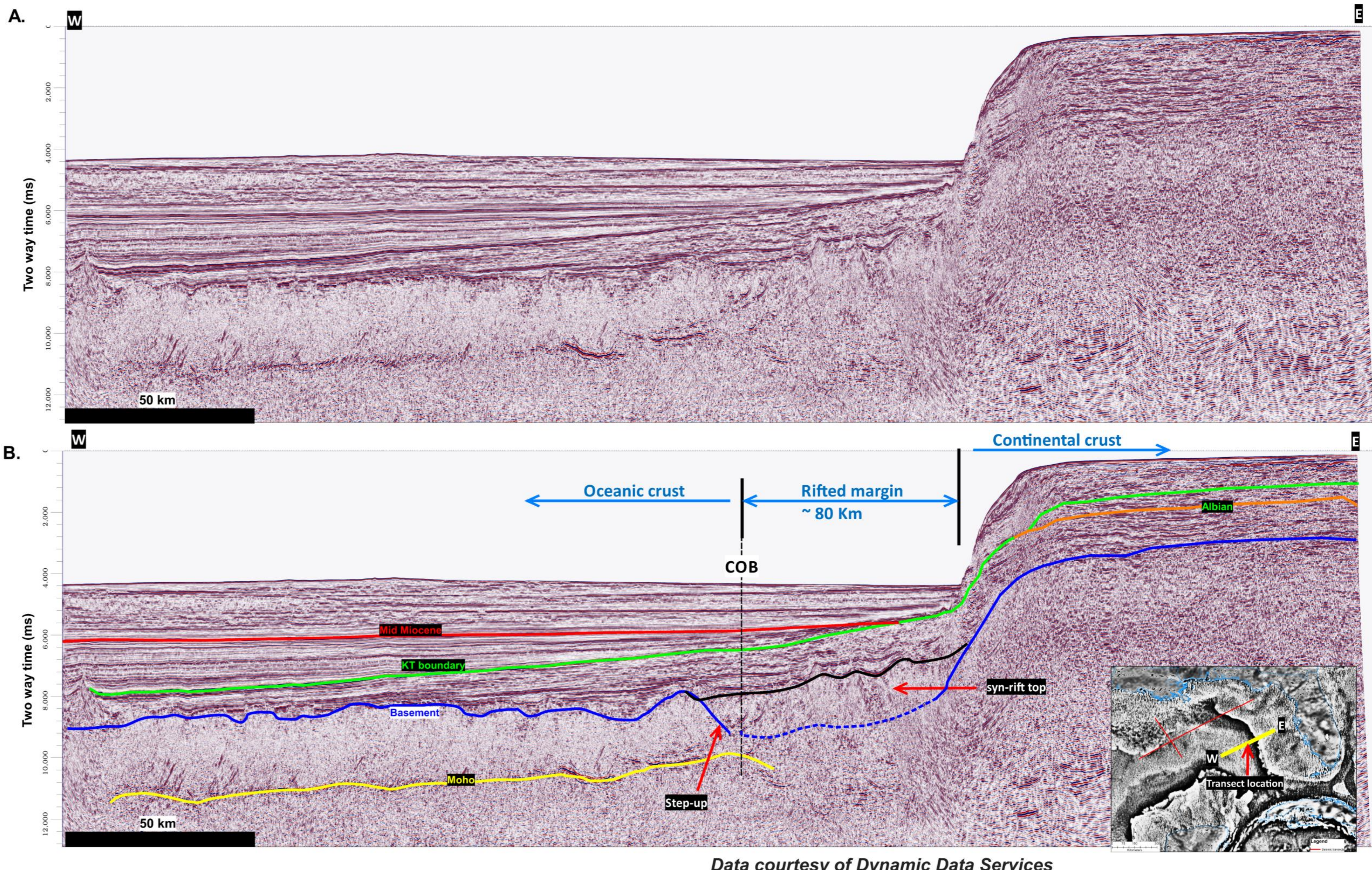
A.
W
E
Two way time (ms)
50 km
B.
W
E
Continental crust
Oceanic crust
Rifted margin
~ 80 Km
COB
Albian
Mid Miocene
KT boundary
Basement
syn-rift top
Moho
Step-up
50 km
Transect location
Data courtesy of Dynamic Data Services

Figure 9

The Cretaceous-Tertiary (KT) boundary forms a continuous surface throughout the deep basin of the GOM and the northeastern shelf shows a strong reflection contrast especially in deepwater GOM presumably as the result of submarine flows following the Chicxulub impact (Galloway, 2008) (Fig. 9). The age of this pick is ~66 Ma and similar to what has been proposed in recent stratigraphic and biostratigraphic studies by several groups (Galloway, 2008; Kruge et al., 1994). Strata predating the KT boundary are relatively flat and depositional in nature that thicken from less than 1 second TWT (~0.5 km) near the extinct spreading center to ~1.5 second TWT (2.5 km) near the COB.

Cenozoic sediment packages thicken toward the central GOM as a result of sediment influx of Mississippi fan (Fig. 9). Accommodation space on the shelf remained almost constant in Cenozoic and has been a site for long term carbonate accumulation (Galloway, 2008).

2.5.1.2 Line 8 Moho pick

The Moho pick on the oceanic crust along Line 8 is a semi-continuous and flat reflector except near COB where two "smile" diffractions are observed (Fig. 9). The basement reflector overlying these two diffractions shows sediment wedging which may be interpreted as recording displacements along basement faults during early rifting and oceanic crust formation. The Moho is at a depth of ~11 seconds TWT (~16 km).

Moho continuity terminates near the basement step-up and this termination is interpreted as the edge of oceanic crust or the COB limit (Fig. 9). The Moho beneath the rifted margin and continental crust of Florida block is less evident than observed in the oceanic crust. The dashed line shown on Figure 9 is my inferred continental Moho based on its slightly stronger reflection signature.

2.5.1.3 Line 8 basement step-up and identifications of COB

Line 8 shows a significant drop in the basement elevation from the oceanic crust to the transitional crust; this drop in elevation is about 1 second TWT (~1.35 km). The nature of deposition of strata on this steep ramp is not well resolved on Line 8 (Fig. 9). Pindell and Horn (2014) proposed various ideas for formation of this steep ramp marking the COB with one idea being the collapse of rift shoulders of the continental crust following breakup.

2.5.1.4 Line 8 extinct GOM spreading center

The extinct spreading center is located about 10 km west of the end of Line 8 and therefore is not observed on Figure 9. The extinct spreading center in GOM is observed on other lines of the Supercache data set shown later in the thesis (Figs. 10, 11) and generally forms an east-west-trending valley that incises the upper oceanic crust.

2.5.2 Line 9 seismic interpretation

Line 9 on Figure 10 is another southwest to northeast strike line, 850 km long, and located north of Line 8 (Figure 9) from Walker Ridge on the oceanic crust to Southern Platform and Apalachicola protection area of offshore Florida (Fig. 5). Salt is present at two locations along this line: the autochthonous Luann salt in the center of the deep basin and Desoto Canyon salt basin (Fig. 5).

Line 9. Regional seismic line from Walker Ridge on the oceanic crust to Southern Platform and Apalachicola protection area offshore Florida. Observations on this line include: oceanic basement is less flat with expressed topography with 10 to 11 seconds TWT (~11.5 to 12.5 km); beneath the rifted continental crust, the basement is less continuous and less evident on the seismic line than the oceanic crust; continental basement is higher on the southern platform at 3.7 seconds TWT (~5.1 km); salt is present on this section and overlies syn-rift strata; salt appears depositional and in situ with the base of salt formed during the sag phase; Cretaceous-Tertiary (KT) boundary is continuous with strata predating KT boundary being thinner than the previous section (less than half second TWT) (~0.75 km) with no landward thickening; Cenozoic sediment packages are thickening toward central GOM due to sediment influx of Mississippi fan; the Moho pick for oceanic crust is intermittent and flat with depth of ~12-13 seconds TWT (~17-20 km); the COB basement step-up is relatively smaller than the previous section (0.5 seconds TWT) (~0.8 km).

2.5.2.1 Line 9 age picks

The top of oceanic basement of Line 9 (Fig. 10) is at a depth of 10 to 11 seconds TWT (~11.5 to 12.5 km). Two lows on the basement are present: one occupies the center of the line (Atwater Valley area) and the other one underlies the autochthonous salt (Fig. 10).

Basement beneath the rifted, continental crust on Figure 10 is shallower than on Line 8 (Fig. 9), where the base of the salt can be mapped. The rifted continental margin along Line 9 widens to ~130 km, continental basement is higher on the southern platform (~3.7 seconds TWT (~5.1 km), and continental basement dips eastward (Fig. 10).

The Cretaceous-Tertiary (KT) boundary is continuous with strata predating the KT boundary being thinner than previous section seen in Figure 8 (less than half second TWT) (~0.75 km) with no landward thickening. The contact between strata predating the KT horizon is depositional and the continuous reflectors are parallel to oceanic basement (Fig. 10).

Figure 10. A. Uninterpreted regional Dynamic Data Services seismic line 9 showing transition from Walker Ridge on the oceanic crust to Southern platform and Apalachicola protection area offshore Florida. **B.** Interpreted line 9 showing: 1) oceanic basement shows significant topography with depth of 10 to 11 seconds TWT (~11.5 to 12.5 km); 2) beneath the thin crust beneath the rift, basement is less continuous and less evident than the oceanic crust; 3) continental basement is higher on the Southern platform (3.7 seconds TWT) (~5.1 km); 4) salt is present on this section and overlies syn-rift strata; 5) salt appears depositional with the base of salt was formed during a post-rift sag phase; 6) Cretaceous-Tertiary (KT) boundary is continuous and strata predating KT boundary are thinner than previous section (less than 0.5 second TWT) (~0.75 km) with no thickening landward; 7) Cenozoic sediment packages are thickening toward central GOM due to the Cenozoic sediment influx of the Mississippi fan; 8) Moho pick on the oceanic crust is intermitted and flat at a depth of 12-13 seconds TWT (~ 17 to 20 km); and 9) basement step-up is relatively smaller than that shown on Figure 8 (0.5 seconds TWT of relief) (0.8 km).

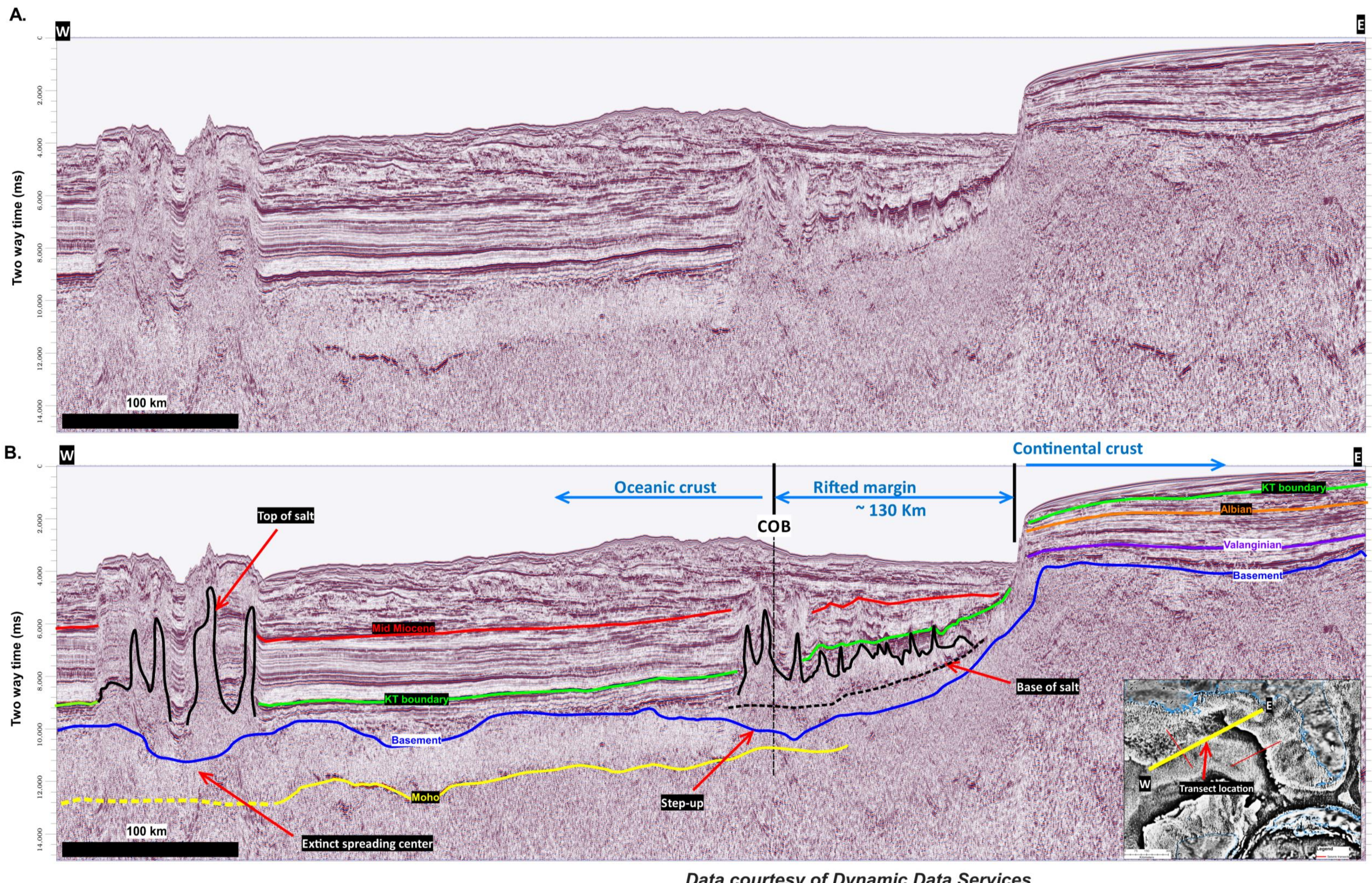

A.
W
E
Two way time (ms)
100 km
B.
W
E
Continental crust
Oceanic crust
Rifted margin
~ 130 Km
COB
Top of salt
KT boundary
Albian
Valanginian
Basement
Mid Miocene
Base of salt
Step-up
Moho
Extinct spreading center
Transect location
Data courtesy of Dynamic Data Services

Figure 10

2.5.2.2 Line 9 Moho pick

The Moho pick of the oceanic crust is not continuous but appears flat at a depth of ~12-13 seconds TWT (~17 to 20 km). Near the COB, the rifted continental crust appears ultra-thin as the Moho pick is very close to the top basement pick (Fig. 10). The Moho beneath the continental crust of Florida is also not certain, although strong reflectors at depths of 12 to 14 seconds TWT (~17 to 24 km) may represent the continental Moho.

2.5.2.3 Line 9 basement step-up and location of COB

Line 9 (Fig. 10) shows less of a drop in basement elevation at the COB from the oceanic crust to the transitional crust relative to Line 8 (Fig. 9). This drop occurs over a longer distance and at a lesser ramp angle of ~20 °.

2.5.2.4 Line 9 extinct spreading center

The extinct spreading center is located beneath the four intrusive salt bodies in Walker Ridge area in the center of the deep GOM and appears as a V-shaped valley incising the top of an oceanic basement. This feature has a topographic profile and width very similar to modern, slow-spreading ridges (Pascoe, 2014).

2.6. Interpretation of one long seismic transects in more salt areas of the NGOM

2.6.1. Line 10 seismic interpretation

Regional north-northwest and south-southeast-trending seismic lines from the Walker Ridge area image oceanic crust of the Green Canyon area adjacent to hyper-extended continental crust (Fig. 11). Line 10 in Figure 11 is a regional north-northwest to south-southeast seismic line from the Walker Ridge area to the oceanic crust in the deep GOM. A key observation for Line 10 is that the top of oceanic basement is flat south of the extinct spreading center but dips northward towards the COB north of the extinct spreading center. Northward dip of the basement north of the spreading center was also described by Hudec et al. (2013) on their lines from the same area as this line 10.

Other seismic lines show that this COB area is underlain by either oceanic crust or exhumed mantle (Pindell and Horn, 2014). Extensive salt is present on this area and overlies a thin section of inferred syn-rift strata (Fig. 11). The COB is ~100 km north of the Sigsbee escarpment indicating that this salt was either deposited originally on the newly formed Jurassic oceanic crust or unroofed mantle or was later remobilized and extruded or thrust upon the oceanic crust as apparent from the Sandwell et al. (2014) gravity image where the spreading ridge disappears and reappears on different sides of the Sigsbee escarpment (Fig. 5).

The Cretaceous-Tertiary (KT) boundary is flat on Figure 11 and strata predating KT boundary are very thin compared to previous sections (less than one half second TWT (~0.7 km). Cenozoic sediment packages thicken northward. The Moho pick on the oceanic crust is not pronounced as previous sections with depth of ~12-13 seconds TWT (~16 to 17.5 km) (Fig. 11). The basement step-up is not observed on this section although the oceanic crust could be as much as 2 km (1 second TWT) higher than the adjacent hyper-extended crust.

2.6.1.1 Line 10 age picks

Oceanic basement remains flat south of the extinct spreading center but deepens northward by about 1 second TWT (2 km) (Fig. 11). Deepening of the basement north of the extinct spreading center was interpreted by Hudec et al. (2013) as the COB as illustrated on one of their lines near this location. This observation required early opening of the GOM in segments with the central GOM being the last segment to undergo continental breakup.

This segmented model for GOM breakup from Hudec et al. (2013) allows more time for salt to be deposited in the central GOM although no direct data on age exists to distinguish which area of salt is older in the GOM. Crust beneath Walker Ridge, Green Canyon, and Atwater Valley may be any of the following crustal types: thin oceanic crust, hyper-extended continental crust, or exhumed mantle. The thinned crust beneath these area is not isostatically compensated in order to support more than approximately 13 km (12 second TWT) of clastic infill (Galloway, 2008). Another important observation is that full closure of the GOM discussed in detail in the discussion of this thesis requires that this area be either oceanic crust or exhumed mantle - if continental breakup was simultaneous along the spreading center.

The Cretaceous-Tertiary (KT) boundary is flat in this section with the strata predating the KT boundary being very thin compared to previous sections (less than half a second TWT) (~0.7 km) (Fig. 11). Cenozoic sediment packages thicken northward.

2.6.1.2 Line 10 Moho pick

The Moho pick of the oceanic crust is not well expressed at a depth of ~12-13 seconds TWT (~16 to 17.5 km). The basement step-up marking the COB is not observed on this section although the oceanic crust is about 1 second TWT (~2 km) higher than the adjacent hyper-extended continental crust. Near the extinct spreading center, the Moho almost merges with the basement surface so the crust is ultra-thin (Fig. 11). The Moho signature abruptly disappears near the Sigsbee escarpment.

Figure 11. (next page) A. Uninterpreted regional Dynamic Data Services seismic line 10 showing transition from Walker Ridge on the oceanic crust to Green Canyon area on the hyperextended continental crust. **B.** Interpreted line 10 showing: 1) oceanic basement is flat south of the extinct spreading center but deepens northward; 2) deepening of the basement north of the spreading center was proposed by Hudec et al. (2013) as the COB; however, to a achieve a full closure of the basin discussed later in this this thesis requires this area to be either oceanic crust or unroofed mantle; 3) transitional crust is hyperextended in this section or possibly does not exist and is instead represented by unroofed mantle; salt is extensive on the section overlying the thin syn-rift strata; 4) the COB is ~100 km north of the Sigsbee escarpment meaning that either this salt was deposited on the incipient oceanic crust or was mobilized onto the ocean crust; 5) the Cretaceous-Tertiary (KT) boundary is flat in this section and strata predating the KT boundary are very thin compared to previous sections (less than 0.5 seconds TWT) (~0.7 km); 6) Cenozoic sediment packages thicken northward in the direction of the Mississippi delta; 7) the Moho pick on the oceanic crust is discontinuous at a depth of ~12-13 seconds TWT (~16 to 17.5 km); and 8) the basement step-up is not observed on this section; however, the oceanic crust could be as much as 1 seconds TWT (~2 km) higher than the hyperextended crust.

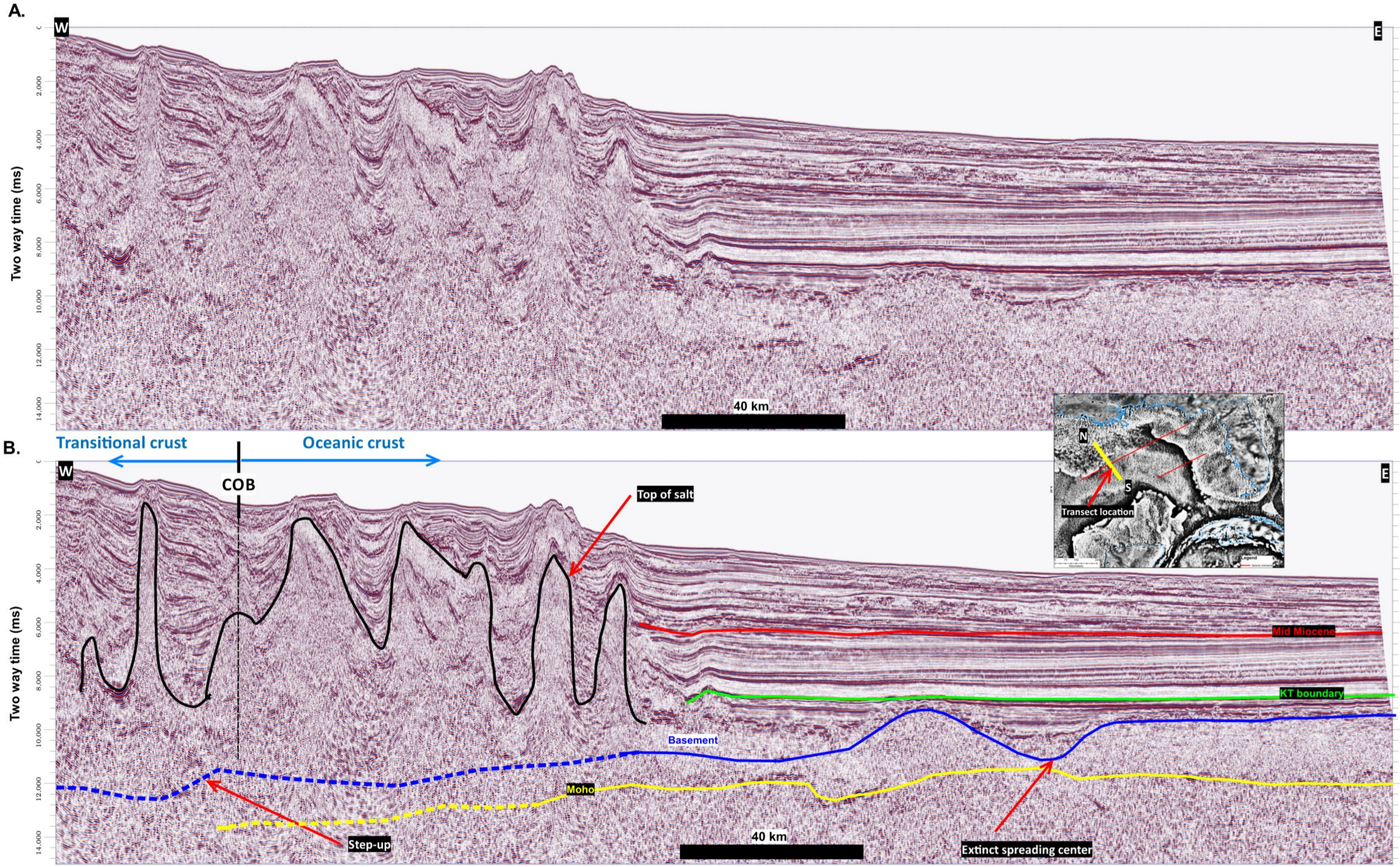
A.
W
E
Two way time (ms)
40 km
B.
Transitional crust
Oceanic crust
COB
Top of salt
N
S
Transect location
Mid Miocene
KT boundary
Basement
Moho
Step-up
Extinct spreading center

Figure 11

2.6.1.3 Line 10 basement step-up and identifications of COB

Line 10 shows drop in basement elevation near Sigsbee escarpment (Fig. 11). Whether this drop in elevation marks the limit of the oceanic crust is not clear from Line 10. A similar drop in the top of the basement surface was also observed on Line 8 (Fig 8), although the COB in that area is located ~50 km landward. This drop in the basement may be related to some other mechanism unrelated to the COB as proposed by Hudec et al. (2013).

Another possible candidate for basement step-up may be located ~120 km north of the first step-up beneath the massive salt canopy (Fig. 11). However, the presence of massive, overlying salt obscures the interpretation of this deeper section.

2.6.1.4 Line 10 extinct spreading center

The extinct spreading center is located ~100 kilometers south of Sigsbee escarpment and is seen on Line 10 (Fig. 11). The extinct spreading forms a valley incising the continuous oceanic crust for depth ~1.3 seconds TWT (~2.2 km) and width of ~20 km. The vertical gravity gradient map of Sandwell et al. (2014) confirms the location of the spreading center seen on the Supercache reflection lines (Fig. 5).

2.7. Zoomed seismic lines showing details of the COB in the more salt-rich area of the northern GOM

The precise limit of oceanic crust and the location of the continent-ocean boundary (COB) in the eastern and central GOM are important both for deepwater oil exploration as well as for achieving a better plate tectonic fit between continental rocks of the Yucatan Peninsula and North America (Fig. 2). Four seismic sections were compiled on Figure 11A-D to show the structure and associated stratigraphy of the basement step-up feature that Hudec et al. (2013) and other authors have proposed to coincide with the COB in the GOM.

.

Figure 12 (next page): A. Interpreted seismic line showing significant drop in basement depth from the oceanic crust to the transitional continental crust (for all locations see map in Figure 7). This drop is about 1.25 seconds TWT (~1.5 km). Transitional crust near the basement step-up is faulted (black lines). Very little salt is present in this location. **B.** This section shows a smaller drop in basement depth from the oceanic crust to the transitional crust relative to section B (~0.75 seconds TWT (~0.8 km). An increased amount of salt is present at this location. **C.** This line shows a small drop in transitional crust basement below the oceanic crust (~0.25 seconds TWT) (~0.3 km). Intensive salt at this sections obscures underlying reflectors, and mapping of basement step-ups at this section is uncertain. **D.** This line also shows a small drop in transitional crust basement below the oceanic crust (~0.25 seconds TWT) (~0.3 km). Intensive salt at this sections obscures underlying reflectors, and mapping of basement step-ups at this section is uncertain.

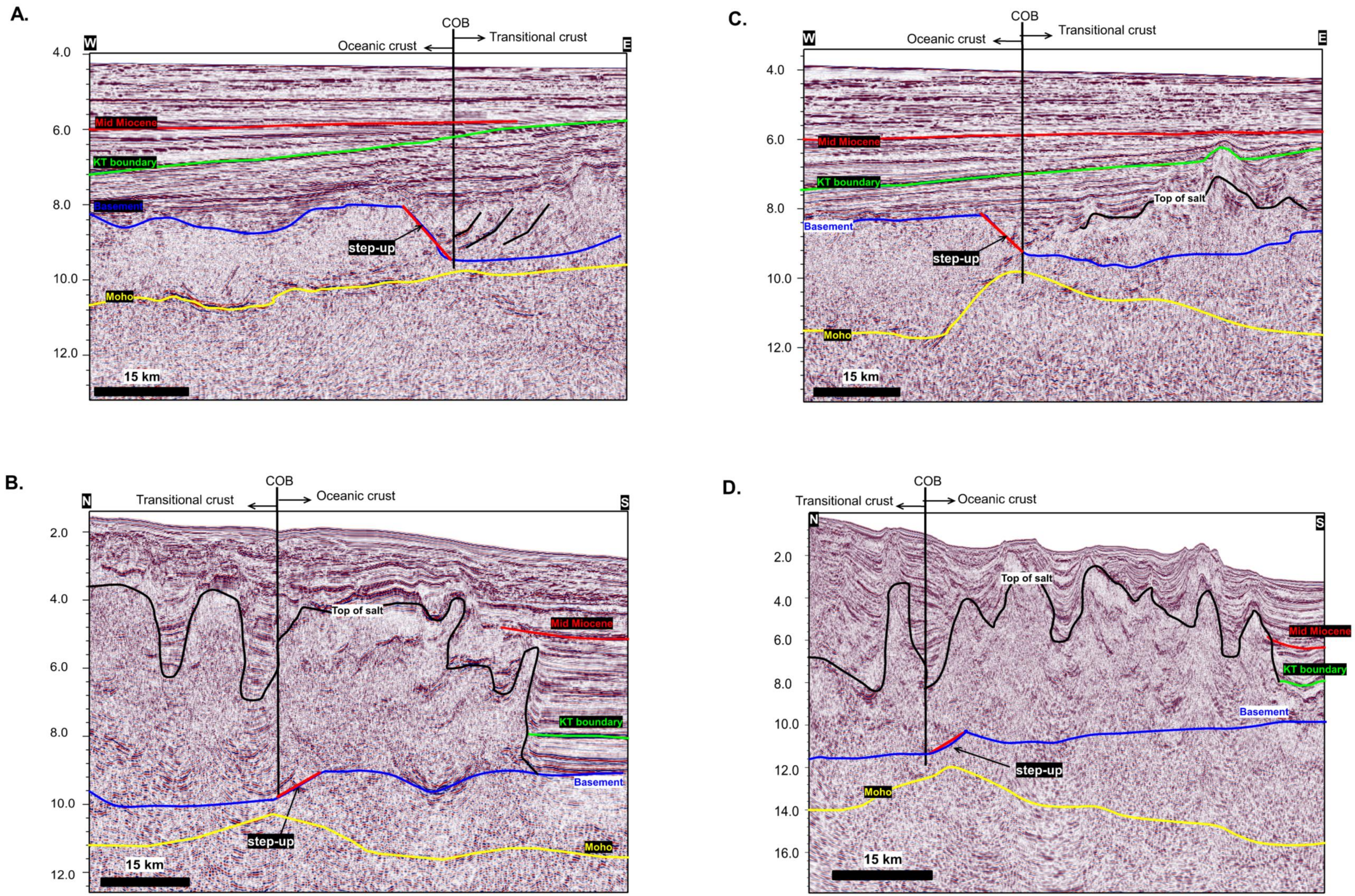
A.
COB
W
E
Oceanic crust
Transitional crust
4.0
6.0
8.0
10.0
12.0
Mid Miocene
KT boundary
Basement
step-up
Moho
15 km
C.
COB
W
E
Oceanic crust
Transitional crust
4.0
6.0
8.0
10.0
12.0
Mid Miocene
KT boundary
Top of salt
Basement
step-up
Moho
15 km
B.
COB
N
S
Transitional crust
Oceanic crust
2.0
4.0
6.0
8.0
10.0
12.0
Top of salt
Mid Miocene
KT boundary
Basement
step-up
Moho
15 km
D.
COB
N
S
Transitional crust
Oceanic crust
2.0
4.0
6.0
8.0
10.0
12.0
14.0
16.0
Top of salt
Mid Miocene
KT boundary
Basement
step-up
Moho
15 km

Figure 12

I compare the positions of the basement step-up in my study area to the proposed COB based on the Sandwell et al. (2014) interpretation of their vertical gradient of gravity (VGG) image. In my study area, the lack of a salt layer allows for better imaging of the basement step-ups than in areas of the central GOM that have extensive salt cover (Hudec et al., 2013). In my area the interpretation of the COB by Sandwell et al. (2014) using the VGG grid image matches the location of my observed basement step-ups seen on the Dynamic seismic profiles to within a distance of 35 km as compared on Figure 8.

The height and angle of the ramp of the basement step-ups varies with its distance from the pole of rotation for the Jurassic opening of the GOM (Fig. 8). The basement step-ups closer to the pole of rotation like those shown in Figure 12A and B show relief of (1.25 seconds TWT) (~1.5 km) along with more abrupt thinning of the underlying Moho.

Northern sections are further away from the pole of rotation shows the basement step-ups with lower angles and less relief along with thinner underlying crust as seen from the inferred Moho reflector (Figure 12C and D) relative to near pole or rotation sections (Figure 12 A and B). I interpret the sections in Figure 12C and D, further from the pole with thinner crust and lower relief (0.75 seconds TWT) (~0.8 km), as representing more extended continental crust. This thinner crust in the northern area is also associated with a much thicker overlying salt layer (Fig. 12C, D). Although much of this salt is remobilized, it is possible that areas of more extended, continental crust acted as the original Triassic-Jurassic depocenter for accommodating greater thicknesses of depositional salt.

The synrift sedimentary section is not present near the basement step-ups or is obscured or highly deformed by remobilized salt. The depositional synrift section is only visible in the salt-free areas to the south such as shown on Figure 9B.

2.8. Well cross section and seismic line showing the passive margin in the southeastern GOM and Yucatan

A 1280-km-long regional well cross section traversing the Yucatan block, the Straits of Florida, and the Florida block, is shown in Figure 13. The picks shown for the wells used in this cross section were based on paleontological information provided by Lexco (2014), BOEM (www.boem.gov) and internal reports from Dynamic Data Services. The lithology of the wells from the Yucatan block are based on Ramos (1975) and Ward et al. (1995). The top basement pick (dashed blue line) shown for the wells Yucatan 1, DSDP 537, Shell offshore 002, and Fl-HAR 1 show similar depths to top basement of ~3 km. All these wells penetrate Paleozoic sedimentary rocks.

This similarity in basement stratigraphy on either side of the Straits of Florida indicate the possibility of a pre-rift proximity, continuity, and similar subsidence history for the now-rifted and separated Yucatan and Florida blocks. Paleozoic sedimentary rocks and overlying Triassic rocks are truncated on both blocks, as the region was topographically elevated prior to the onset of rifting - possibly reflecting the influence of a large mantle plume centered on the area of the Bahamas platform (Fig. 2). In general, the top Paleozoic basement of Florida deepens eastward from a top basement depth of

~1.7 km at well P19 on the Middle Florida arch to ~ 3.0 km near the west Florida coastline (Fig. 13). Late Jurassic redbeds and siliclastic sediments overlie Paleozoic basement in Yucatan 1, Yucatan 4, and DSDP 537 - but are absent in the Florida shelf wells, perhaps reflecting the preexisting topographic upper surface of the eroded Paleozoic basement (Fig. 13).

Figure 13 (next page): A. Regional well cross section crossing the Yucatan block, the Straits of Florida, and the Florida block. The picks on the wells were based on paleontological information provided in reports by Lexco (2014), BOEM (2012) and Dynamic Data Services (R. Pascoe, personal communication, 2013). The lithology of the wells on the Yucatan block are based on Ramos (1975) and Salvador (1987). The basement picks (dashed blue line) on Yucatan 1, DSDP 537, Shell offshore 002, and Fl-HAR 1 are similar with a depth of approximately 3 km and are all overlain by Paleozoic sedimentary rocks. This strong similarity in basement lithologies indicates pre-opening proximity and a similar subsidence history for both the Yucatan and Florida blocks. In general, the basement in Florida dips eastward from a depth of 1.7 km at well P19 located on the Middle Florida arch to a depth of 3.0 km near the Florida coastline. Late Jurassic redbeds and siliclastic sedimentary rocks overlie basement in wells Yucatan 1, Yucatan 4 and DSDP 537 - but are absent in the West Florida shelf wells. This difference in Mesozoic stratigraphy is likely attributed to the preexisting topography of the Paleozoic basement. During the earliest Cretaceous to Albian (dashed orange line) both the Yucatan and Florida blocks underwent passive margin phase I, where 1-1.25 km of evaporites were deposited on the Yucatan block with a similar thickness of limestone and dolomite deposited during the same interval on the Florida shelf while a hiatus continued through the Albian on the Middle Florida arch. Passive margin phase I continued during the late Cretaceous (Albian-dashed orange line) to Maestrichtian (dashed green line) where about 1.5 km of limestone, dolomite and breccia were deposited on the Yucatan platform and 700 – 900 m of limestone and dolomite were deposited on the Florida shelf. From Maestrichtian to present, a second passive margin phase (Passive Margin phase II) deposited thin (< 200 m) limestone on the Yucatan shelf, whereas, 1.5 km of limestone and dolomite were accumulated on the Florida block. **B.** Index map showing the location of wells in the cross section. **C.** E-W seismic section showing three mapped horizons with planar stratigraphy dominant on the Florida shelf because this area has been in passive margin phase with very little terrigenous sedimentary input since the late Jurassic.

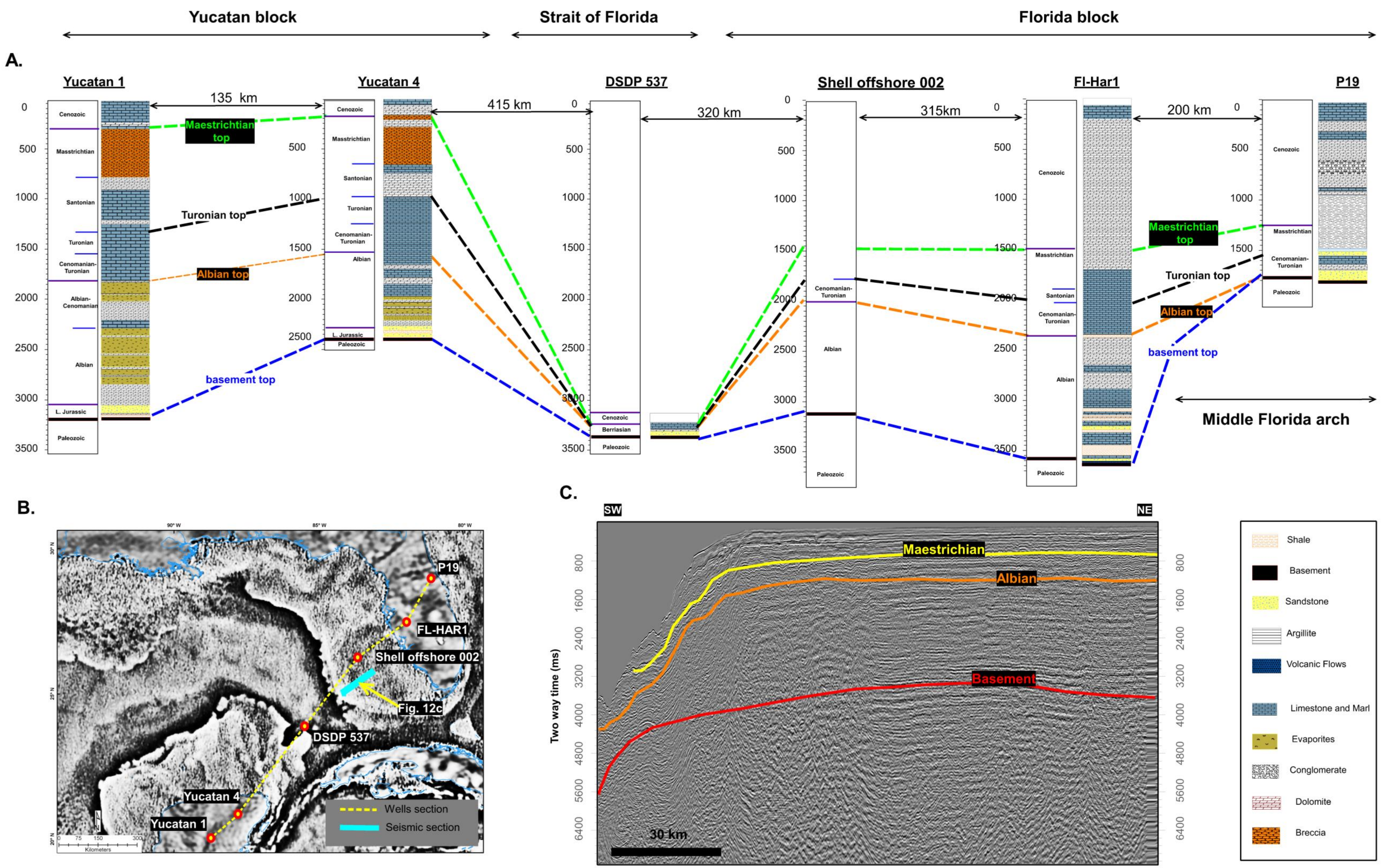
Yucatan block
Strait of Florida
Florida block
A.
Yucatan 1
Yucatan 4
DSDP 537
Shell offshore 002
Fl-Har1
P19
135 km
415 km
320 km
315km
200 km
Maestrichtian top
Turonian top
Albian top
basement top
Middle Florida arch
B.
P19
FL-HAR1
Shell offshore 002
Fig. 12c
DSDP 537
Yucatan 4
Yucatan 1
Wells section
Seismic section
C.
SW
NE
Two way time (ms)
Maestrichian
Albian
Basement
30 km
Shale
Basement
Sandstone
Argillite
Volcanic Flows
Limestone and Marl
Evaporites
Conglomerate
Dolomite
Breccia

Figure 13

During the Earliest Cretaceous to Albian, both Yucatan and Florida blocks experienced a similar period of passive margin subsidence recorded by the deposition of 1-1.25 km of evaporites deposited on Yucatan block and a similar thickness of mainly limestone and dolomite deposited on Florida shelf - followed by an erosional hiatus that continued through the Albian on the Middle Florida arch. A first passive margin phase continued during the Late Cretaceous (Albian) to Maestrichtian, when ~1.5 km of limestone, dolomite, and breccia were deposited on Yucatan platform and a thinner section (700 – 900 m) of limestone and dolomite were deposited on Florida shelf. From the Maestrichtian to present, a second phase of passive margin developed, where a thin section (< 200 m) of limestone was deposited on Yucatan shelf, while at the same time, a thick accumulation of 1.5 km of limestone and dolomites accumulated on Florida block.

There is no evidence of a Jurassic rifting event affecting the Florida block, although Escalona and Yang (2013) propose that the Straits of Florida underwent a second phase of rifting during the middle Jurassic that they related to the continuous CCW rotation of the Yucatan block. Late Jurassic redbeds and siliclastic sediments overlie basement in wells Yucatan 1, Yucatan 4, and DSDP 537, but the late Jurassic is absent from the Florida shelf wells, possibly as a result of preexisting Paleozoic topography. Dating of redbeds in Yucatan 1 and 4 is problematic and their ages are not well constrained (Ward et al, 2001). Pindell and Kennan (2009) proposed that these sediments are Late Triassic in age and were deposited during a Late Triassic rifting episode prior to the breakup of Pangea.

2.9. Seismic lines and well cross sections showing the passive margin in the eastern GOM

A regional, 425-km-long, well-log cross section, constructed parallel to the margin, uses four wells obtained from BOEM: Shell 001 from the Southern Platform; Chevron 001 from the Middle Ground arch; Mobil 001 near the Tampa embayment; and Shell 002 on the Sarasota arch (Fig. 14). Picks from paleontological reports and Gamma ray signal variations were used to make correlations. The top basement pick from the Southern Platform (Shell 001) and Middle Ground arch (Chevron 001) are identical with depth at ~4.2 km, while the top basement surface is ~6 km deep beneath the Tampa embayment (Mobil 001) and 3.25 km beneath the Sarasota arch (Shell 002).

Late Jurassic – Earliest Cretaceous sedimentary rocks are significantly thicker in Mobil 001 as compared to the other wells. For example, the Tithonian- Berriasian Cotton Valley Formation consisting of siliclastic sedimentary rocks are ~700 m thick in Mobil 001 and less than 300 meters in the other three wells.

This variation in late Jurassic – Earliest Cretaceous is clearly depositional and controlled by basement topography of the time. In the earlier passive margin phase during the Aptian-Albian, 1.5-2.0 km of mainly limestone and dolomite deposited on the shelf and from Albian to Maestrichtian thin, 400-700-m thick section of limestone and dolomite overlain by shale was deposited on the shelf. From Maestrichtian to present, thin section (300-1000 m) of limestone, dolomite, and shale was deposited, during the earlier passive margin phase from early Aptian to uppermost Albian, a thick, 1.5-2.0 km section of mainly limestone and dolomite was deposited on the shelf with a northward thickening into the Tampa embayment. From Albian to Maestrichtian, a thin section of 400-700-m thickness consisting of initially limestone and dolomite that gradually increased in shale content deposited. The thickest part of this section occupied a basement low within the Tampa Embayment. From Maestrichtian to present, thin section (300-1000 m) of limestone dolomites and shale was deposited with southward thickening.

Figure 14 (next page): A. Regional well cross section across the northeastern GOM. Correlated wells and their locations include: **Shell 001** on the Southern Platform; **Chevron 001** on the Middle Ground arch; **Mobil 001** near the Tampa embayment; and **Shell 002** on the Sarasota arch. Basement picks (dashed blue line) on Southern Platform (Shell 001) and Middle Ground arch (Chervron 001) are identical with a depth of roughly 4.2 km. Top basement is about 6 km deep beneath the Tampa embayment as penetrated by well Mobil 001 and 3.25 km deep beneath the Sarasota arch as penetrated by Shell 002. Late Jurassic-earliest Cretaceous sedimentary rocks are significantly thicker in the Mobil 001 well than other wells in the area. For example, Tithonian-Berriasian age siliclastic sedimentary rocks of the Cotton Valley Formation are 700 m thick in Mobil 001 and less than 300 meters in the other three wells. This strong lateral variation in late Jurassic-earliest Cretaceous thickness was likely controlled by basement topography at the time. During passive margin phase I, from Aptian (dashed blue line) to Albian (dashed orange line) 1.5-2.0 km of mainly limestone and dolomite was deposited on the shelf. From the Albian (dashed orange line) to Maestrichtian (dashed green line) a thin unit (400-700 m) of limestone, dolomite and shale were deposited on the shelf. From the Maestrichtian to the present, a thin unit (300-1000 m) of shallow marine carbonates deposited. **B.** Location map for the well cross section shown in A. **C.** North-south seismic section 8 km from Chevron 001 well and 3 km from Mobil 001 well showing major mapped horizons. Mobil 001 well is located on the flank of the Tampa embayment while Chevron 001 is located on basement high of Middle Ground arch.

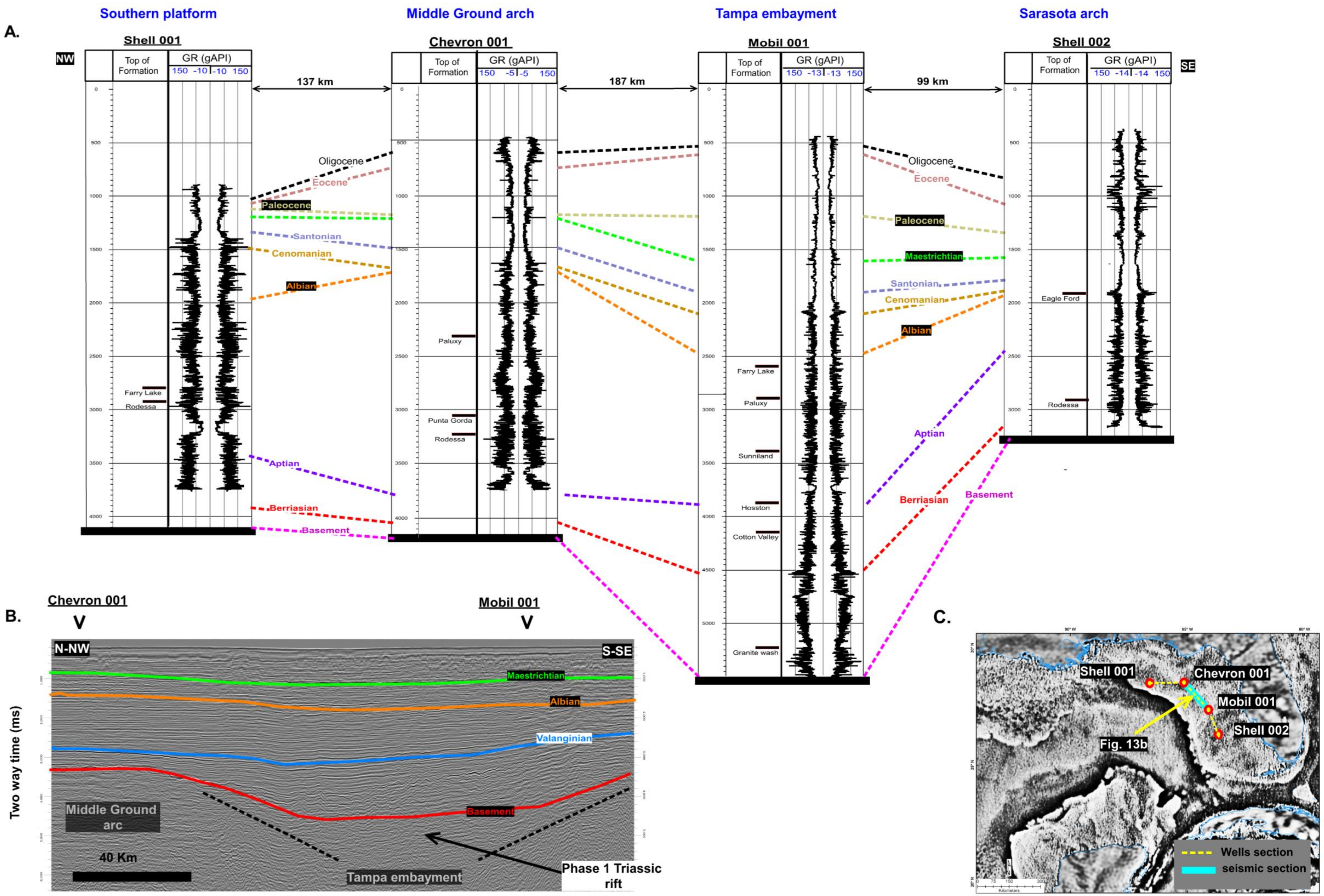

A.
Southern platform
Middle Ground arch
Tampa embayment
Sarasota arch
Shell 001
Chevron 001
Mobil 001
Shell 002
NW
SE
Top of Formation
GR (gAPI)
137 km
187 km
99 km
Oligocene
Eocene
Paleocene
Maestrichtian
Santonian
Cenomanian
Albian
Aptian
Berriasian
Basement
Farry Lake
Rodessa
Paluxy
Punta Gorda
Sunniland
Hosston
Cotton Valley
Granite wash
Eagle Ford
B.
Chevron 001
Mobil 001
N-NW
S-SE
Maestrichtian
Albian
Valanginian
Basement
Two way time (ms)
Middle Ground arc
40 Km
Tampa embayment
Phase 1 Triassic rift
C.
Shell 001
Chevron 001
Mobil 001
Shell 002
Fig. 13b
Wells section
seismic section

Figure 14

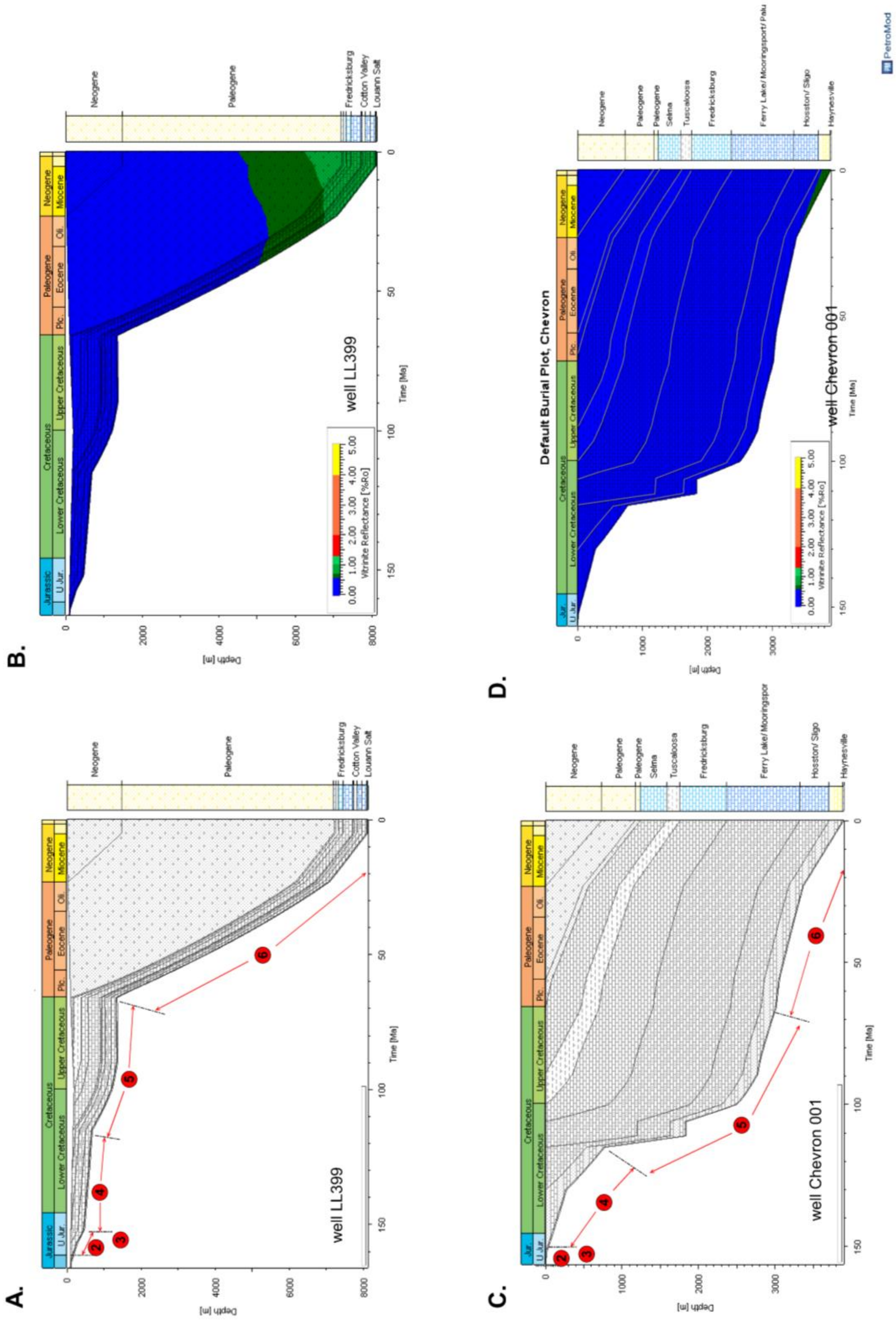

A.
B.
C.
D.
well LL399
well Chevron 001
Default Burial Plot, Chevron
Vitrinite Reflectance [%Ro]
Time [Ma]
Depth [m]
Neogene
Paleogene
Fredricksburg
Cotton Valley
Louann Salt
Selma
Tuscaloosa
Ferry Lake/ Mooringspor
Hosston/ Sligo
Haynesville
Jurassic
Cretaceous
Lower Cretaceous
Upper Cretaceous
Eocene
Miocene
PetroMod

2.10 Subsidence analysis of the deepwater eastern GOM and the Middle Ground arch

One-D backstripping and subsidence analysis were performed on two wells to quantify uplift and subsidence episodes for syn-rift and passive margin phases: 1) well LL399 located on Lloyd Ridge in the deepwater central GOM near the COB; and 2) Chevron 001 located on the Middle Ground arch on the west Florida shelf. Ages picks from BOEM well reports provided the ages for the tops of formations. (Fig. 14a).

For this subsidence analysis, five unconformities and their accompanying erosion were integrated into the subsidence history: 1) the breakup unconformity at 163 Ma; 2) the Valanginian unconformity at 137 Ma; 3) the Upper Albian unconformity (known as Mid Cenomanian unconformity by previous workers) at 100 Ma; 4) the Turonian unconformity at 91.5 Ma; and 5) the K-T unconformity at 66 Ma. (Wu et al., 1990; Haq et al. 1987; Addy and Buffler 1984; Buffler et al. 1980).

Figure 15: **A.** Subsidence plot for well LL339 located in the deepwater GOM near the COB. Tectonic phases inferred from subsidence history include: **Phase 2** = Middle Jurassic rifting; **Phase 3** = Luann salt deposition (166 – 163 Ma) during a sag phase following Phase 2 rifting; **Phase 4** = separation and drifting stage of central GOM following oceanic crust opening (163 – 137 Ma); **Phase 5** = Cretaceous passive margin stage (137-66 Ma); and **Phase 6** = Cenozoic passive margin stage (66 – 0 Ma).;
B. Maturation plot showing Early Jurassic source rock within the oil generation window.
C. Subsidence plot for Chevron 001 located on the Middle Ground arch of Florida shelf. The same tectonic phases seen in Chevron 001 are also observed in well LL339ell. A significant difference between the two wells is that Cenozoic subsidence related to infilling of the Mississippi delta is not as prominent in LL339 as compared to Chevron 001 because LL339 was drilled on the higher-standing Middle Ground arch that was not covered by the deep-sea fan of the Mississippi delta. **D**. Maturation plot showing that only a thin section of Late Jurassic has reached the oil generation window.

2.10.1 Well LL339

For well LL339, an initial subsidence of 50-100 m was followed by middle Jurassic Phase 2 rifting (Fig. 15A). This initial subsidence created accommodation space for salt deposition (phase 3) and allowed the deposition and preservation of a relatively thin salt layer during the post-rift sag phase.

Between the Callovian and Valanginian (163 -137 Ma), seafloor spreading in the central GOM continued, while areas near the COB maintained higher elevations where mainly thin sections of shallow-water carbonate rocks were deposited (Phase 4). Basement continued to subside to a depth of about 1.5 km below sea level during the Late Cretaceous, where ~1 km of mainly carbonate rocks of the Fredericksburg and equivalent Aptian to Albian formations were deposited during Phase 5. Since the Maestrichtian, more than 6 km of siliclastic sediments derived from the Mississippi delta and deep-sea fan caused rapid subsidence during Phase 6. The top of basement has reached a depth of ~8 km below sea level at this location (Fig. 15B).

2.10.2. Well Chevron 001

Neither initial subsidence (phase 2) nor salt deposition (phase 3) is recognized in well Chevron 001 (Fig. 14B). A carbonate buildup (phase 4) continued between (163-137 Ma) as basement subsided to ~1 km below sea level. Basement continued to subside to about 3.0 km below sea level during the Late Cretaceous, when carbonate and anhydrite sections of the Hosston/Silgo/Ferry Lake/Fredericksburg Formations and equivalent Aptian to Albian formations were deposited (Phase 5) (Galloway, 2008). Since

Maestrichtian time, more than 2 km of carbonate buildups have accumulated and basement continued to subside during Phase 6 to depth of about 4 km below sea level at this location (Fig. 14b).

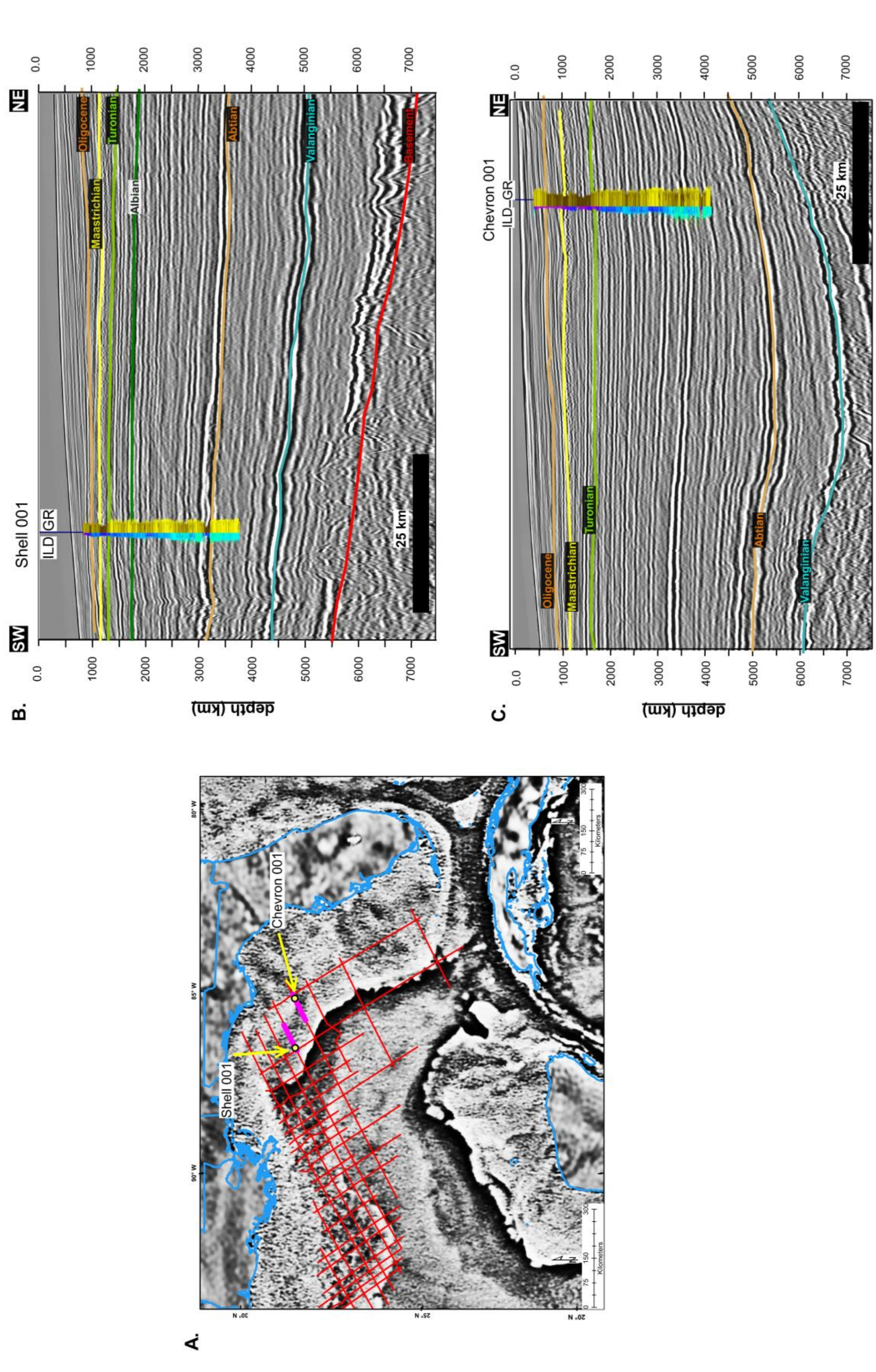
A.
Shell 001
Chevron 001
Kilometers
B.
SW
NE
Shell 001
ILD
GR
Oligocene
Maastrichtian
Turonian
Albian
Abtian
Valanginian
Basement
25 km
depth (km)
C.
Chevron 001
ILD_GR
25 km

2.11 Seismic-well correlation for two selected wells

2.11.1 Line 14 in the northeast GOM

Supercache seismic data were made available for my study in both time and depth domain. For the purpose of this study, I performed seismic-well correlation in the depth domain to verify the accuracy of the velocity model used for the depth conversion and to precisely define the ages of the main reflectors on the seismic lines crossing the well (Fig. 16A and B). The dates of various horizons are based on the BOEM well report the stratigraphic information and the velocity model that I used for converting seismic data from the time domain to the depth domain.

Figure 16: **A.** Index map showing the location of two wells, Shell 001 and Chevron 001, penetrating the Cenozoic and Cretaceous passive margin sequence and used for the seismic-well tie. Bold red lines are the extent of seismic sections shown in B and C. Both wells are located within 25 km of the seismic line. **B.** Well tie to line Shell 001. Gamma ray and deep-induced resistivity log (ILD) for Shell 001 are both superimposed on the seismic section in depth. The Maestrichtian pick at a depth of 1189 m corresponds to a drop in gamma ray and resistivity measurement values. The Turonian pick is at a depth of 1350 m, the Albian pick at a depth of 1956 m, and the Aptian pick at a depth of 3520 m. All picks are based on the well reports provided with the BOEM well information. **C.** Well tie to line Shell 001. Gamma ray and deep-induced resistivity log (ILD) for Chevron 001 are both superimposed on a seismic section in depth. The Maastrichtian pick at a depth of 1206 m corresponds to a drop in gamma ray and resistivity. The Turonian pick is at a depth of 1627 m, the Albian pick at a depth of 1709 m, and the Aptian pick at a depth of 3712 m. All picks based on the well report provided with the BOEM well information.

2.12 Basement structure and isochron maps

2.12.1. Basement and rift structures marking the COB of the northeastern GOM

Phase 2 Middle Jurassic rifting that preceded the onset of seafloor spreading in the GOM resulted in an arcuate system of grabens and half-grabens that rimmed the eastern and northern margins of the GOM (Salvador, 1987; Hudec et al. 2013) (Fig. 17). These middle Jurassic rift systems trend north to northwest in the eastern GOM, formed by rotation of the Yucatan block (Fig. 4), and differ in trend from Phase 1 late Triassic rifts filled by the Eagle Mills formation in the northern GOM that exhibit northeast trends that are collinear with rifts along the east coast of the USA (Fig. 2).

The arcuate rifted margin along the eastern GOM closely follows a gravity low parallel to the margin that I mapped on the Supercache seismic reflection data grid as a full graben underlain by hyperextended, continental crust (Fig. 17A). This narrow, 50-130 km band of hyperextended crust widens to the north and formed as Yucatan rotated CCW and produced northeast-southwest extension in the north-central GOM and east-northeast extension in the eastern GOM. Figure 17A is a map of the top basement surface showing the basement low underlying the full graben at a depth of 10-11 seconds TWT (~12.5 km). The basement surface deepens to the northwest as the full graben widens in that direction as a result of increasing extension to the northwest and becomes obscured by the thick salt layer in the north-central GOM. The western edge of the full graben marked by a basement step-up that is inferred by most workers to represent the COB (Hudec et al., 2013).

A.

B.

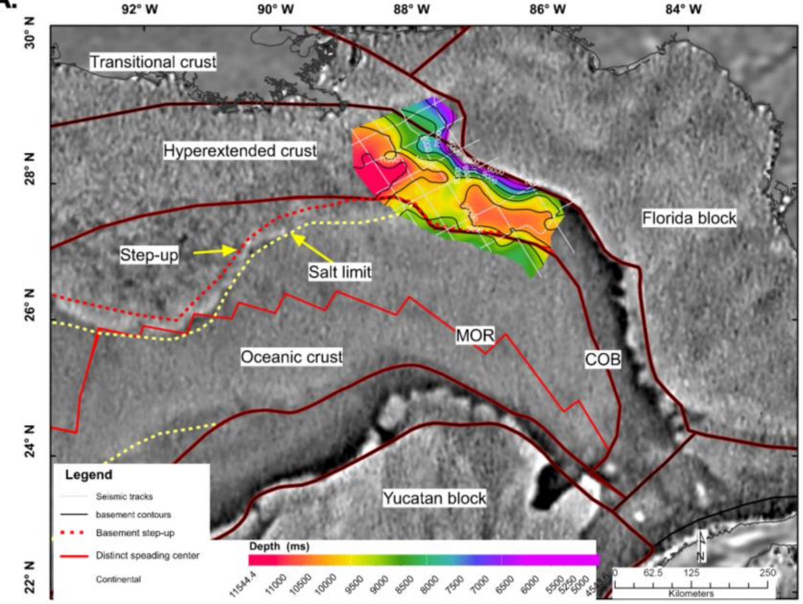

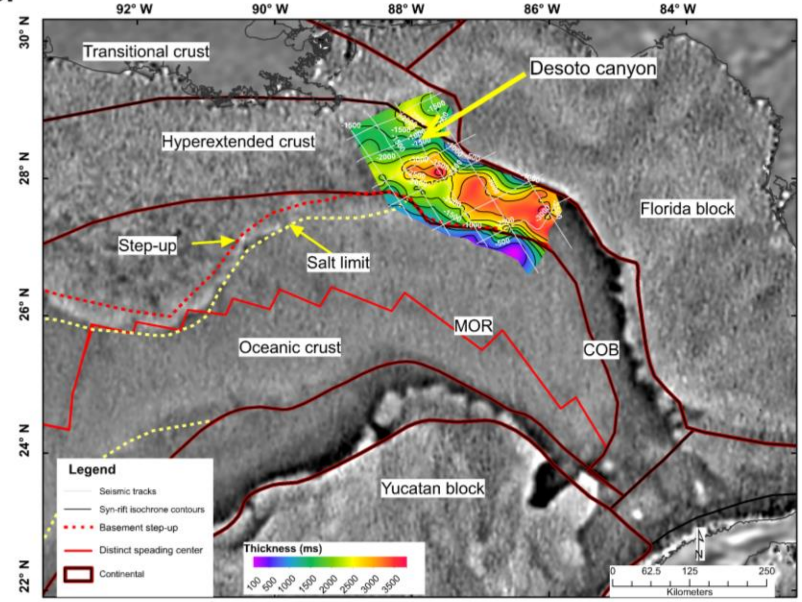

Figure 17: A. Top of basement structure map (red is deep and purple is shallow) for the northeastern GOM along the proposed NE GOM rifted margin superimposed on Sandwell et al. (2014) VGG map. This map area is the only area where the top of basement is clearly mappable from the Dynamic seismic grid. The deepest basement horizon and thickest overlying Late Jurassic synrift sediment is located directly adjacent to the basement step-up marking the COB on the seismic lines (dashed red) and on the VGG map of Sandwell et al. (2014). Inferred hyperextended continental crust is inferred to underlie a 125-km-wide rift zone that widens to the west, presumably in the direction of greater extension in the northern GOM. Two main basement depocenters are identified, one as deep as 11.5 seconds TWT (~12.5 km) near the edge of salt at the Desoto Canyon salt basin and one to the southeast at a depth of 10 seconds TWT (~11.0 km). **B.** Isopach map for Late Jurassic syn-rift sediments along the proposed rift axis superimposed on the Sandwell et al. (2014) map. The thickest syn-rift sediments are found near the present-day shelf break with thicknesses as great as ~2 km. The Jurassic syn-rift sediments thin to zero near the basement step-up and COB.

The thickness map (Fig. 17B) of the infill of the full graben shows a relatively thick late Jurassic section (~2 to 4 km) that I infer is mostly syn-rift and chaotic Luann salt in the northern area, possibly deposited at the top of the rift during a post-rift sag phase (Figs. 9, 10). Synrift sediments wedges from zero thickness near the basement step-up to the west to a depth of more than 3 km near the shelf. There are no wells that penetrate to this great depth so there is no direct age control for this section. Sediments wedging from zero kilometer thickness near basement step-up to more than 3.9 km near the shelf.

2.12.2 Basement structure and isochron maps for the Jurassic rift stage and the earliest passive margin stage

Top of basement was mapped in time for the study area and is shown in Figure 18A. Top basement is defined as the top of oceanic crust in the deep GOM and as the breakup unconformity on thinned continental rocks of the shelf and slope of the eastern GOM. The basement map and its overlying isochron show a series of basement highs and lows that trend east-northeast, and are interpreted as a series of horsts and grabens, possibly formed during Phase 1 early Triassic rifting (Salvador, 1987).

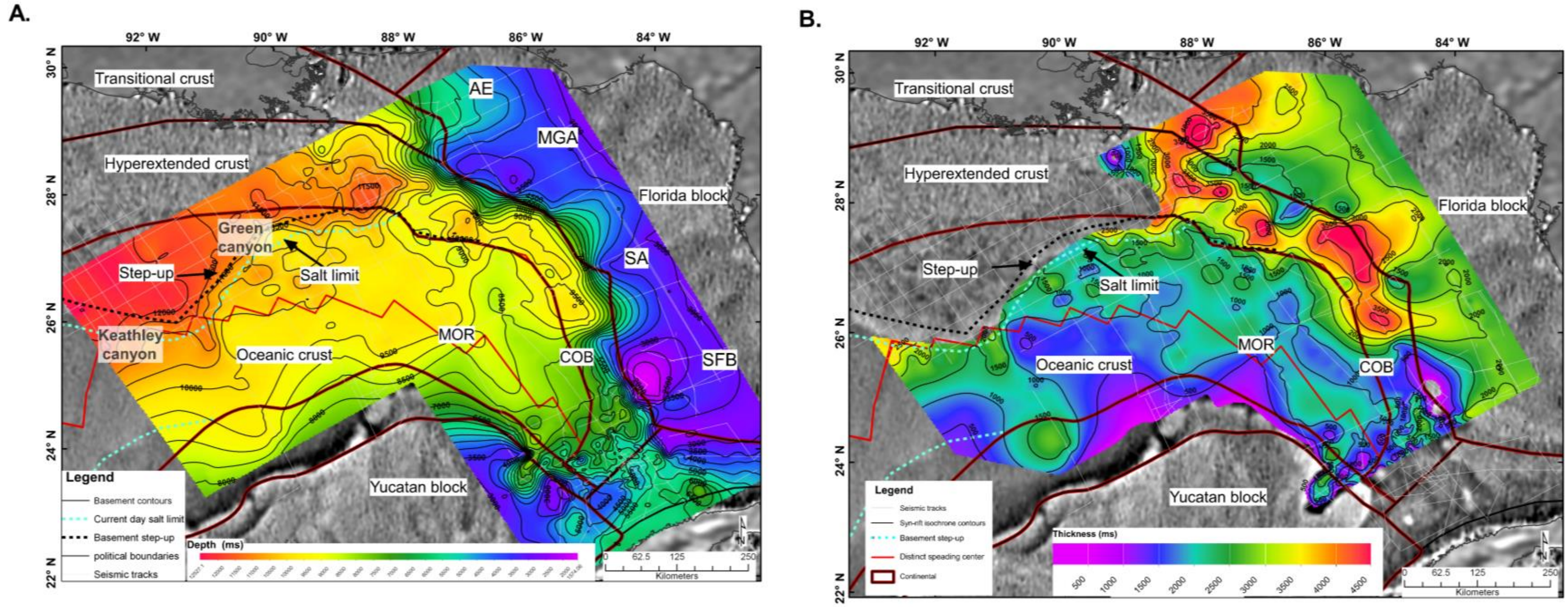

Figure 18: A. Top basement structure map in milliseconds (two-way travel time) with the shallowest areas in red and deepest areas in purple superimposed on VGG basemap of Sandwell et al. (2014). On the Florida shelf, a series of east-northeast-trending basement highs and lows are present. The east-northeast-trending Apalachicola embayment (AE) is the largest inferred rift roughly 200 km in length and 100 km wide. The Florida Platform and the Middle Ground arch (MGA) are aligned with a depth of roughly 3 seconds TWT (~5.2 km) to their top basement surface. The Tampa embayment is a V-shaped inferred rift with its widest section located to the SW near the GOM margin. The Sarasota arch (SA) is a basement high on the southern shelf whose top basement is 2.5 seconds TWT (~4.3 km). The South Florida basin (SFB) reaches a top basement depth of 3.5 seconds TWT (~5.9 km) with the deepest basement down to 12 seconds TWT (~13 km) in the areas of Keathley and Green Canyons. The basement step-up shown as a dashed red line marks the basinward limit of Jurassic rift and position of the COB with oceanic crust in the central GOM. **B.** Thickness map showing thickness of syn-rift sediments and early passive margin stage (late Jurassic to Early Cretaceous) superimposed on Sandwell et al. (2014) VGG map.

The Apalachicola embayment (AE) is ~200 km in length and ~100 km in width, and is the largest of these basins, although the northern extent of this basin is outside the area of my data coverage. Basement underlying the Florida Platform and the Middle Ground arch (MGA) are at the same depth range with a TWT depth of ~3 seconds TWT (~5.2 km). The Tampa embayment is a V-shaped basin that widens basinward. The Sarasota Arch (SA) is another basement high on the southern shelf that is ~2.5 seconds TWT (~4.3 km) at its shallowest point. The South Florida Basin (SFB) is as deep as 3-3.5 seconds TWT (~5.2 to 5.9 km). Basement is deepest in the northern area with the deepest point to top basement at ~12 seconds TWT (~13 km) in the Keathley and Green Canyons. The basement step-ups marking the COB are particularly well imaged in the southern area lacking salt.

Sedimentary sections of syn-rift Late Jurassic rocks and upper Cretaceous (to end of Albian) passive margin rocks (Fig 18B) was mapped as time thickness to show the main depocenters active during the Jurassic syn-rift phase and earliest Cretaceous passive margin phase at the scale of the NE GOM. The main depocenters for the syn-rift phase and early passive margin phase are located in basement lows that were formed during Phase 2 Late Triassic rifting. These basement lows include the same basement features describe above that include the Apalachicola embayment, the Tampa embayment and several small depocenters near the COB.

2.12.1 Top structure map for KT boundary and isochron map for the Cenozoic

The Cretaceous-Tertiary (KT) boundary is marked by a basin-wide seismic reflector found in the deepwater GOM that corresponds to a major unconformity present throughout the GOM basin (Keller et al. 1993). This unconformity marks a global stratigraphic event related to sea-level changes and is not an exclusively related to events unique to the GOM basin. The composition of sediments deposited above this boundary have been a subject a number of detailed studies all showing an event layer composed of a catastrophic "cocktail" deposit containing fossils from many water depths, fragments of reworked strata, and other Chicxulub-related impact ejecta. The age of this unconformity is Maestrichtian (~65-66 Ma) in age (Bralower and Leckie, 1998)

The KT boundary was formed due to Chicxulub impact that produced the largest known, single, mass-wasting deposit in Earth history. The KT boundary deposit is thicker in the deepwater area of the GOM (100- 200 m) and thinner on its shelves (10-20 m) (Denne et al., 2013). The KT boundary conforms to the underlying morphology of the top basement surface. On the Florida shelf, the interpreted KT boundary reflector is flat and maintains a depth range of 0.5-1.0 seconds TWT (~1 to 2 km) (Fig. 18A). The Florida escarpment serves as the terminating boundary between shelf strata and deep basin strata and forms an edge across which the KT boundary deepens by as much as 4 seconds TWT (~4.3 km) and by as much as 10 seconds TWT (~10 km) near the Sigsbee escarpment in the north. This deepening toward the center of the GOM basin is related to the increased rate of subsidence and extensive sedimentation from the Mississippi delta and deep-sea fan (Fig. 19A).

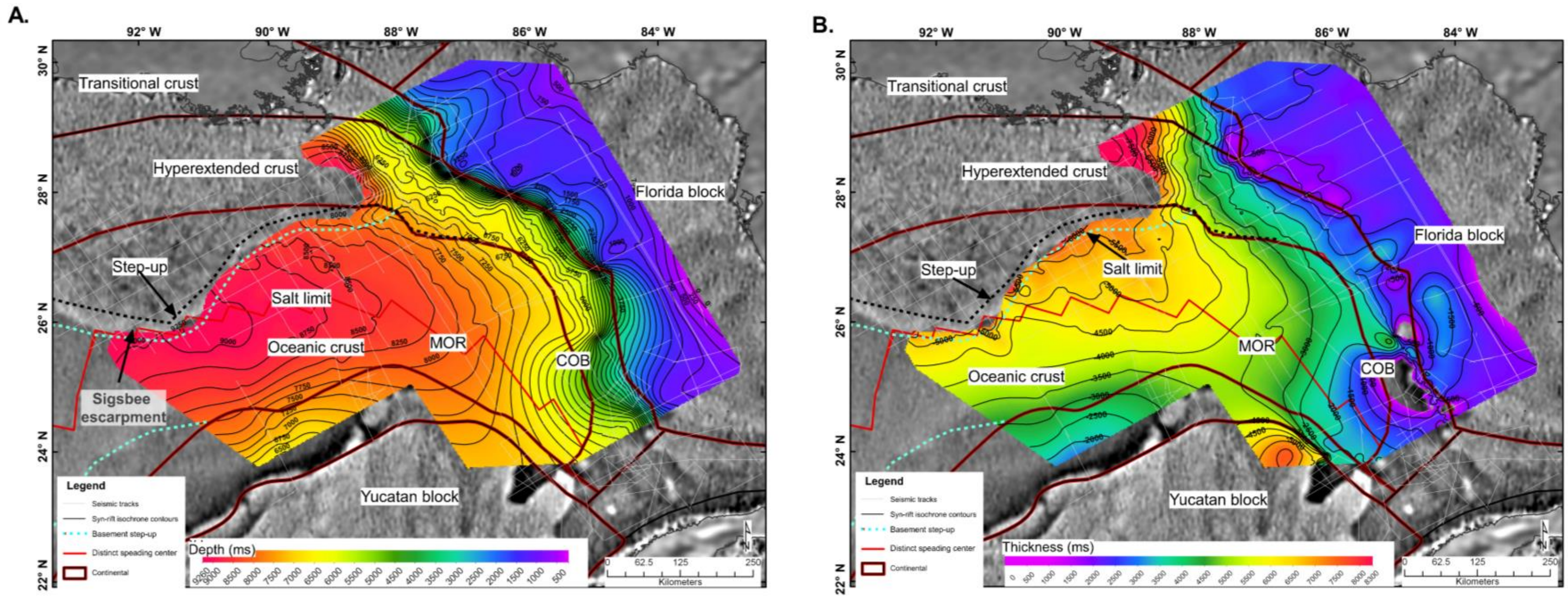

Figure 19: **A.** Top of Cretaceous-Tertiary (KT) boundary structure map in seconds TWT superimposed on Sandwell et al. (2014) VGG map. This surface follows the general morphology of the underlying basement shown on Figure 17A. Red to dark purple represents shallow to deeper depths, respectively. On the Florida shelf, the KT boundary is flat and maintains a depth range of 0.5-1.0 seconds TWT (~1 to 2 km). Overlying oceanic crust of the central GOM, the KT boundary is as deep as 10.0 seconds TWT (~10.5 km) near the Sigsbee escarpment. This deepening toward the center of the GOM reflects increased subsidence due to the sediment load of the Mississippi delta and deep-sea fan. **B.** Thickness map showing the thickness of sediments deposited during the Cenozoic superimposed on Sandwell et al. (2014) VGG map. The thickest Cenozoic section coincides with the proximal Mississippi fan where sediments (up to 7 seconds TWT thick/9 km) have accumulated. Carbonate rocks less than 2 seconds TWT (1.7 km) thick have accumulated on the shelf.

The thickness of sediments overlying the KT boundary varies significantly from deepwater to shelf environments. The thickest Cenozoic section coincides with the proximal Mississippi deep-sea fan which are up to 7 seconds TWT in time thickness (~9 km). Carbonate rocks less than 2 seconds TWT (~1.7 km) in time thickness have accumulated on the Florida shelf (Fig 19B).

2.13. PaleoGIS tectonic reconstructions of the GOM

2.13.1. Previous GOM reconstructions and methods

Early attempts to reconstruct plates in the GOM and circum-Atlantic region can be traced back to the work of Bullard et al. (1965). Other reconstructions have emerged over the years and include: Hudec et al. (2013), Kneller and Johnson (2011), Pindell and Kennan (2009), Buffler and Thomas (1994), Hall and Najmuddin (1994), Pindell (1985a; 1993), Ross and Scotese (1988), Salvador (1987), Buffler and Sawyer (1985), and Burke (1984). Most, if not all of these models propose a counterclockwise rotation of Yucatan to reconstruct the GOM part of the supercontinent Pangea. The amount of rotation of Yucatan and closure is constrained by the locations of the COB and the amount of crustal stretching in the largely inferred rift zones.

I created tectonic reconstructions of the Gulf of Mexico and circum-Atlantic using PaleoGIS software with six time steps (200, 174, 163, 154, 147, and 137 Ma) (Figs. 20-25) These six geological time steps were chosen because they represent geological events that have been well dated and can be used as control points for the reconstruction.

2.13.2 Earliest Jurassic reconstruction (200 Ma):

During this stage, the supercontinent Pangea rifted apart (Fig. 20). Amalgamated continental crust of Gondwanan and Laurentian affinity underwent extreme stretching along an intracratonic rift system that separated the North American plate from the Gondwanan affinity plates (South American and African plates). This intracratonic rift system included the well-documented and subaerially exposed eastern North American rift system that extends through Northern Florida and Georgia and as far south as northern South America in Venezuela and Colombia (Bartok et al., in press).

The northeast alignment of the interpreted Triassic rift system (Pindell and Kennan, 2009) suggests that GOM was being extended in a northwest direction relative to the Africa and South America. This northwest extension of this Triassic rift system formed structural trends visible on gravity and magnetic maps of the eastern GOM in Florida shelf and Yucatan, although the age and exact lithologies forming these anomalies are unknown (Fig. 20).

Circum-Atlantic closure between the North American plate and African plate is based on the location and reconstruction of the East Coast Magnetic Anomaly (ECMA). In my reconstructions I adopted the matching markers on the Atlantic side from Labails et al. (2010) including the New England seamounts and Jacksonville fracture zone (JFZ) on the eastern margin of North America that are conjugate on the African side to the Canary Islands and Cape Verde fracture zone (CVFZ), respectively. (Fig. 20).

Early Jurassic (200 Ma)

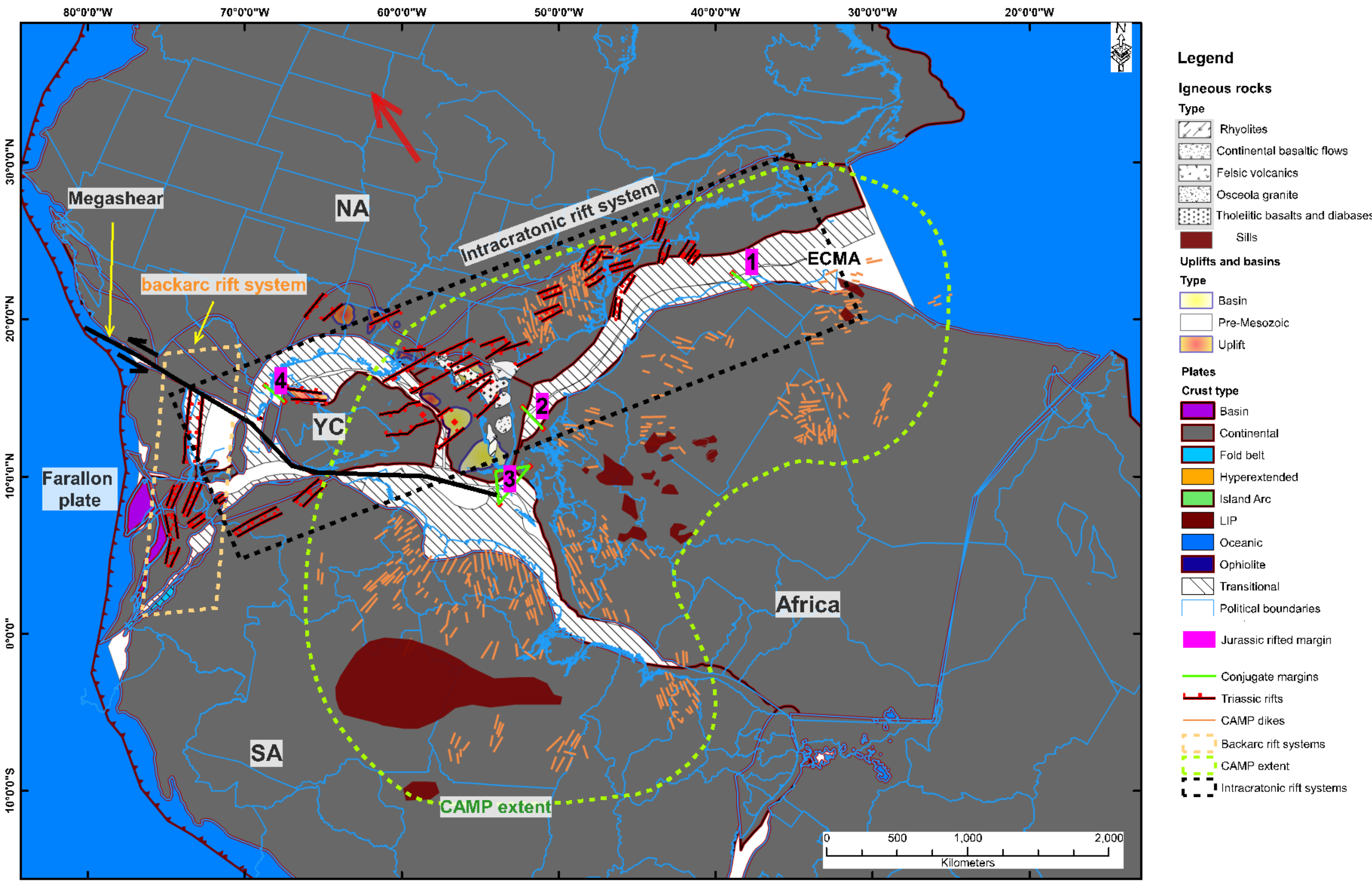

This precise fit of the ECMA requires the Yucatan block to rotate 39° clockwise from its present position with an additional 250 to 300 km of shortening along the northwestern edge of the block. Block rotation creates an overlap problem between Yucatan and northern South America in the reconstruction. For Yucatan to fit between North and South America without overlapping continental blocks, an addition 250 to 300 km of extension must have occurred. This rotation and shortening aligns trends in gravity and magnetic anomalies in Yucatan and Florida that may correspond to buried rift systems. In the reconstruction continental crust of the Chiapas massif in southern Mexico is dealt with separately (Bartok et al., in press).

Figure 20: Early Jurassic (200 Ma) reconstruction of the central Atlantic and Gulf of Mexico. Reconstruction of the Central Atlantic is based on realigning the East Coast magnetic anomaly (ECMA) of the USA and African West Coast magnetic anomaly (AWCMA). Match points include the New England seamounts (**number 1**) and Jacksonville fracture zone (JFZ) (**number 2**) on North American eastern margin that are conjugate to the Canary Islands and Cape Verde fractures zone (CVFZ) on the African margin (Labails et al., 2010). Match points also include placing Guinea-Bissau in central Africa against French Guiana and southern Florida (**number 3**) and placing the Tabasco province of southern Mexico against Texas in the USA (**number 4**). Late Triassic (230-190 Ma) rifts (red and black lines) formed along the eastern coast of the North American plate, eastern Yucatan block, and northern South American plate as a result of the earliest rift phase between North America, South America and Africa. The Central Atlantic Magmatic Province (CAMP) event occurred over a short period of time about 201 Ma that formed an immense pattern of radiating (orange lines) and basaltic sills (red polygons) centered on the area of the Bahamas and southeast Florida. The center point of this radial pattern is inferred to be the site of a mantle plume (Withjack, 2012; Oslen, 1999). The reconstruction of the Yucatan peninsula requires ~39° clockwise rotation and translation of the block in a northwesterly direction by 250-300. This fit assumes that the basement of the Bahamas is completely oceanic and that the Florida block has remained a single, rigid block since the Late Triassic.

Kinematically, migration of North American plate in the NW direction requires pervasive left-lateral shearing of a broad zone of Mexican terranes. Mexican terranes overlap with northwestern South American plate if they remain in their current, geographic position. The Sonora-Mojave megashear has been proposed as possible accommodation zone for North America breakup (Salvador, 1987). In my reconstruction I propose a left-lateral shear zone through southern Yucatan and Coahuila block as a possible transform zone that accommodated the early opening in the GOM and Caribbean regions.

Mexican terranes overlap with NW South American plate if they remained in their current position. The Sonora-Majova Megashear is one candidate for accommodating late Jurassic displacement to overcome overlap problem.

Middle Jurassic (174 Ma)

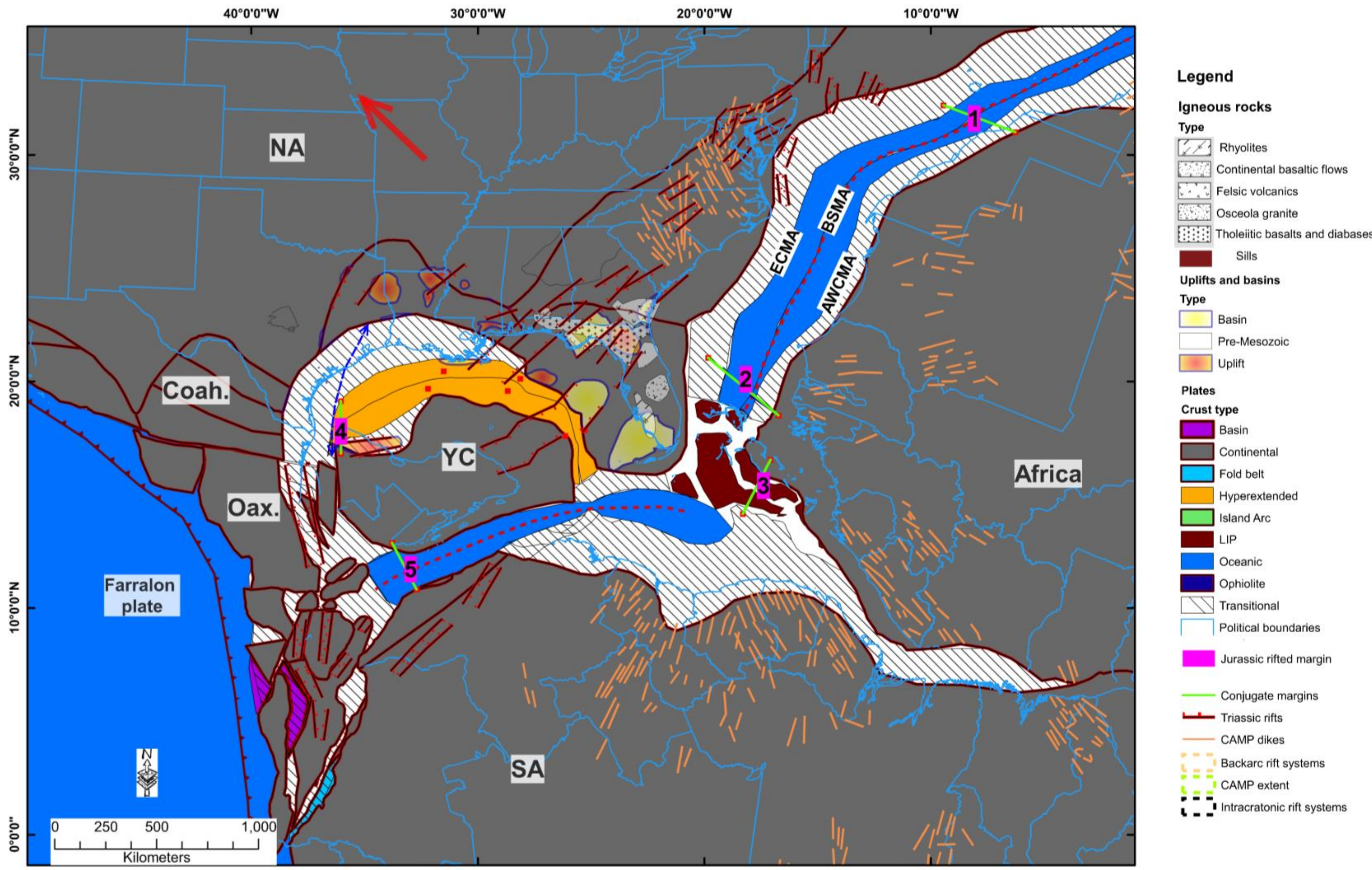

2.13.4 Middle Jurassic reconstruction (174 Ma)

Reconstruction of the Central Atlantic in Earliest Middle Jurassic reunites the Blake Spur Magnetic Anomaly (BSMA) with an equivalent anomaly known as African Blake spur magnetic anomaly (ABSMA) (Labails et al., 2010). The age of the BSMA is 170+-4 Ma (Withjack et al., 2012; Bird et al., 2007)

At this stage, opening of the Atlantic Ocean continued at a slow spreading rate of 1.19 cm/year with a possible ridge jump (Bird et al., 2007). A proto-Caribbean Sea must have opened at this stage given the fit of the BSMA and the fact that the oceanic crust had not propagated into the GOM by this time. My interpretation differs from the Pindell and Kennan (2009) conclusion that the Gulf of Mexico opened first followed by opening of the Proto-Caribbean Sea. Evidence for the earlier opening of the Proto-Caribbean being that the GOM is a result of kinematic model presented in this work. (Fig. 21)

Extension of ~100-150 km in a northwest-southeast opening direction occurred at this stage and was focused mainly in the deep central GOM with a minor rotational component.

Figure 21: Middle Jurassic reconstruction (174 Ma) of the central Atlantic and GOM. The reconstruction shown for the Central Atlantic between the Blake Spur Magnetic Anomaly (BSMA) and the African West Coast magnetic anomaly (AWCMA) is modified from Labails et al. (2010). Breakup of the Central Atlantic and seafloor spreading occurred between 190-170 Ma at a slow spreading rate of 1.19 mm/year. During this period, the Proto- Caribbean Sea opened and extension continued in the GOM. The direction of opening of the GOM at this time as northwest-southeast with CCW rotation of the Yucatan block.

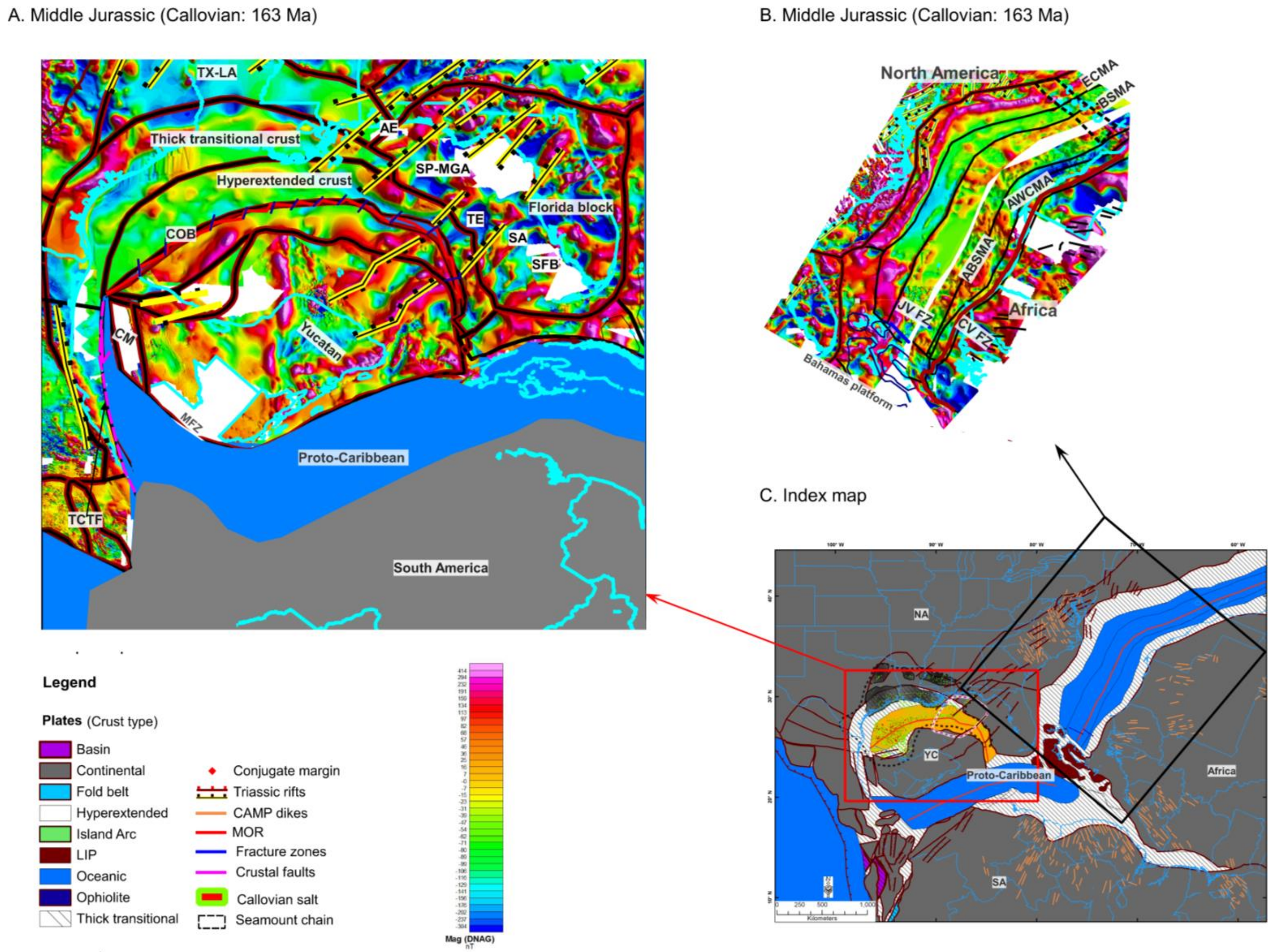
A. Middle Jurassic (Callovian: 163 Ma)
TX-LA
AE
Thick transitional crust
SP-MGA
Hyperextended crust
Florida block
TE
COB
SA
SFB
CM
Yucatan
MFZ
Proto-Caribbean
TCTF
South America
Legend
Plates (Crust type)
Basin
Continental
Fold belt
Hyperextended
Island Arc
LIP
Oceanic
Ophiolite
Thick transitional
Conjugate margin
Triassic rifts
CAMP dikes
MOR
Fracture zones
Crustal faults
Callovian salt
Seamount chain
Mag (DNAG)
nT
B. Middle Jurassic (Callovian: 163 Ma)
North America
ECMA
BSMA
AWCMA
ABSMA
Africa
JV FZ
CV FZ
Bahamas platform
C. Index map
NA
YC
Proto-Caribbean
Africa
SA
Kilometers

2.13.5 Callovian reconstruction (163 Ma)

Rifting ceased at this stage in the GOM basin and basement subsidence became the dominant element in the GOM basin evolution. During the sag phase, extensive salt was deposited in subsiding grabens systems above hyperextended, transitional crust with two main depocenters and several secondary depocenters. The main depocenters were located in the central GOM where up to 4 km of salt was deposited. The other main salt depocenter was located in northeast GOM in the Desoto Canyon salt basin. Thin salt sections were also deposited in Houston embayment salt basin, the Louisiana salt basin, the Mississippi salt basin, and along on the hyperextended crust in the eastern GOM with thickening of the salt in an east to west direction.

Figure 22: A. Callovian (163 Ma) reconstruction of the GOM showing grid of DNAG magnetic anomalies layered onto the plates. This closure is based on the newly mapped COB in the GOM and the arcuate shape of the fracture zones. The signature of magnetic anomalies on both the Yucatan and Florida blocks that are inferred be buried Triassic or Jurassic rifts once aligned and continuous with each other and with rift systems extending along the east coast of the USA. Buried, high amplitude magnetic anomalies along the northeastern Yucatan align with mapped basement highs of Florida (Sarasota Arch, Southern Platform and Middle Ground arch) while lower magnetic amplitudes correspond to deeper basement of the Tampa embayment, South Florida basin and Apalachicola embayment. At this stage rifting ceased and salt was deposited within the subsided rifted margin. **B.** Callovian (163 Ma) reconstruction of the Atlantic between the Blake Spur Magnetic Anomaly and magnetic anomaly M25. The New England seamounts and Jacksonville fracture zones (JFZ) on the eastern margin of North American used as conjugates to the Canary Islands and Cape Verde fracture zone (CVFZ) on the African margin (Labails et al., 2010). The rate of seafloor spreading increased to ~3.5 cm/yr. This rate is based on previous fit at the Blake Spur Magnetic anomaly and M25 with a constant rate of separation. **C.** Map showing full reconstruction during Callovian time (163 Ma).

The Callovian fit of GOM is based on matching: 1) the COB boundary of the conjugate margins; 2) the orientation of the circular Sandwell et al. (2014) VGG anomalies that correspond to fracture zones; and 3) the length and curvature of Tamaulipas-Chiapas Transform Fault (TCTF) mapped by Nguyen (2014, personal communication), and the arcuate shape of the extinct spreading center (Fig. 5).

Closure of the GOM shows a remarkably close alignment between magnetic anomalies of the Florida shelf and anomalies on the Yucatan peninsula (Fig. 22A). High-amplitude magnetic anomalies along the northeastern Yucatan align with mapped basement highs of Florida (Sarasota arch, Southern Platform and Middle Ground arch) while lower-amplitude magnetic amplitudes correspond to deeper basement of the Tampa embayment, South Florida basin and Apalachicola embayment. These alignments provide additional evidence for the tectonic model that I am proposing in this thesis.

This precise alignment of magnetic anomalies in the eastern GOM following GOM closure can be used as an argument that pre-Callovian northwest to southeast extension was focused in the central GOM. These alignments also disprove the hypothesis of Klitgord (1984) that fracture zones offset the Florida block. These strike-slip offsets would have disrupted the precise matches I describe from Yucatan and Florida.

Reconstruction of the Atlantic between the Blake Spur Magnetic Anomaly and magnetic anomaly M25 is challenging because there is no reference anomaly or isochrons to use as matching points. To the north, matching points between the diverging North American plate and the South American plate include the New England seamounts and

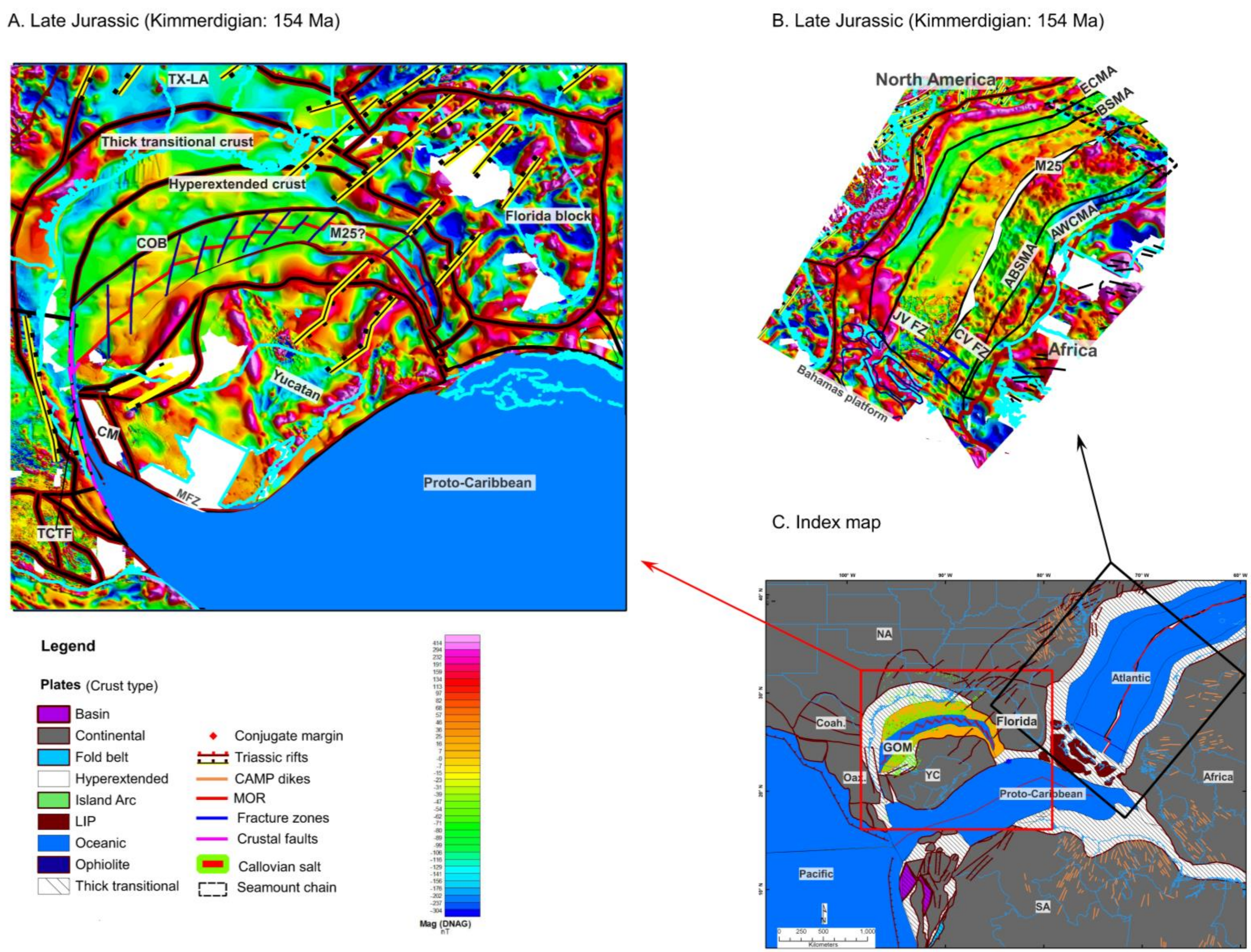
A. Late Jurassic (Kimmerdigian: 154 Ma)
TX-LA
Thick transitional crust
Hyperextended crust
Florida block
COB
M25?
Yucatan
CM
MFZ
TCTF
Proto-Caribbean
Legend
Plates (Crust type)
Basin
Continental
Fold belt
Hyperextended
Island Arc
LIP
Oceanic
Ophiolite
Thick transitional
Conjugate margin
Triassic rifts
CAMP dikes
MOR
Fracture zones
Crustal faults
Callovian salt
Seamount chain
Mag (DNAG)
B. Late Jurassic (Kimmerdigian: 154 Ma)
North America
ECMA
BSMA
M25
AWCMA
ABSMA
JV FZ
CV FZ
Africa
Bahamas platform
C. Index map
NA
Coah.
GOM
Oax.
YC
Florida
Atlantic
Proto-Caribbean
Africa
Pacific
SA

Jacksonville fracture zone (JFZ) on the eastern margin of North American that are used as conjugates to the Canary Islands and Cape Verde fracture zone (CVFZ) on the African margin (Labails et al., 2010). (Fig, 22B).

2.13.5 Kimmeridgian reconstruction (154 Ma)

Oceanic spreading in GOM initiated shortly after salt deposition in the Callovian (Table 1) and split the salt into two distinct provinces: the northern province of Luann salt in the USA and the southern province of Campeche salt in Mexico (Salvador, 1987). CCW rotation of Yucatan around the fixed pole in in the deepwater southeastern GOM resulted in right-lateral displacement along the TCTF. This rotation regime produced curvilinear fractures zone arc in shape with their center pointing to the pole of rotation. (Fig. 5, 23A)

Figure 23: A. Kimmeridgian (154 Ma) reconstruction of the GOM showing grid of DNAG magnetic anomalies layered onto the plates. During this time, early oceanic crust in GOM continued to form as Yucatan rotated in a CCW direction around a single pole located in the Straits of Florida with a resulting, right-lateral displacement of 320 km along the Tamaulipas-Chiapas transform fault (TCTF). Magnetic anomalies on the Jurassic oceanic crust are not present due the Jurassic magnetic quiet zone as also observed in the central Atlantic Ocean. **B.** Kimmeridgian 154 Ma reconstruction of Atlantic at magnetic anomaly M25 using the same conjugate points as on Figure 21. Rate of spreading in the central Atlantic Ocean became more rapid at a rate of ~3.9 cm/year based on the previous fit at 163 Ma and M25 and with constant rate of separation. **C.** Map showing full reconstruction at 154 Ma.

The geometry of spreading caused the shape of the GOM spreading center to be oriented north-south in eastern GOM, east-west in central GOM and northeast-southwest in the western GOM. The proximity of the pole of rotation to the GOM also produced different spreading rates along the margin with slow spreading in the eastern GOM and fast spreading in the western GOM. The farther from the pole of rotation, the faster the spreading of the oceanic crust; the closer to the pole the slower the spreading. For this simple geometric and kinematic reason, the GOM oceanic crust is twice as wide in the west as in the east (Fig. 5).

Magnetic anomalies of the GOM oceanic crust (Fig. 23A) are not well expressed with low amplitudes and long wavelengths similar to those in the central Atlantic (Fig. 23B) and correlate in age to the period of the Jurassic magnetic quiet zone (Bird et al., 2007). For the central Atlantic reconstruction at 154 Ma (Fig. 23B), the reconstruction is based on aligning the M25 isochron.

2.13.6 Tithonian reconstruction (147 Ma)

Opening of GOM continued with right-lateral displacement along the TCTF that led to a total of 550 km of predicted fault offset along the east coast of Mexico. No evidence from magnetic or subsurface seismic observations show any different rates of separation. Slow, asymmetric separation continued during this stage in the eastern GOM because the rate of separation is faster in the west than in the east due to the kinematics of basin opening and proximity of the pole of rotation.

While there are no significant magnetic anomalies on the ocean crust of GOM at this time (Fig. 24A), there are several, aligned magnetic highs present in the western GOM that were interpreted by Bird et al. (2005) as traces of a fossil hotspot. These anomalies could also be related to lithologic variation since they have short wavelengths (Fig. 24A).

Reconstruction of the central Atlantic in the Tithonian (147 Ma) at magnetic anomaly M21 uses the New England seamounts and Jacksonville fracture zones (JFZ) on the eastern margin of North American as conjugates to the Canary Islands and Cape Verde fracture zone (CVFZ) on the African margin (Labails et al., 2010).

Figure 24: **A.** Tithonian (147 Ma) reconstruction of the GOM showing DNAG magnetic anomalies layered onto the plates. At this stage, early oceanic crust in GOM continued to form as a result of the CCW rotation of the Yucatan block around a single pole located in the Straits of Florida resulting in total of ~550 km of right-lateral displacement along the TCTF. Magnetic anomalies on the Jurassic oceanic crust are not present due the Jurassic magnetic quiet zone as also observed in the central Atlantic Ocean. **B.** Reconstruction of the Atlantic to the Tithonian (147 Ma) at magnetic anomaly M21 using the same conjugate points as in Figure 23. The rate of spreading has slowed to ~3.6 cm/year. This rate is based on a previous fit at M25 and M21 and with constant rate of separation in between. **C.** Map showing full reconstruction at 147 Ma.

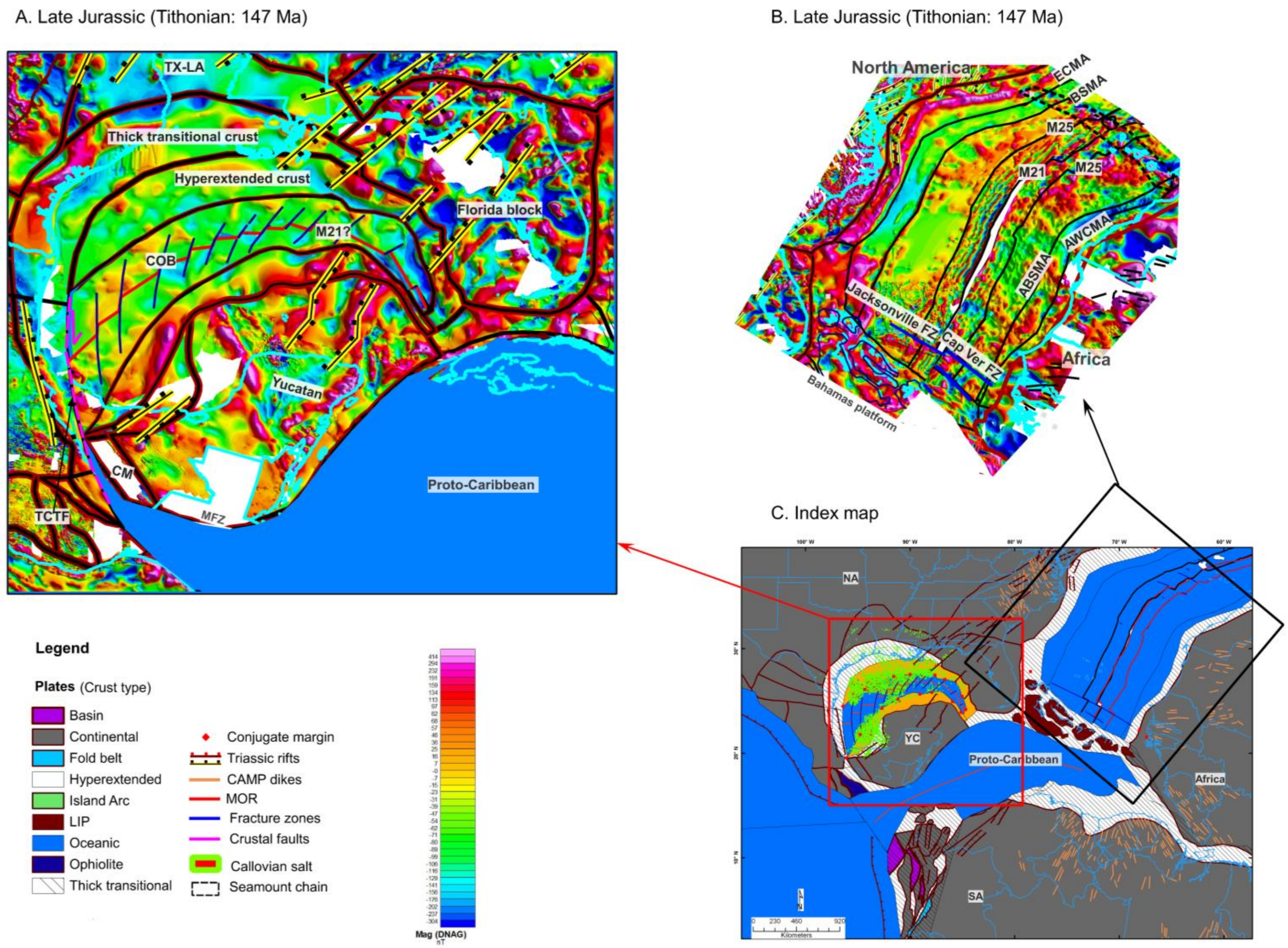
A. Late Jurassic (Tithonian: 147 Ma)
TX-LA
Thick transitional crust
Hyperextended crust
Florida block
M21?
COB
Yucatan
CM
MFZ
TCTF
Proto-Caribbean
B. Late Jurassic (Tithonian: 147 Ma)
North America
ECMA
BSMA
M25
M21
M25
AWCMA
ABSMA
Jacksonville FZ
Cap Ver FZ
Africa
Bahamas platform
C. Index map
NA
YC
Proto-Caribbean
Africa
SA
Kilometers
Legend
Plates (Crust type)
Basin
Continental
Fold belt
Hyperextended
Island Arc
LIP
Oceanic
Ophiolite
Thick transitional
Conjugate margin
Triassic rifts
CAMP dikes
MOR
Fracture zones
Crustal faults
Callovian salt
Seamount chain
Mag (DNAG)
nT

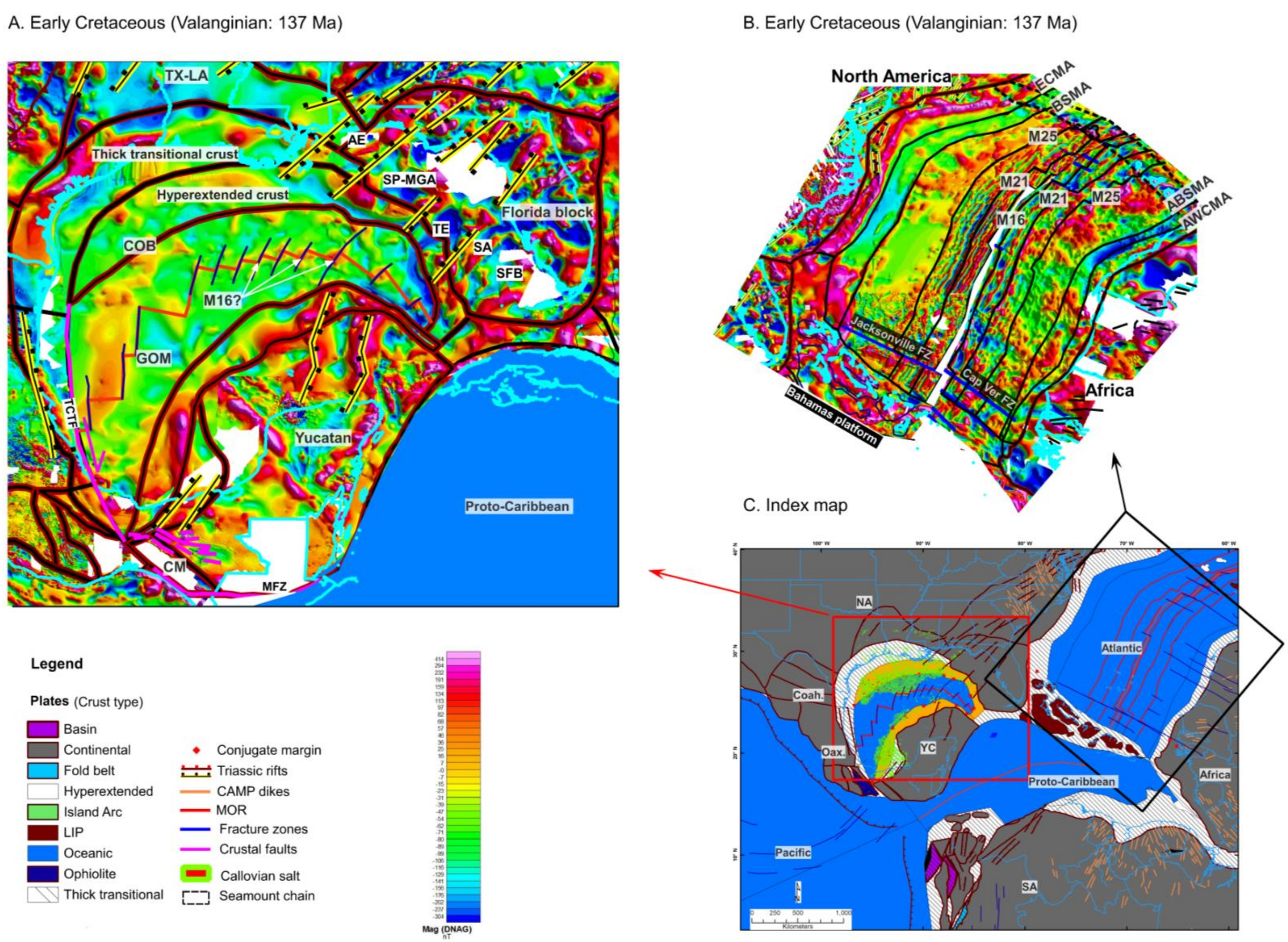

A. Early Cretaceous (Valanginian: 137 Ma)
TX-LA
AE
Thick transitional crust
Hyperextended crust
SP-MGA
TE
SA
Florida block
SFB
COB
M16?
GOM
TCTF
Yucatan
Proto-Caribbean
CM
MFZ
Legend
Plates (Crust type)
Basin
Continental
Fold belt
Hyperextended
Island Arc
LIP
Oceanic
Ophiolite
Thick transitional
Conjugate margin
Triassic rifts
CAMP dikes
MOR
Fracture zones
Crustal faults
Callovian salt
Seamount chain
Mag (DNAG)
B. Early Cretaceous (Valanginian: 137 Ma)
North America
ECMA
BSMA
M25
M21
M21
M16
M25
ABSMA
AWCMA
Jacksonville FZ
Cap Ver FZ
Bahamas platform
Africa
C. Index map
NA
Coah.
Oax.
YC
Atlantic
Proto-Caribbean
Africa
Pacific
SA

2.13.7 Valanginian reconstruction (137 Ma)

By early Valanginian, opening of the GOM was completed and basin evolution transitioned from the drift stage to a passive margin stage. This opening completed the CCW rotation of Yucatan by 39° with right-lateral displacement of ~800 km along eastern offshore Mexico. Asymmetric spreading is evident in the eastern GOM where the extinct spreading center is closer to Yucatan than to the Florida block. This asymmetry disappears in the central and western GOM where oceanic crust is evenly distributed on both sides of the ridge. (Fig 25A). It is unclear why the Yucatan rotation stopped abruptly in the Valanginian.

Figure 25: A. Valanginian (137 Ma) reconstruction of the GOM showing DNAG magnetic anomalies layered onto the plates. At this time, the opening and drift stage of the GOM is complete with about 39 degrees of CCW rotation of the Yucatan block and a total right-lateral displacement of ~800 km along the TCTF. **B.** Valanginian (137 Ma) reconstruction of the central Atlantic at M16. Rate of spreading in central GOM slowed down significantly to ~1.7 cm/year. This rate is based on previous fit at M21and M16 with a constant rate of separation in between. **C.** Map showing full reconstruction at 137 Ma.

2.14 Discussion

2.14.1 Kinematic model for the Jurassic opening of the GOM basin (Phase 4 in Figure 27)

This study has shown an excellent correlation between the locations of the extinct spreading ridges and transform faults shown on the gravity image of Sandwell et al. (2014). Their concentric nature about the pole of rotation they define near northwestern Cuba and the locations of the NE and eastern GOM COB's suggests Yucatan angle of rotation at 39 degrees (Fig. 26). The pole of rotation calculated from the Sandwell et al. (2014) gravity image falls closest to the previous pole position of Pindell and Kennan (2009) as shown on Figure 3. The close correspondence of the predicted small circles of opening to the pattern of spreading ridges and transform faults indicates that the Jurassic opening phase that produced the oceanic crust occurred about this single pole of rotation to the northwest of Cuba (Fig. 26). From a structural point of view the nearby pole means that the spreading ridge is highly arcuate and subdivided into many short spreading segments that are generally shorter than 200 km in length.

The mapped location of COB in my work and supported by the Sandwell et al. (2014) gravity data is similar to Hudec et al (2013) in eastern GOM and western GOM; however, in the central GOM, the width of the oceanic crust area in my study is wider than that shown by Hudec et al. (2013) based on an independent data set. I also disagree with the authors who suggested COB in the northern GOM extends to near the southern coastlines of the SE USA (Kneller and Johnson, 2011; Marton and Buffler, 1994) (Fig. 4). Instead, the seismic lines (Fig 9, 10, 11, and 12) presented earlier in this thesis shown this boundary to be much further to the south and in accordance with the gravity interpretation by Sandwell et al. (2014) d (Fig. 5) It is important to note that the COB mapped along the western side of GOM is much less constrained that the COB of the eastern and central GOM described in this thesis. My proposal for a single stationary pole of rotation in my work in the late Jurassic opening phase for the GOM is different from the migrating pole of rotation proposed by Pindell and Horn (2014). The proposed pole agrees with earlier studies by Pindell and Kennan (2009), Shephard (1983) and Marton and Buffler (1994).

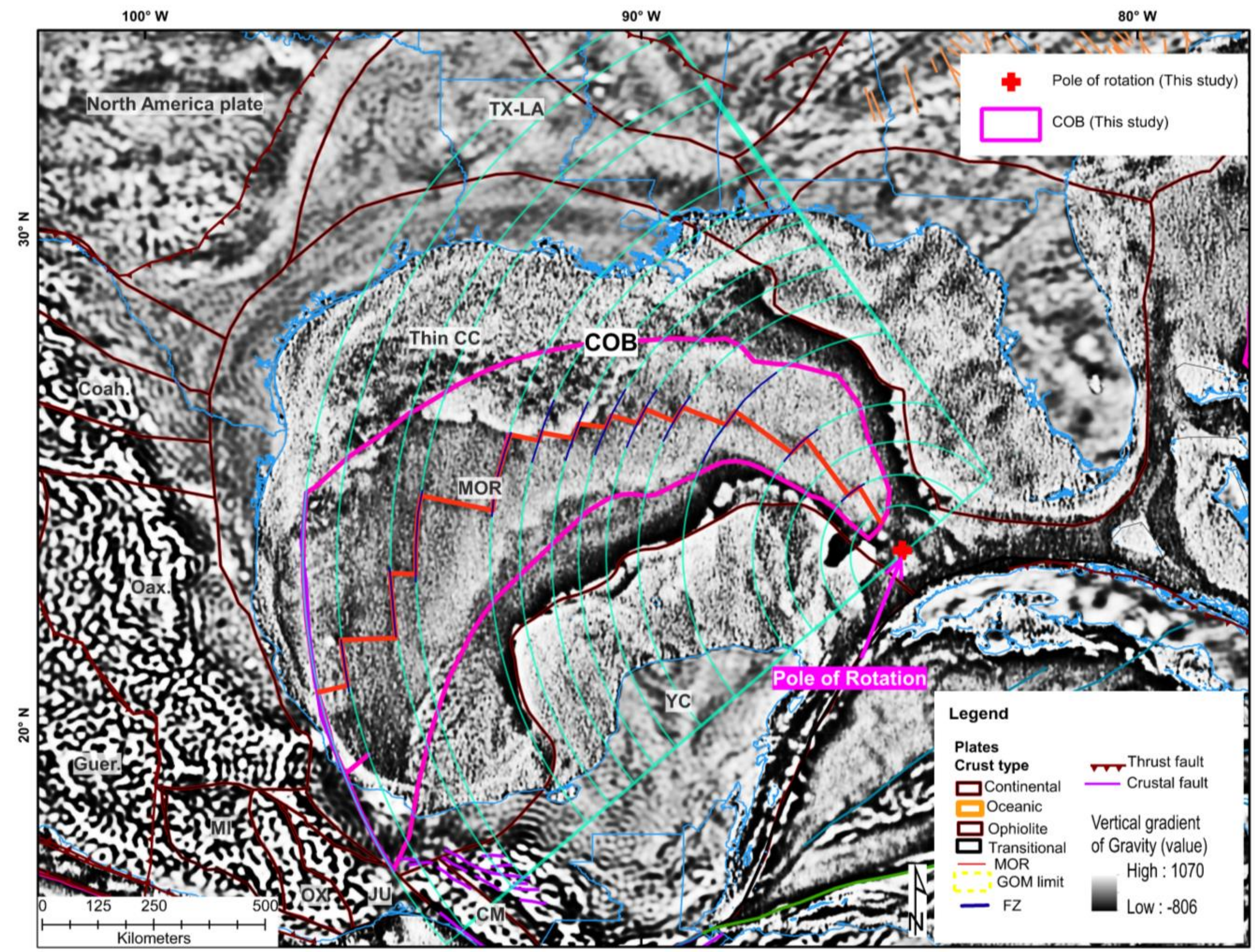

Figure 26: Sandwell (2014) VGG grid showing location of pole of rotation for Yucatan and Chiapas Massif (red plus sign), COB (purple line) and extinct spreading center (red line) proposed in this study. Circle arcs shows predicted location of fractures zones and conjugate which is in agreement with Sandwell grid.

The late Triassic period of extension (Phase 1 in Figure 27) was not imaged or studied in the GOM for this thesis as these features are mainly known from the subsurface of the northern GOM (Fig. 22A). However, the restorations shown in Figure; 22A, 23A, 24A, and 25A all show the progressive rotation of preexisting late Triassic rift trends in Florida and the Yucatan block as they are rotated through an angle of 39 degrees during the opening of the central GOM. This relation suggests that the GOM underwent rifting in two directions at two different times: first, Late Triassic stage 1 rifting to the southeast, apparently about a the same pole as the central Atlantic, and second, stage 2 Middle Jurassic rifting about the pole to the northeast of Cuba (Fig. 25A).

2.14.2 Timing of Mesozoic-Cenozoic tectonostratigraphic events of the eastern and central GOM

Six tectonostratigraphic phases of the opening of the GOM are summarized on Figure 26 based on the data and interpretations taken from this thesis or previous workers at six different localities in the eastern GOM or Yucatan block (locations of columns in the modern GOM are shown on figure 27G: 1) ultradeep GOM basin in the Walker Ridge; 2) ultradeep GOM basin in the northeastern Atwater Valley; 3) the Florida shelf at the Destin dome; 4) the Florida shelf at Charlotte harbor; 5) Straits of Florida; and 6) Yucatan block.

Figure 27: (next page) Regional chart summarizing my proposed tectonostratigraphic phases of the eastern GOM. On the vertical scale, major lithological units and six major phases for the eastern GOM evolution are identified. On the horizontal scale, six depositional environments are selected for correlation, from east to west: 1) ultra-deepwater in the center of GOM near the Atwater valley area overlying normal oceanic crust; 2) ultra-deepwater of GOM near Walker Ridge that overlies hyperextended transitional crust; 3) northern Florida shelf at Destin dome area that overlies thick transitional crust; 4) southern Florida shelf at the Charlotte Harbor area where the crust can be classified as normal continental crust that may have undergone minor stretching during Phase 1 Late Triassic rifting; 5) southeastern GOM in Strait of Florida where the crust has undergone two phases of rifting in Late Triassic (Phase 1) and Middle Jurassic (Phase 2); and 6) on the Yucatan platform where the crust has undergone minor rifting during phase 1 of Late Triassic rifting. On the oceanic crust, only thin accumulations (0.5 to 0.75 seconds TWT) of deep marine sediments (gray blocks) were deposited in the basin during phase 4 (phase of oceanic crust formation) and phase 5 (passive margin phase 1). During these two phases, the oceanic crust has been loaded with 4 to 5 seconds TWT of siliciclastic sediments from the Mississippi fan and its equivalents (light green). Phase 1 through phase 6 of evolution can be observed on hyperextended crust and thick transition crust (columns 2 and 3), during Phase 1 with late Triassic redbeds deposited and extensive magmatism starting with the CAMP event at 201 Ma (Smith, 1982; Muller et al, 2003). During the Middle Jurassic rifting (Phase 2), redbeds and sandstone were deposited followed by extensive salt (Phase 3). As the drift phase continued (Phase 4), shallow marine carbonates were deposited on the shelf (Smackover formation and equivalents) while deep marine sediments accumulated basinward. Similar deposition continued during Phase 5 on hyperextended and thick continental crust with deep marine sediments were deposited basinward and shallow marine carbonates deposited landward. In Phase 6, siliciclastic sediments from the Mississippi river became dominant. On the stretched continental crust beneath the Florida shelf (column 4), no evidence for phase 2 rifting in the Middle Jurassic can be identified. This crustal province has served as an area of extensive carbonate deposition throughout basin (phases 5 and phase 6). In the Straits of Florida (column 5) there is no significant sedimentary accumulation although evidence for both Phase 1 of Late Triassic rifting and Phase 2 of middle Jurassic rifting are evident (Escalona and Yang, 2013). On the Yucatan block (column 6), similar tectonostratigraphic phases as described on Florida shelf (column 4) suggest that the two areas were once continuous prior to rifting.

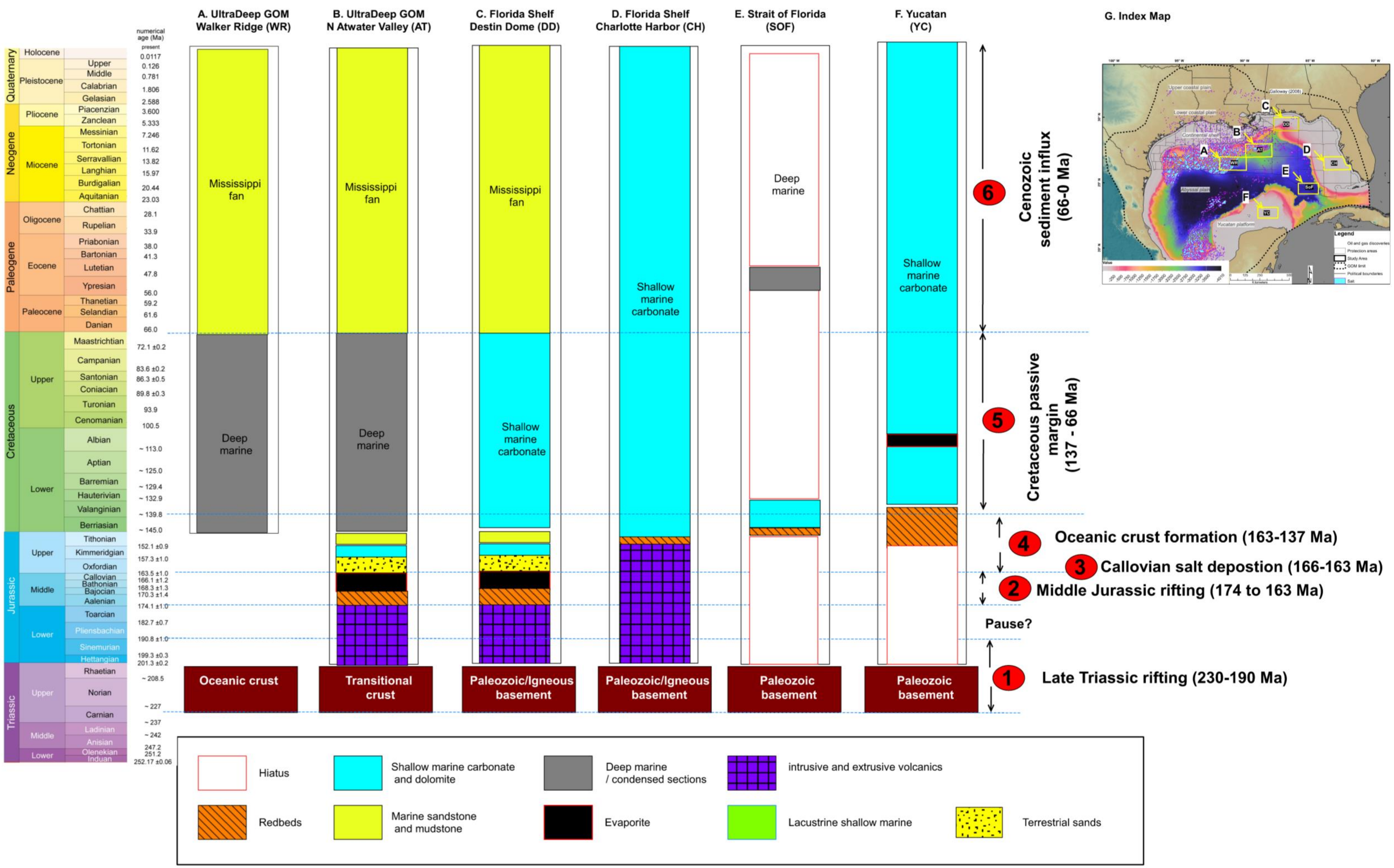

A. UltraDeep GOM Walker Ridge (WR)
B. UltraDeep GOM N Atwater Valley (AT)
C. Florida Shelf Destin Dome (DD)
D. Florida Shelf Charlotte Harbor (CH)
E. Strait of Florida (SOF)
F. Yucatan (YC)
G. Index Map
numerical age (Ma)
Mississippi fan
Deep marine
Shallow marine carbonate
Oceanic crust
Transitional crust
Paleozoic/Igneous basement
Paleozoic basement
6 Cenozoic sediment influx (66-0 Ma)
5 Cretaceous passive margin (137 - 66 Ma)
4 Oceanic crust formation (163-137 Ma)
3 Callovian salt depostion (166-163 Ma)
2 Middle Jurassic rifting (174 to 163 Ma)
Pause?
1 Late Triassic rifting (230-190 Ma)
Hiatus
Shallow marine carbonate and dolomite
Deep marine / condensed sections
intrusive and extrusive volcanics
Redbeds
Marine sandstone and mudstone
Evaporite
Lacustrine shallow marine
Terrestrial sands
Quaternary
Neogene
Paleogene
Cretaceous
Jurassic
Triassic
Holocene
Pleistocene
Pliocene
Miocene
Oligocene
Eocene
Paleocene
Upper
Lower
Middle
Calabrian
Gelasian
Piacenzian
Zanclean
Messinian
Tortonian
Serravallian
Langhian
Burdigalian
Aquitanian
Chattian
Rupelian
Priabonian
Bartonian
Lutetian
Ypresian
Thanetian
Selandian
Danian
Maastrichtian
Campanian
Santonian
Coniacian
Turonian
Cenomanian
Albian
Aptian
Barremian
Hauterivian
Valanginian
Berriasian
Tithonian
Kimmeridgian
Oxfordian
Callovian
Bathonian
Bajocian
Aalenian
Toarcian
Pliensbachian
Sinemurian
Hettangian
Rhaetian
Norian
Carnian
Ladinian
Anisian
Olenekian
Induan

Figure 27

The stratigraphic, facies, and biostratigraphic information compiled on the chart is taken from well reports used in this study (Galloway, 2008; Mancini and Puckett, 2002). The six phases are defined on the basis of major breaks in the stratigraphic record including unconformities and changes in sedimentary environments and water depths as shown on the stratigraphic columns on Figure 27 : 1) **Late Triassic rifting** (230 -190 Ma); 2) **Middle Jurassic rifting** (174 to 166 Ma); 3) **deposition of extensive salt** (166-163 Ma); 4) **formation of the oceanic crust in central GOM** (163-137 Ma); 5) **subsidence of the Cretaceous passive margin** (137-66 Ma); and 6) **influx of Cenozoic sediments related to the formation of the Mississippi delta** (66-0 Ma). The timing of these events based on the results of this thesis can be compared to results from previous workers that are summarize on Table 1.

Each of the six different areas (Fig. 27G) overlies three different type of basement - or a basement that has undergone a different amount of extension than areas above the same type of basement located in different areas.   The three types of basement include: 1) **Jurassic oceanic crust** of the ultradeep GOM at southern Walker Ridge (Fig. 27A); only thin accumulations (0.5 to 0.75 seconds TWT) of deep marine sediments (gray blocks) were deposited in the basin during phase 4 (phase of oceanic crust formation) and phase 5 (passive margin phase 1); during these two phases, the oceanic crust has been loaded with 4 to 5 seconds TWT of siliciclastic sediments from the Mississippi fan and its equivalents (Fig. 27); 2) **transitional, thinned, or hyperextended continental crust** of the northern Walker Atwater Valley (Fig. 27B); Phase 1 through phase 6 of evolution can be observed on hyperextended crust and thick transition crust (columns on Fig. 27B and C), during Phase 1 with late Triassic redbeds deposited and extensive magmatism starting with the CAMP event at 201 Ma (Smith, 1982); and 3) Paleozoic continental crust with varying amounts of extension at the Destin dome (Fig. 27C), Florida shelf (Fig. 27D); Charlotte Harbor, Florida Strait - where the crust may have undergone minor stretching during Phase 1 Late Triassic rifting; on the stretched continental crust beneath the Florida shelf (column 4), no evidence for phase 2 rifting in the Middle Jurassic can be identified; this crustal province has served as an area of extensive carbonate deposition throughout basin Phases 5 and 6) (Fig. 27D); Straits of Florida where the crust underwent two phases of rifting in the late Triassic (Phase 1) and the Middle Jurassic (Phase 2) (Fig. 27E); in the Straits of Florida (column 5) there is no significant sedimentary accumulation although evidence for both Phase 1 of Late Triassic rifting and Phase 2 of middle Jurassic rifting are observed (Escalona and Yang, 2013).

2.14.3 Comparison of the GOM sequence of rifting, massive salt deposits, breakup and seafloor spreading to the central Atlantic and the Red Sea

In order to understand the tectonic forces controlling the GOM opening and their tectonostratigraphic response, Figure 28 compares the sequence of opening events proposed in this thesis with the sequence of events known from previous workers in the central Atlantic Ocean and the Red Sea.

Several hypotheses have been proposed for the opening of the GOM from a plate tectonic prospective: 1) the western GOM basin opened from west to east by a triple junction located offshore eastern Mexico or along a triple junction located between Florida and Yucatan (Pindell and Kennan, 2007a, 2009; Jacques and Clegg, 2002); 2) the GOM basin opened first in its center along a hotspot track (Bird, 2005); 3) the GOM opened as the result of a mantle plume located in the central GOM (Dobson and Buffler, 1991, 1997; Buffler and Thomas, 1994); and 4) the GOM opened along two segmented spreading ridges, one the east and one in the west (Hudec et al., 2013).

Due to the deep burial of the older rocks of the GOM, the amount and exact distribution of volcanism accompanying early Mesozoic opening of the basin remains uncertain. Imbert (2005) and I have both mapped massive lava flows of ~8 km in thickness with eastward dips (seaward-dipping reflectors or “SDR’s”) that cover an area ~16,600 km^2 around Lloyd ridge in the northeastern GOM.

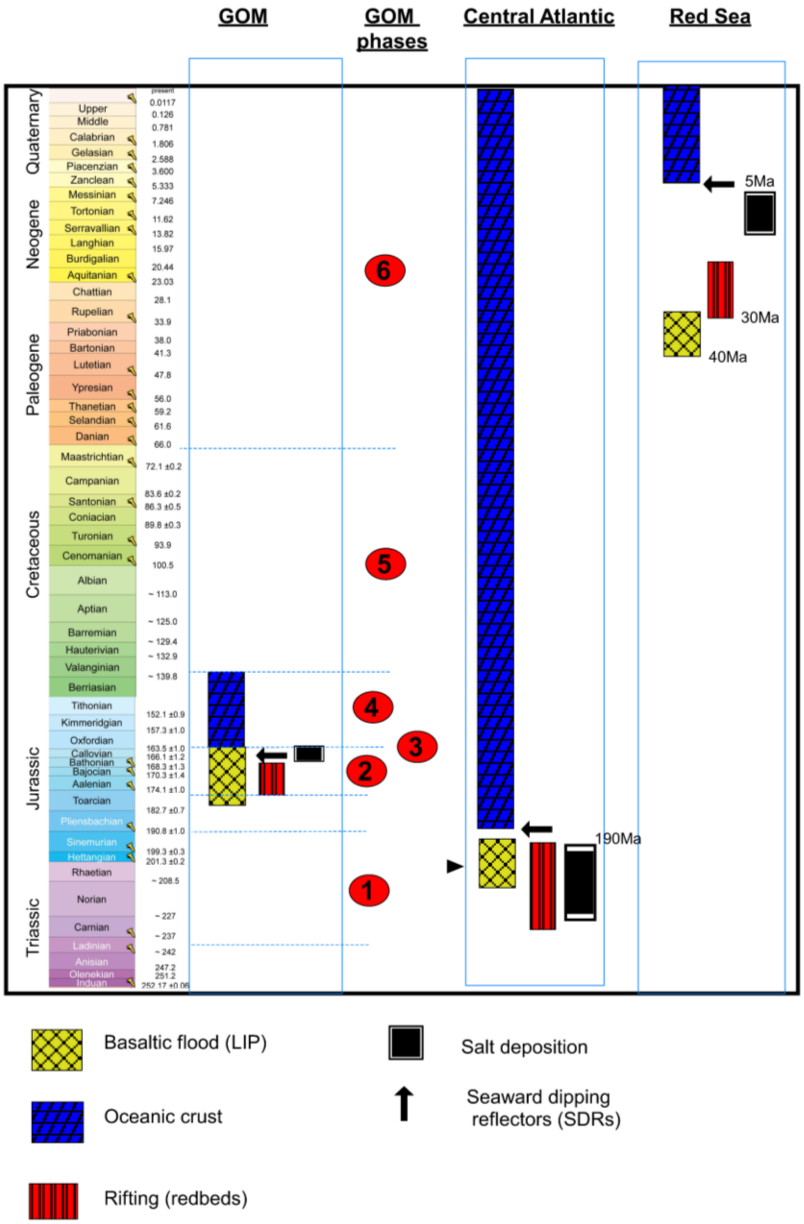

Figure 28: Chart comparing the sequence, duration, and timing of major stages of the basin evolution of the GOM to stages studied by previous workers in the Central Atlantic and Red Sea. In the GOM, magmatism in the form of continental basaltic flows and seaward-dipping reflectors, or SDR's, modified the continental basement beneath the northeastern GOM (Imbert, 2005; Eddy et al. 2014). I propose this pulse of magmatism in the northeastern and eastern GOM predated the Middle Jurassic rifting (Phase 2) but continued to accompany all of the

Middle and Late Jurassic rifting stages. SDR's formed prior to breakup at ~163 Ma and were followed by formation of the oceanic crust (phase

4) and passive margin phases (Phases 5 and phase 6). In the central Atlantic, rifting predated extensive magmatism (CAMP and central Atlantic SDRs) and salt was deposited over a prolonged geological time (220 to 190 Ma). Breakup occurred roughly at 190 Ma followed by generation of oceanic crust. In the Red Sea, magmatism first started at ~40 Ma followed by rifting at ~30 Ma and salt deposition at ~10 Ma. Oceanic crust (in red) in the east started to form at 5-6 Ma. The Red Sea is an analog for active rifting due to mantle convection (extensive magmatism and upwelling that leads to rifting) while the central Atlantic may be considered a passive rift (rifting that leads to extensive magmatism). GOM seems to fall into the active rifting category, although the distinction is less obvious than Red Sea analog.

However, to the south in the southeastern GOM in the Supercache grid of seismic data, I could see no evidence for widespread magmatic activity of the type associated with volcanic margins (Franke et al., 2012). Christeson et al. (2014) and Eddy et al. (2014) proposed underplated, high-density crust in the northeastern GOM that is consistent with the presence of SDR's in this area. Along the northwestern GOM margin in Texas, Mickus et al. (2009) proposed the presence of a Jurassic volcanic margin formed during early rifting based on refraction studies.

Although the age and distribution of a widespread magmatic event in the GOM remains poorly documented, I propose that the known pulse of magmatism in the northeastern and eastern GOM predated the period of Middle Jurassic rifting (Phase 2) but continued to accompany all of the Middle and Late Jurassic rifting stages as SDR's continued to form prior to breakup at ~163 Ma as shown on Figures 27 and 28. This same sequence of long-lived magmatism during protracted rifting and culminating with the formation of oceanic crust is observed at other volcanic margins believed to be driven by active rifting, or the influence of mantle plumes (Franke et al., 2012) such as in the case of the Red Sea (Fig. 28).

The Red Sea is a well-studied modern analog of active type rift system controlled by an ascending mantle plume that has been documented with geophysical surveying. Extensive magmatism first started at ~40 Ma and constructed a large igneous province for a period of 10 million years before rifting commenced at ~30 Ma. Rifting was followed by extensive deposition of salt in a sag basin setting at ~10 Ma and, finally, formation of oceanic crust in the central Red Sea from 5-6 Ma (Bastow and Keir, 2012; Bosworth et al., 2005).

In the central Atlantic Ocean, Triassic rifting predated extensive, late Triassic magmatism at 201 Ma (CAMP event and its associated central Atlantic SDR's). Salt was deposited in a sag basin over a prolonged geological time (230 to 190 Ma) prior to breakup and formation of oceanic crust starting at 190 Ma.

GOM shares characteristics with both margins: the sequence of an early phase of Triassic rifting (stage 1 in Figure 27) followed by magmatism, and finally oceanic crust formation is similar to the central Atlantic margin. Early rifting in the GOM indicates the possibility of a passive rift mechanism, not involving an initial mantle plume event. Klitgord and Schouten (1980) proposed that the GOM and rotation of the Yucatan block was a passive rift response to a shear couple set up by oblique subduction along the Pacific margin of Mexico (Fig. 2). On the other hand, evidence for large-scale basalt flows in the northeastern GOM indicates the possibility of mantle-driven, active rifting. I propose this pulse of magmatism in the northeastern and eastern GOM predated the Middle Jurassic rifting (Phase 2) but continued to accompany all of the Middle and Late Jurassic rifting stages as seen on other volcanic margins. SDR's formed prior to breakup at ~163 Ma and were followed by formation of the oceanic crust (Phase 4) and passive margin phases (Phases 5 and 6) (Fig. 27).

2.15 Conclusions

1. Based on data presented in this thesis, the opening of the Gulf of Mexico occurred in six stages: 1) Triassic stage 1 rifting (230-190 Ma); 2) Late Jurassic stage 2 rifting (174-166 Ma); 3) Late Jurassic stage 3 sag basin (166-163 Ma); 4) Late Jurassic stage 4 separation and formation of 6-8-km-thick oceanic crust (163-137 Ma); 5) Cretaceous stage 5 passive margin stage and deposition of overlying stratigraphic sections (137-66 Ma); and 6) Cenozoic stage 6 sediments influx stage (66-0 Ma).
2. Gulf of Mexico opening phase that produced the oceanic crust in the deep GOM basin occurred about a single pole of rotation to the northwest of Cuba where Yucatan rotated 39 degrees counterclockwise during the late Jurassic (163-137 Ma).
3. Late Jurassic stage 2 rifting (174-166 Ma) occurred in eastern Gulf of Mexico in a relatively narrow, 50-130 km-wide zone near the continent-ocean boundary.

4. Both Triassic stage 1 rifting (230-190 Ma) and Late Jurassic stage 2 rifting (174-166 Ma) were accompanied by extensive magmatism northeast Gulf of Mexico followed by formation of seaward-dipping reflectors prior to breakup at ~163 Ma.
5. Syn-rift strata thicken in a full graben adjacent to the COB in the east and central GOM. This rift zone widens to the north and northwest but is obscured by thick salt. Salt may have been focussed in this wider rift beneath the northern GOM.
6. The eastern GOM is a narrow rifted margin due to east-west extension near the pole of rotation. Along the arcuate spreading ridge the extension direction varied from northeast in the northeastern to north-south in the central GOM.
7. The oceanic crust in central GOM in 6-8-km thick and the COB is marked with a step-up in the basement.
8. The extinct Jurassic spreading ridge is recognizable on both gravity images and on seismic reflection data.

REFERENCES

Alaniz-Alvarez, e., 1996, Radiometric and kinematic evidence for Middle Jurassic strike-slip faulting in southern Mexico related to the opening of the Gulf of Mexico: Geology, v. 24, p. 443-446.

Bartok, P., 1993, Pre-breakup geology of the Gulf of Mexico-Caribbean; its relation to Triassic and Jurassic rift systems of the region: Tectonics, v. 12, p. 441-459.

Bird, D.E., Burke, K., Hall, S.A., and Casey, J.F., 2005, Gulf of Mexico tectonic history: Hotspot tracks, crustal boundaries, and early salt distribution: AAPG Bulletin, v. 89, p. 311-328.

Bird, D.E., Hall, S.A., Burke, K., Casey, J.F., and Sawyer, D.S., 2007, Early Central Atlantic Ocean seafloor spreading history: Geosphere, v. 3, p. 282-298.

Bralower, T.J., Paull, C.K., and Leckie, R.M., 1998, The Cretaceous-Tertiary boundary cocktail: Chicxulub impact triggers margin collapse and extensive sediment gravity flows: Geology, v. 26, p. 331-334.

Buffler, R.T., 1991, Early evolution of the Gulf of Mexico Basin, in Goldthwaite, D., ed., An Introduction to Central Gulf Coast Geology: New Orleans, Louisiana, New Orleans Geological Society, p. 1-15.

Buffler, R.T., Dobson, L.M., and DeBalko, D.A., 1993, Middle Jurassic through Early Cretaceous evolution of the Northeastem Gulf of Mexico Basin, in Pindell, J.L., and Perkins, R.F., eds., Mesozoic and Early Cenozoic Development of the Gulf of Mexico and Caribbean Region: A Context for Hydrocarbon Exploration, Gulf Coast Section Society of Economic Paleontologists and Mineralogists Foundation, p. 33-50.

Buffler, R.T., and Sawyer, D.S., 1985, Distribution of crust and early history, Gulf of Mexico basin: Gulf Coast Association of Geological Societies Transactions, v. 35, p. 333-334.

Buffler, R.T., Shaub, F.J., Huerta, R., Ibrahim, A.B.K., and Watkins, J.S., 1981, A model for the early evolution of the Gulf of Mexico basin: Oceanologica Acta, v. 14, p. 129-136.

Buffler, R.T., and Thomas, W.A., 1994, Crustal structure and evolution of the southeastern margin of North America and the Gulf of Mexico basin, in Speed, R., ed., Phanerozoic Evolution of North American Continent-Ocean Transitions, Volume CTV-1:

Geology of North America: Boulder, Colorado, Geological Society of America, p. 219-263.

Buffler, R.T., Watkins, J.S., Worzel, J.L., and Shaub, F.J., 1980, Structure and early geologic history of the deep central Gulf of Mexico Basin, in Pilger, R., ed., Proceedings of a Symposium on the Origin of the Gulf of Mexico and the Early Opening of the Central North Atlantic, Louisiana State University, Baton Rouge, LA, March 1980: Baton Rouge, Louisiana State University, p. 3-16.

Bullard, E., Everett, J.E., and Smith, A.G., 1965, The fit of the continents around the Atlantic: Philosophical Transactions of the Royal Society of London. Series A, Mathematical and Physical Sciences, v. 258, p. 41-51.

Burke, K., Cooper, C., Dewey, J.F., Mann, P., and Pindell, J.L., 1984, Caribbean tectonics and relative plate motions: Geological Society of America Memoirs, v. 162, p. 31-64.

Centeno-García, E., Guerrero-Suástegui, M., and Talavera-Mendoza, O., 2008, The Guerrero composite terrane of western Mexico: Collision and subsequent rifting in a supra-subduction zone: Geological Society of America Special Papers, v. 436, p. 279-308.

Christeson, G.L., Van Avendonk, H.J.A., Norton, I.O., Snedden, J.W., Eddy, D.R., Karner, G.D., and Johnson, C.A., 2014, Deep crustal structure in the eastern Gulf of Mexico: Journal of Geophysical Research: Solid Earth, v. 119, p. 2014JB011045.

Dobson, L.M., and Buffler, R.T., 1991, Basement rocks and structure, northeast Gulf of Mexico, in Schumacher, D., and Rosen, N.C., eds., Gulf Coast Association of Geological Societies; transactions of the 41st annual convention, Volume XLI: New Orleans, LA, Gulf Coast Association of Geological Societies, p. 191-206.

Dobson, Laura M., and Richard T. Buffler, 1997, Seismic stratigraphy and geologic history of Jurassic rocks, northeastern Gulf of Mexico: AAPG Bulletin, v. 81, p. 100-120.

Dunbar, J.A., and Sawyer, D.S., 1987, Implications of continental crust extension for plate reconstruction: An example from the Gulf of Mexico: Tectonics, v. 6, p. 739-755.

Eddy, D.R., Van Avendonk, H.J., Christeson, G.L., Norton, I.O., Karner, G.D., Johnson, C.A., and Snedden, J.W., 2014, Deep crustal structure of the northeastern Gulf of Mexico: Implications for rift evolution and seafloor spreading: Journal of Geophysical Research: Solid Earth, v. 119, p. 6802-6822.

Escalona, A., and Yang, W., 2013, Subsidence controls on foreland basin development of northwestern offshore Cuba, southwestern Gulf of Mexico: AAPG Bulletin, v. 97, p. 1-25.

Franke, D., 2013, Rifting, lithosphere breakup and volcanism: Comparison of magma-poor and volcanic rifted margins: Marine and Petroleum Geology, v. 43, p. 63-87.

Galloway, W.E., 2008, Chapter 15 Depositional evolution of the Gulf of Mexico sedimentary basin, in Andrew, D.M., ed., Sedimentary Basins of the World, Volume Volume 5, Elsevier, p. 505-549.

Hall, S.A., and Najmuddin, I.J., 1994, Constraints on the tectonic development of the eastern Gulf of Mexico provided by magnetic anomaly data: Journal of Geophysical Research: Solid Earth, v. 99, p. 7161-7175.

Heatherington, A.L., and Mueller, P.A., 2003, Mesozoic igneous activity in the Suwannee Terrane, Southeastern USA: Petrogenesis and Gondwanan affinities: Gondwana Research, v. 6, p. 296-311.

Hudec, M.R., Norton, I.O., Jackson, M.P.A., and Peel, F.J., 2013, Jurassic evolution of the Gulf of Mexico salt basin: AAPG Bulletin, v. 97, p. 1683-1710.

Imbert, P., and Phillippe, Y., 2005, The Mesozoic opening of the Gulf of Mexico: Part 2, Integrating seismic and magnetic data into a general opening model, 25th Annual GCS-SEPM Foundation Bob F. Perkins Research Conference: Houston, Texas, p. 1151-1168.

Jacques, J.M., and Clegg, H., 2002, Late Jurassic source rock distribution and quality in the Gulf of Mexico: Inferences from plate tectonic modelling: Transactions - Gulf Coast Association of Geological Societies, v. 52, p. 429-440.

Keir, D., Bastow, I.D., Pagli, C., and Chambers, E.L., 2013, The development of extension and magmatism in the Red Sea rift of Afar: Tectonophysics, v. 607, p. 98-114.

Klitgord, K.D., Popenoe, P., and Schouten, H., 1984, Florida: A Jurassic transform plate boundary: J. Geophys. Res., v. 89, p. 7753-7772.

Klitgord, K.D., and Schouten, H., 1980, Mesozoic evolution of the Atlantic, Caribbean and Gulf of Mexico, in Pilger, R.H., Jr., ed., The Origin of the Gulf of Mexico and the Early Opening of the Central North Atlantic, proceedings of a symposium at Louisiana State University, Baton Rouge, Louisiana, March 3-4-5, 1980: Baton Rouge, LA, Louisiana State University, p. 100-101.

Kneller, Erik A., and Christopher A. Johnson, 2011 Plate kinematics of the Gulf of Mexico based on integrated observations from the Central and South Atlantic: Gulf Coast Association of Geological societies Transactions, v. 61, p. 283-300.

Kruge, M.A., Stankiewicz, B.A., Crelling, J.C., Montanari, A., and Bensley, D.F., 1994, Fossil charcoal in Cretaceous-Tertiary boundary strata: Evidence for catastrophic firestorm and megawave: Geochimica et Cosmochimica Acta, v. 58, p. 1393-1397.

Mancini, E.A., Badali, M., Puckett, T.M., Llinas, J.C., and Parcell, W.C., 2001, Mesozoic carbonate petroleum systems in the northeastern Gulf of Mexico area, Petroleum Systems of Deep-Water Basins: GCS-SEPM Foundation 21st Annual Research Conference, p. 423-451.

Mancini, E.A., and Markham Puckett, T., 2002, Transgressive-regressive cycles in Lower Cretaceous strata, Mississippi Interior Salt Basin area of the northeastern Gulf of Mexico, USA: Cretaceous Research, v. 23, p. 409-438.

Marton, G., and Buffler, R.T., 1994, Jurassic reconstruction of the Gulf of Mexico Basin: International Geology Review, v. 36, p. 545-586.

Mickus, K., Stern, R.J., Keller, G.R., and Anthony, E.Y., 2009, Potential field evidence for a volcanic rifted margin along the Texas Gulf Coast: Geology, v. 37, p. 387-390.

Molina-Garza, R.S., Van der Voo, R., and Urrutia-Fucugauchi, J., 1992, Paleomagnetism of the Chiapas Massif, southern Mexico: Evidence for rotation of the Maya Block and implication for the opening of the Gulf of Mexico: Geological Society of America Bulletin, v. 104, p. 1156-1168.

Mueller, P.A., Heatherington, A.L., Foster, D.A., Thomas, W.A., and Wooden, J.L., 2013, The Suwannee suture: Significance for Gondwana-Laurentia terrane transfer and formation of Pangaea: Gondwana Research, v. 26, p. 365-373.

Olsen, P.E., 1997, Stratigraphic record of the early Meoszoic breakup of Pangea in the Laurasia-Gondwana rift system: Annual Review of Earth and Planetary Science, v. 25, p. 337-401.

Pindell, J., and Dewey, J.F., 1982, Permo-Triassic reconstruction of western Pangea and the evolution of the Gulf of Mexico/Caribbean region: Tectonics, v. 1, p. 179-211.

Pindell, J., Graham, R., and Horn, B., 2014, Rapid outer marginal collapse at the rift to drift transition of passive margin evolution, with a Gulf of Mexico case study: Basin Research, v. 26, p. 154-182.

Pindell, J., and Kennan, L., 2007, Rift models and the salt-cored marginal wedge in the northern Gulf of Mexico: Implications for deep-water Paleogene Wilcox deposition and basinwide maturation, in Kennan, L., Pindell, J., and Rosen, N., eds., Proceedings, 27th Annual GCS-SEPM Foundation Bob F. Perkins Research Conference: Houston, Texas, p. 1-30.

Pindell, J.L., and Kennan, L., 2009, Tectonic evolution of the Gulf of Mexico, Caribbean and Northern South America in the mantle reference frame: an update: Geological Society, London, Special Publications, v. 328, p. 1-55.

Poole, F.G., Perry, W.J., Madrid, R.J., and Amaya-Martínez, R., 2005, Tectonic synthesis of the Ouachita-Marathon-Sonora orogenic margin of southern Laurentia: Stratigraphic and structural implications for timing of deformational events and plate-tectonic model: Geological Society of America Special Papers, v. 393, p. 543-596.

Ramos, E.L., 1975, Geological summary of the Yucatan Peninsula, The Gulf of Mexico and the Caribbean, in Boletín Asociación Mexicana de Geólogos Petroleros, v. XXV, no. 1–3, 1973

Ross, M.I., and Scotese, C.R., 1988, A hierarchical tectonic model of the Gulf of Mexico and Caribbean region: Tectonophysics, v. 155, p. 139-168.

Rychert, C.A., Hammond, J.O., Harmon, N., Kendall, J.M., Keir, D., Ebinger, C., Bastow, I.D., Ayele, A., Belachew, M., and Stuart, G., 2012, Volcanism in the Afar Rift sustained by decompression melting with minimal plume influence: Nature Geoscience, v. 5, p. 406-409.

Sacks, P.E., and Secor, D.T., 1990, Delamination in collisional orogens: Geology, v. 18, p. 999-1002.

Salvador, A., 1987, Late Triassic-Jurassic paleogeography and origin of Gulf of Mexico basin: AAPG Bulletin, v. 71, p. 419-451.

Salvador, Amos, 1991, Origin and development of the Gulf of Mexico basin, in Salvador, A., ed., The Gulf of Mexico Basin, Volume J: The Geology of North America: Boulder, Colorado, Geological Society of America, p. 389-444.

Sandwell, D.T., Müller, R.D., Smith, W.H., Garcia, E., and Francis, R., 2014, New global marine gravity model from CryoSat-2 and Jason-1 reveals buried tectonic structure: Science, v. 346, p. 65-67.

Sawyer, D.S., Buffler, R.T., and Pilger, R., 1991, Crust and mantle of the Gulf of Mexico basin, in Salvador, A., ed., The Gulf of Mexico Basin, Volume J: Geology of North America: Boulder, Colorado, Geological Society of America, p. 53-72.

Schouten, H., and Klitgord, K., D., 1994, Mechanistic solutions to the opening of the Gulf of Mexico: Geology, v. 22, p. 507-510.

Shephard, A., 1983, A Study of the Magnetic Anomalies in the Eastern Gulf of Mexico. Doctoral dissertation, University of Houston-University Park.

Smith, D.L., 1982, Review of the tectonic history of the Florida basement: Tectonophysics, v. 88, p. 1-22.

Stern, R.J., and Dickinson, W.R., 2010, The Gulf of Mexico is a Jurassic backarc basin: Goesphere, v. 6, p. 739-754.

Ward, W., Keller, G., Stinnesbeck, W., and Adatte, T., 1995, Yucatán subsurface stratigraphy: Implications and constraints for the Chicxulub impact: Geology, v. 23, p. 873-876.

Withjack, M.O., Schlische, R.W., and Olsen, P.E., 2012, Development of the passive margin of eastern North America: Mesozoic rifting, igneous activity, and breakup: Principles of Phanerozoic Regional Geology, v. 1, p. 301-335.

Wu, S., Vail, P.R., and Cramez, C., 1990, Allochthonous salt, structre and stratigraphy of the north-eastern Gulf of Mexico. Part I: Stratigraphy: Marine and Petroleum Geology, v. 7, p. 318-349.